

Modulators of Toll-like Receptors-4 and -2

By

**C2009
Wenyan Wu**

**Submitted to the graduate degree program in Medicinal Chemistry and the
Graduate Faculty of the University of Kansas
in partial fulfillment of the requirements for the degree of
Master of Science.**

Dissertation Committee:

Chairperson

Date defended: _____

**The Thesis Committee for Wenyan Wu certifies
that this is the approved version of the following thesis:**

Modulators of Toll-like Receptors-4 and -2

Dissertation Committee:

Chairperson

Date approved: _____

Abstract

The toxicity of Gram-negative bacterial endotoxin (lipopolysaccharide, LPS) resides in its structurally highly conserved glycolipid component called lipid A. The major goal of the first project was to further explore structure-activity relationships in small-molecules that would sequester LPS by binding to the lipid A moiety, so that it may find application in the prophylaxis or adjunctive therapy of Gram-negative sepsis. Several guanylhyazones had earlier been identified in rapid-throughput screens as potent LPS binders. It was desirable to examine if grafting the guanylhyazone functionality on the scaffold of a lead *N*-alkyl polyamine compound would afford greater LPS sequestration potency. In the first project, a congeneric set of guanylhyazone analogues were synthesized and evaluated for LPS-sequestering potency. It was found that a C₁₆ alkyl substitution was optimal in the *N*-alkylguanylhyazone series; a homospermine analogue with the terminal amine *N*-alkylated with a C₁₆ chain with the other terminus of the molecule bearing an unsubstituted guanylhyazone moiety was marginally more active suggesting very slight, if any, steric effects. Neither C₁₆ analogue was significantly more active than the *N*-C₁₆-alkyl or *N*-C₁₆-acyl compounds that we had characterized earlier, indicating that basicity of the phosphate-recognizing cationic group is not a determinant of LPS sequestration activity.

The N-terminus of bacterial lipoproteins are acylated with a (*S*)-(2,3-bisacyloxypropyl)cysteinyll residue. Lipopeptides derived from lipoproteins activate innate immune responses by engaging Toll-like receptor 2 (TLR2), and are highly immunostimulatory and yet without apparent toxicity in animal models. The lipopeptides may therefore be useful as potential immunotherapeutic agents. Previous structure-activity relationships in such lipopeptides have largely been obtained using murine cells and it is now clear that significant species-specific differences exist between human and murine TLR responses. In the second project, I have examined in detail the role of the highly conserved Cys residue as well as the geometry and stereochemistry of the Cys-Ser dipeptide unit. (*R*)-diacylthioglycerol analogues were maximally active in reporter gene assays using human TLR2. The Cys-Ser dipeptide unit represents the minimal part-structure, but the stereochemistry of neither amino residues of the dipeptide was found to be a critical determinant of activity. The thioether bridge between the diacyl and dipeptide units was determined to be crucial, and replacement by an ether bridge resulted in a dramatic decrease in activity. Moreover, the replacement of the two ester-linked C₁₆ hydrocarbons by ether or amide linkages led to a dramatic loss in activity, while the replacement of one of the ester-linked fatty acyl moiety (internal) with an amide linkage remained partially active.

Acknowledgments

Firstly I would like to acknowledge and thank my advisor Professor Sunil David for his advice, guidance and mentorship during my graduate studies. In the course of my work, he has provided me constant help and support and has inspired and encouraged me and I owe him a deep gratitude for having shown me this way of research. I also would like to thank the David research group and greatly appreciate their support and assistance without which it would have been impossible for me to accomplish my research.

I would like to thank the members of my dissertation committee – Professors Apurba Dutta, Blake Peterson and Teruna Siahaan for their time and effort. I am also thankful to the faculty members of the department of medicinal chemistry and their valuable instructions and support.

I am also very grateful to my parents and all my friends for their love, encouragement and their never-ending support.

Wenyan Wu

8.28.2009

Table of Contents

List of Figures	10
List of Abbreviations	12

Chapter 1

Introduction: Gram-negative Sepsis

1.1 Background	17
1.2 Complexation of LPS by macromolecules as a therapeutic strategy	22
1.2.1 Polyclonal and monoclonal antibodies	22
1.2.2 Non-antibody LPS-binding proteins	23
1.3 The paradigm of non-immunologic sequestration of LPS by small molecules	24
1.3.1 Polymyxin B	24
1.3.2 Structural correlates of affinity of LPS binding in nonpeptide small molecules	26
1.4 Structural correlates of LPS binding and neutralization	27
1.4.1 Elucidation of the pharmacophore for lipid A binding	27
1.4.2 Lipid A binding is necessary, but not sufficient for LPS Neutralization	32
1.4.3 Structural correlates of neutralization of endotoxicity	34
1.5 Lipopolyamines as lead compounds for development of LPS Sequestrants	35

Chapter 2

Structure –Activity Relationships of Lipopolysaccharide Sequestration

in Guanylhydrazone-bearing Lipopolyamines

2.1 Introduction and rationale	39
2.2 Syntheses of compounds bearing alkylguanylhydrazone on one end, and a free amino group at the other terminus	41
2.3 Synthesis of an analog bearing an <i>N</i> -alkyl substituent on one end and an unsubstituted guanylhydrazone at the other terminus	41
2.4 LPS sequestration activities of the guanylhydrazone compounds	44
2.5 Conclusions	47
2.6 Experimental Data	
2.6.1 Experimental Procedures	49
2.6.1.1 Syntheses of compounds bearing alkylguanylhydrazone on one end, and a free amino groups at the other terminus	49
2.6.1.2 Synthesis of an analog bearing an <i>N</i> -alkyl substituent on one end and an unsubstituted guanylhydrazone at the other terminus	57
2.6.2 Materials and Methods	61
2.6.2.1 Chemistry	61
2.6.2.2 Assays	62

Chapter 3

Toll-like Receptors (TLRs) and TLR2

3.1 Background	65
3.2 TLR1/TLR2/TLR6 agonistic bacterial lipoteichoic acid and lipopeptides	66
3.2.1 Structural basis for the interactions of PAM ₂ CSK ₄ with TLR2 and PAM ₃ CSK ₄ with TLR2/TLR1	68
3.2.2 Effects of the TLR2 agonistic lipopeptides on professional antigen presenting cells and effector lymphocytes	70

Chapter 4

Structure-Activity Relationships in TLR2-Agonistic Diacylthioglyceryl Lipopeptides

4.1 Introduction and rationale	72
4.2 Syntheses and evaluation of cysteamine and cysteamine—inverse serine analogs	79
4.3 Syntheses and evaluation of PAM ₂ C-OMe, PAM ₂ CS-OH and PAM ₂ CS-OMe analogs	82
4.4 Syntheses and evaluation of <i>O</i> -linkage and ether analogs	83
4.5 Syntheses and evaluation of monoamide and diamide analogs	88
4.6 Conclusions	93

4.7 Experimental Data	
4.7.1 Experimental Procedures	94
4.7.1.1 Scheme1 (cysteamine and cysteamine-inverse serine analogs)	94
4.7.1.2 Scheme 2 (PAM ₂ C-OMe, PAM ₂ CS-OH and PAM ₂ CS-OMe analogs)	102
4.7.1.3 Scheme 3 (<i>O</i> -linkage analogs)	113
4.7.1.4 Scheme 4 (ether analog)	121
4.7.1.5 Scheme 5 (monoamide analog)	128
4.7.1.6 Scheme 6 (diamide analog)	135
4.7.2 Materials and Methods	143
4.7.2.1 Chemistry	143
4.7.2.2 Assays	143
References	147

List of Figures

Figure 1. Incidence of sepsis in the U.S.	17
Figure 2. Schematic and crystal structure of lipopolysaccharide and the structure of enterobacterial lipid A	18
Figure 3. Schematic representation of immune activation by LPS	19
Figure 4. Outcomes of clinical trials of anti-inflammatory agents in sepsis	21
Figure 5. The primary structure of Polymyxin B (PMB) and NMR-derived conformation of the lipid A: PMB complex	25
Figure 6. Affinity of cationic amphiphilic drugs toward lipid A measured by DC displacement	27
Figure 7. Relationship between inter-nitrogen distance of α , ω -diaminoalkanes, polyamines, and bisamidines, and binding affinity to lipid A	29
Figure 8. Model of the pentamidine: <i>bis</i> -phosphoryl lipid-A complex	31
Figure 9. Inhibition of TNF- α in LPS (10 ng/mL)-stimulated human PBMC by pentamidine and polymyxin B.	33
Figure 10. Structures of acylpolyamines and inhibition of TNF- α induction in J774 cells stimulated LPS	34
Figure 11. Structures of mono- and <i>bis</i> -acyl polyamine analogs	36
Figure 12. Correlation between carbon number of the hydrocarbon group in mono- and <i>bis</i> -acyl compounds and TNF- α inhibition in human blood and NO inhibition in murine cells	37

Figure 13. Molecular model of a mono-homologated, mono-alkyl polyamine docked on LPS	40
Figure 14. Comparison of activities of the guanyldihydrazone compounds according to the IC ₅₀ of NF-κB and NO inhibition	44
Figure 15. LPS-induced proinflammatory cytokine production of compound 8f	46
Figure 16. Structure of lipoteichoic acid (LTA), a constituent of the cell envelope of Gram-positive organisms	66
Figure 17. Structure of MALP-2, the first TLR2 agonistic, immunostimulatory lipopeptide identified	67
Figure 18. Crystal structure of PAM ₃ CSK ₄ bound to a heterodimer of TLR1 and TLR2	69
Figure 19. <i>Top:</i> Structure of PAM ₂ CSK ₄ ; <i>Bottom:</i> the crystal structure of PAM ₃ CSK ₄ bound to TLR1/TLR2 heterodimer	76
Figure 20. Pyrogenicity responses to LPS and PAM ₂ CSK ₄ in rabbits	77
Figure 21. Induction of cytokine release by LPS and PAM ₂ CSK ₄ in human blood	77
Figure 22. Induction of NO and phosphorylation of p38MAPK with LPS and PAM ₂ CSK ₄	78
Figure 23. Expansion of CD25 ⁺ /CD56 ⁺ double-positive natural killer (NK) cells population upon stimulation of human whole blood with 1 μg/ml LPS or PAM ₂ CSK ₄ .	79
Figure 24. TLR2 agonistic activities of the lipopeptide analogues	87
Figure 25. TLR2 agonistic activities of the lipopeptide analogues (continued)	92

List of Abbreviations

AcOH – acetic acid

APC antigen presenting cell

BF₃•OEt₂ – boron trifluoride diethyl etherate

BnBr – benzyl bromide

br - broad

Boc – di-*tert*-butyl carbonate

BPI – bactericidal permeability increasing protein

CH₃CN – acetonitrile

C₁₅H₃₁COCl – palmitoyl chloride

CTL – cytotoxic T lymphocyte

DAB – α , γ -diaminobutyric acid

DC –dendritic cell

DC displacement – Dansyl-cadaverine displacement

DCM – dichloromethane

DMF - dimethylformamide

DMAP – 4-dimethylaminopyridine

ED₅₀ – 50% effective displacement

EDCI – 1-Ethyl-3-(3-dimethylaminopropyl)carbodiimide

EDIPA – *N,N*-Diisopropylethylamine

ENP – endotoxin binding protein

eq. – equivalent

ESI – electron spray ionization

EtOAc – ethyl acetate

EtOH – ethanol

FDA – federal drug administration

H-Bonds – hydrogen bonds

HCOOH – formic acid

HCl – hydrochloric acid

HEK – human embryonic kidney cells

HIV – human immunodeficiency virus

HPLC – high performance liquid chromatography

IL – interleukin

KDO – 3-ketodeoxy-D-manno-octulosonic acid

i.p. – intraperitoneally

i.v. – intravenously

K_d – dissociation constant

IC₅₀ – 50% inhibitory concentration

LC-MS – liquid chromatography mass spectrometry

LD₁₀₀ – lethal dose

LiBH₄ – lithium borohydride

LiOH – lithium hydroxide

LPS – lipopolysaccharide

LBP – LPS binding protein

LRR – leucin-rich repeat

LTA – lipoteichoic acid

m – multiplet

MALP-2 – mycoplasma associated lipopeptide-2kDa

mg – milligram

MHC – major histocompatibility complex

mL – mililiter

M ϕ – microphage

MeOH – methanol

NaH – sodium hydride

NaHCO₃ – sodium bicarbonate

NaN₃ – sodium azide

Na₂SO₄ – sodium sulfate

Na₂S₂O₃ – sodium thiosulfate

ng – nanogram

nM – nanomolar

NF- κ B – nuclear factor- κ B

NK cells – natural killer cells

NMR – nuclear magnetic resonance

NO – nitric oxide

p38MAPK – p38 mitogen activated protein kinase

PAMP – pathogen associated molecular pattern

PCC – pyridinium chlorochromate

Pd(OH)₂ – palladium hydroxide

PE – phycoerythrin

PGN – peptidoglycan

Phe – phenylalanine

PMB – polymyxin B

PMN – polymyxin B nonapeptide

PPh₃ – triphenylphosphine

p-TsCl – *para*-toluenesulfonyl chloride

pyr – pyridine

r.t. – room temperature

s - singlet

sAP – secreted Alkaline Phosphatase

SAR – structure-activity relationship

sat. – saturated

t – triplet

T_{1/2} - Half-life

TBAF – tetra-*n*-butylammonium fluoride

TBDMS – *tert*-butyldimethylsilyl

TFA – trifluoroacetic acid

THF – tetrahydrofuran

TIR – Toll/IL-1 receptor

TLR – Toll-like Receptor

TNF- α – Tumor necrosis factor- α

TOF – time of flight

TRIF – TIR-domain-containing adapter-inducing interferon- β

Chapter 1

Introduction: Gram-negative Sepsis

1.1 Background.

Gram-negative sepsis, or "blood poisoning" in lay terminology, is a common and serious clinical problem. While fewer than 100 cases were reported prior to 1920¹, it is now the thirteenth leading cause of overall mortality² globally, and the number one cause of deaths in the intensive care unit³ accounting for some 200,000 fatalities in the US annually⁴ (**Figure 1**). While the incidence continues to rise worldwide^{5,6} due to increased invasive procedures, immunosuppression and cytotoxic chemotherapy, mortality has essentially remained unchanged at about 45%⁷ due to the lack of specific therapy aimed at the pathophysiology of sepsis.

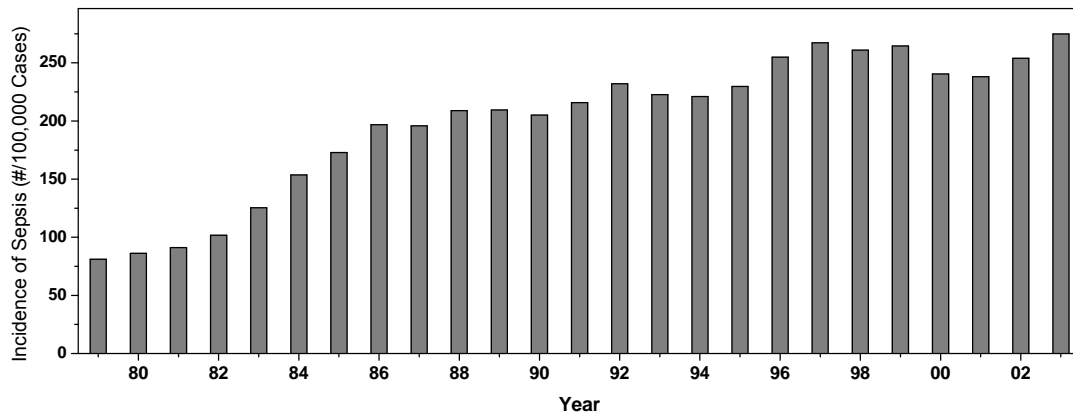


Figure 1. Incidence of Sepsis in the U.S. Data provided by Greg Martin.^{5,6}

The primary trigger in the gram-negative septic shock syndrome is endotoxin, a constituent of the outer membrane of all gram-negative bacteria. Endotoxins consist

of a polysaccharide portion and a lipid called lipid A, and are therefore also called lipopolysaccharides (LPS) (**Figure 2**).

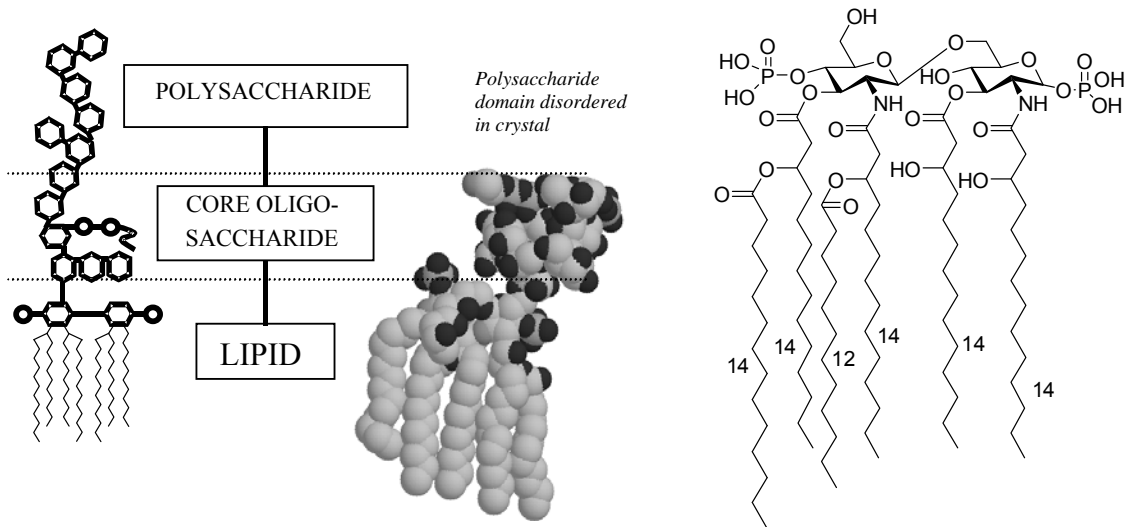


Figure 2. Schematic (*left*) and crystal structure (*middle*) of lipopolysaccharide (LPS). Shown on the right is the structure of enterobacterial lipid A.

The polysaccharide portion consists of an *O*-antigen-specific polymer of repeating oligosaccharide units, the composition of which is highly varied among gram-negative bacteria. A relatively well-conserved core hetero-oligosaccharide covalently bridges the *O*-antigen-specific chain with the structurally highly conserved lipid A^{8;9}. Lipid A is the active moiety of LPS^{9;10} and is composed of a hydrophilic, negatively charged bisphosphorylated diglucosamine backbone, and a hydrophobic domain of 6 (*E. coli*) or 7 (*Salmonella*) acyl chains in amide and ester linkages (**Figure 2**).¹¹⁻¹³

Whereas LPS itself is chemically inert, the presence of LPS in blood (endotoxemia), often a consequence of antibiotic therapy of preexisting bacterial infections, sets off a cascade of exaggerated host responses, which under normal,

homeostatic conditions serve to orchestrate innate immune defenses. It is the uncontrolled, overwhelming, and precipitous systemic inflammatory response that ultimately manifests clinically in the frequently fatal shock syndrome characterized by endothelial damage, coagulopathy, loss of vascular tone, myocardial dysfunction, tissue hypoperfusion, and multiple-system organ failure.¹⁴ LPS activates almost every component of the cellular and humoral (plasma protein) limbs of the immune system (**Figure 3**), resulting in the production of a plethora of proinflammatory mediators, important among which are the cytokines tumor necrosis factor α (TNF- α), interleukin 1 β (IL-1 β), and IL-6, secreted mainly by monocytes and macrophages (M ϕ).¹⁵ These cytokines and other mediators act in concert, amplifying the resultant

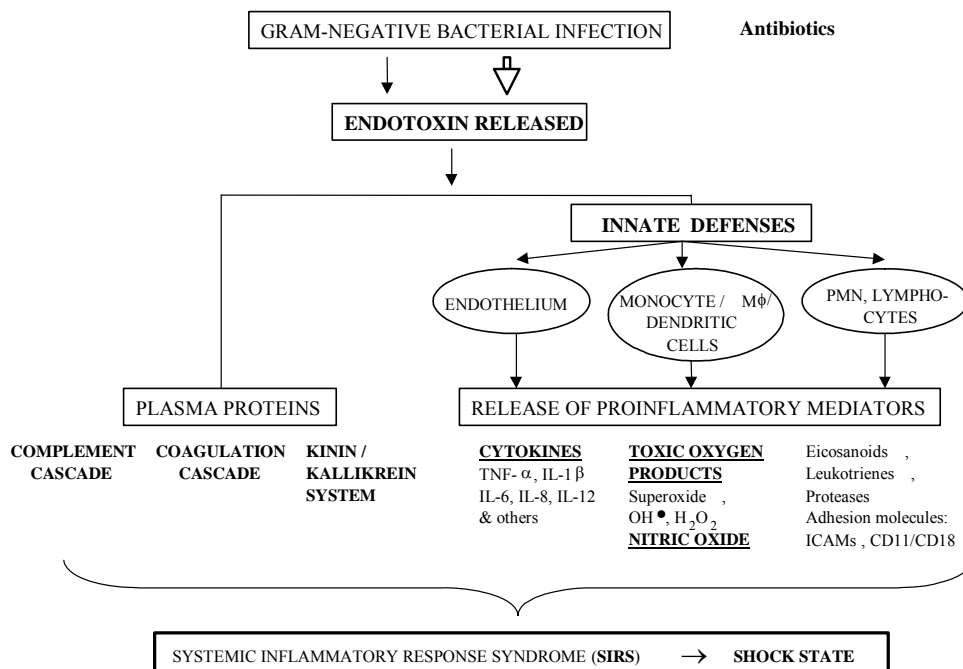


Figure 3. Schematic representation of immune activation by LPS

generalized inflammatory processes. Endotoxemia and its deleterious sequelae may arise even in the absence of systemic gram-negative bacterial infections; conditions such as trauma¹⁶, burns¹⁷, and splanchnic ischemia during cardiac surgery¹⁸ or gram-positive sepsis¹⁹ increase intestinal permeability, resulting in the spill-over into the portal circulation of LPS from the colon which is abundantly colonized by gram-negative bacteria.

Our understanding of basic mechanisms underlying the cellular response to LPS has increased vastly in recent years. Important research contributions include LPS recognition²⁰ by CD14²¹⁻²⁴ [and other cell surface recognition molecules]^{25;26} via an LPS-binding acute-phase plasma protein (LBP),²⁷⁻²⁹ initiation of signal transduction by toll-like receptor-4^{30;31}, and downstream cellular activation events mediated by mitogen-activated kinase p38 and c-Jun N-terminal kinase, leading to nuclear translocation of NF- κ B^{32;33-35} resulting in cytokine mRNA transcription. These advances will likely offer novel therapeutic possibilities in the future. However, after more than two decades of intensive effort at evaluating more than 30 investigational compounds, specific therapeutic options for sepsis have remained elusive. On June 29, 2000, Eli Lilly announced that favorable results had been obtained in Phase III clinical trials for Xigris™ (recombinant human activated protein C), an anticoagulant that targets a component of the humoral activation pathway and ameliorates disseminated intravascular coagulation. Clinical trials of recent years aimed at blocking various proinflammatory mediators including TNF- α , IL-1 β , platelet-activating factor, and prostaglandins produced by the activated cellular components

have all been disappointing³⁶ (**Figure 4**), suggesting that targeting downstream cellular inflammatory processes once immune activation has already progressed is unlikely to be of benefit.

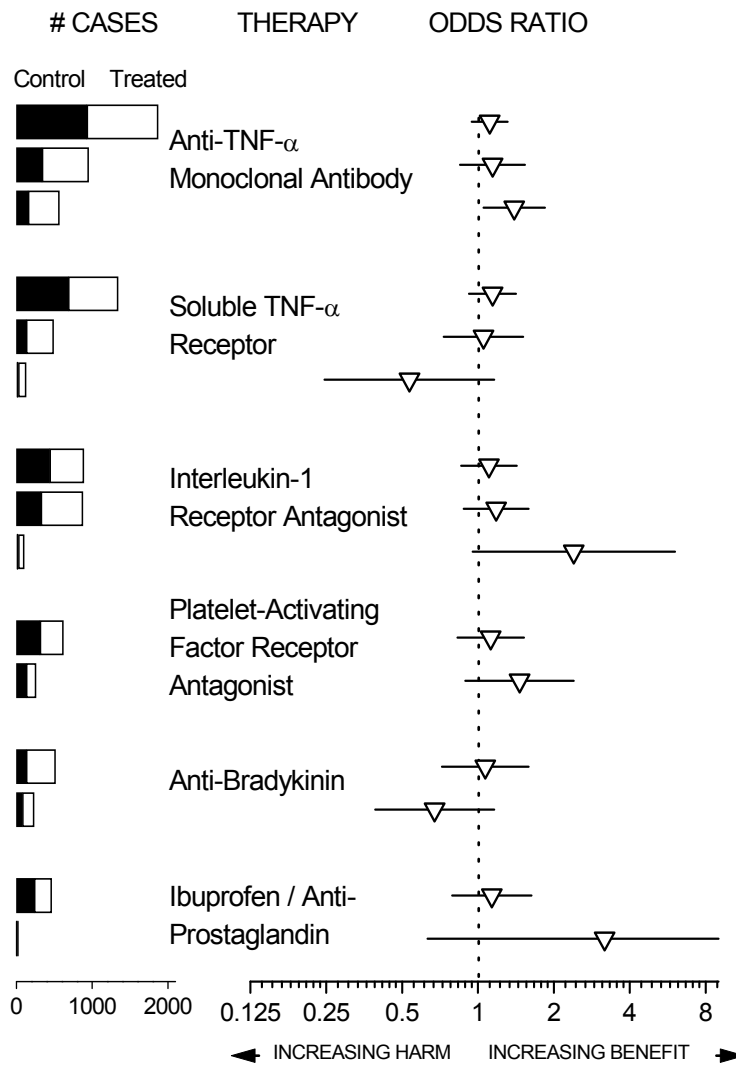


Figure 4. Outcomes of clinical trials of anti-inflammatory agents in sepsis. Adapted from Zeni *et al.*, 1997 (Ref. 37).

1.2 Complexation of LPS by Macromolecules as a Therapeutic Strategy.

1.2.1 Polyclonal and Monoclonal Antibodies: As mentioned earlier, the polysaccharide portion of LPS is extremely variable and serologically distinct for each strain of the same species of gram-negative organisms. Although anti-O-polysaccharide antibodies afford protection in experimental models where animals are challenged with homologous bacteria³⁷, these are not likely to be of significant clinical value since sepsis runs an acute course before the pathogen is identified and appropriate specific immunotherapy is instituted. The biologically active part of LPS, lipid A, as well as the core oligosaccharide portion are structurally highly conserved across gram-negative genera, and thus are attractive targets for sequestration, and elimination of circulating LPS would, in principle, prevent the activation of inflammatory cascades. Experimental studies as early as 1968 suggested that antibodies directed toward epitopes in the core region of LPS may be broadly cross-protective against a range of gram-negative organisms. However, neither human (HA-1A)³⁸ nor murine (E5)³⁹ anti-lipid A monoclonal antibodies afforded significant protection in large, multiple, placebo-controlled clinical trials.⁷ In the wake of these failures, it became apparent that these monoclonal antibodies had been expedited through clinical trials without rigorous preclinical evaluation. Both HA-1A and E5 exhibited low intrinsic binding affinities to LPS⁴⁰ ($<10^4 \text{ M}^{-1}$), neutralized LPS poorly, bound promiscuously to a wide range of hydrophobic ligands such as lipoproteins and cardiolipin, as well as to a variety of human B cell and erythrocyte proteins,⁴¹ and proved to be toxic in a canine model of septic shock. Although the validity of

circulatory LPS as a therapeutic target is still viable, and efforts at developing core region-directed antibodies continue^{42, 43} disappointing results obtained thus far could point to intrinsic problems with lipid antigens: poor immunogenicity, inaccessibility of neutralizing epitopes, the generation of nonspecific cross-reactive antibodies against irrelevant hydrophobic epitopes⁴⁴, and potential problems with the antibody molecule itself: predominant intravascular compartmentalization, and possible tissue damage induced by activation of complement. Other immunotherapeutic strategies include the blockade of LPS binding to CD14 (the predominant cell-surface receptor for LPS) with anti-CD14 antibodies^{45;46} or anti-LBP antibodies.⁴⁷

1.2.2 Non-Antibody LPS-binding Proteins: The approach of neutralizing LPS or preventing cellular recognition by its cognate receptor (s) using non-antibody protein macromolecules is being actively pursued⁴⁸, and notable developments in the area is bactericidal/permeability-increasing protein (BPI), a neutrophil azurophilic granule-derived, antibacterial protein involved in innate host defense.⁴⁹⁻⁵¹ On September 14, 2000, Xoma Inc. announced favorable results of rBPI₂₁ in preliminary clinical trials of severe pediatric meningococemia, and has since obtained an FDA Subpart E designation for Phase III trials. Further ongoing trials will likely provide valuable data on the clinical efficacy of LPS neutralization by large, protein macromolecules of a size (23kDa) that would not efficiently cross endothelial barriers into interstitial spaces.

1.3 The Paradigm of Non-immunologic Sequestration of LPS by Small Molecules

1.3.1 Polymyxin B: The structurally invariant and biologically active center of LPS, lipid A, is a logical therapeutic target for neutralization. The anionic amphiphilic nature of lipid A enables it to interact with a variety of cationic hydrophobic ligands.⁵²⁻⁵⁵ Polymyxin B (PMB), a cationic amphiphilic cyclic decapeptide antibiotic isolated from *Bacillus polymyxa*⁵³ has long been recognized to bind lipid A,⁵⁴ and neutralize its toxicity *in vitro* and in animal models of endotoxemia.^{55-56;57} PMB has served as a "gold standard" for endotoxin-sequestering agents and is routinely used in experimental studies when a biological effect is to be verified as that due to LPS, or to abrogate activity of contaminating LPS. Listed in the US Pharmacopeia as a topical antibiotic, PMB is too toxic for parenteral use, which, while precluding its utility as an LPS-neutralizer in patients with sepsis, has stimulated the search for nontoxic PMB analogs⁵⁸, PMB derivatives⁵⁹⁻⁶⁰ as well as other structurally diverse cationic amphiphilic peptides^{61;620}, as candidate LPS-binding agents which are yet to be evaluated in clinical trials. A cartridge based on polymyxin B covalently immobilized via one of its NH₂ groups to a polystyrene based fiber became available in Japan in late 2000 for clinical use ("Toraymyxin", Toray Industries Inc., Tokyo).⁶³⁻⁶⁶ While this provides a clinically validated proof-of-principle for the value of sequestering circulating LPS, opportunities for extracorporeal hemoperfusion are rare: the typical patient is often profoundly hypotensive, with circulatory failure, refractory even to maximal vasopressor and intravenous fluid therapy regimens, underlining the need to develop alternate strategies for LPS sequestration.

The solution structure of PMB has been determined both in its free, aqueous, (Figure 5) as well as LPS-bound states.^{67,68} The cyclic moiety of aqueous PMB in its

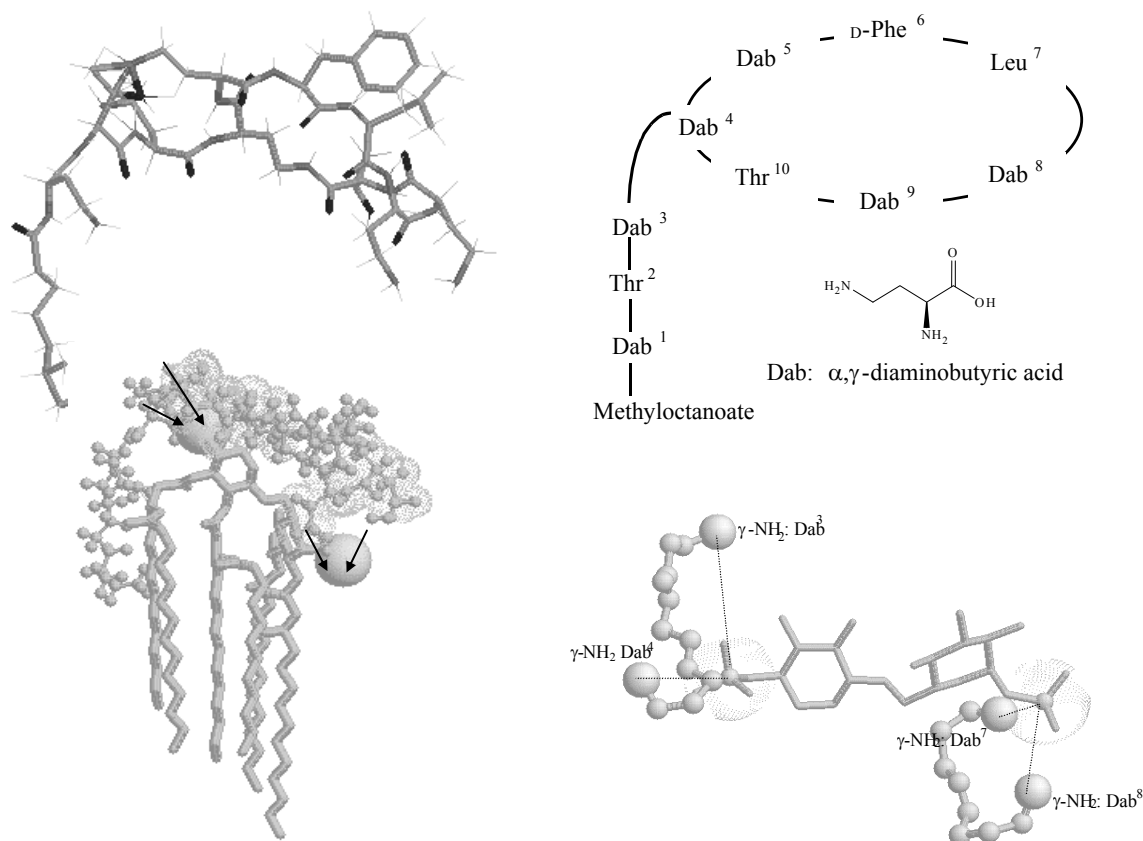


Figure 5. Solution structure (*top left*), primary structure of Polymyxin B (PMB) (*top right*), NMR-derived conformation of the lipid A: PMB complex (*bottom left*) Arrows indicate salt-bridges. The methyloctanoyl acyl moiety attached to Dab1 is oriented normal to the plane of PMB. *Bottom Right:* Detail showing bidentate ionic H-bonds (dotted lines) between Dab sidechain pairs of PMB and the phosphates of lipid A (only glycosidic backbone is shown).

unbound form is characterized by a type II' β -turn centered at D-Phe⁵, and a γ turn at Thr⁹ with no transannular H-bonds, features that are preserved also in the LPS-bound form. In the lipid A-PMB complex, (**Figure 5**) the carbonyl groups form a polar surface on one face of the cyclic portion which overlies the glycosidic hydrophilic backbone of lipid A, and the linear part, bearing the hydrocarbon chain, is parallel to the long axis of lipid A, and is apposed to the acyl chains of lipid A, the basis of the hydrophobic interaction of the peptide with LPS. The γ -NH₂ groups of pairs of the Dab residues (Dab³/Dab⁴ and Dab⁷/Dab⁸) form bidentate ionic H-bonds with the lipid A phosphates (**Figure 5**).

1.3.2 Structural correlates of affinity of LPS binding in nonpeptide small

molecules: A number of classes of cationic amphiphilic drugs already in therapeutic use were screened for lipid A binding and LPS neutralization, among them 4-aminoquinoline antimalarials, phenothiazine antipsychotics, biguanide hypoglycemics, the bis-diguanide antimicrobial, chlorhexidine, and the diamidine antiprotozoal, pentamidine. The criteria for selection of these classes was simply that these drugs were cationic amphiphiles.⁶⁹ It was noted from these early, exploratory studies that dicationic bolaamphiphiles such as pentamidine and chlorhexidine bound lipid A strongly with apparent K_d values of 0.12 and 0.87 μ M, respectively, the K_d for PMB, the reference compound being 0.37 μ M (**Figure 6**). The bisguanidine, chlorhexidine, bound lipid A with an affinity about 80 times that of the monobiguanides, metformin and phenformin, and the K_d of pentamidine was greater

than that of PMB (**Figure 6**). Both compounds antagonized LPS activity in the *Limulus* (horseshoe crab) amoebocyte lysate gelation assay, an extremely sensitive *in vitro* test with a detection limit of 1 ng/mL of uncomplexed, bioactive LPS.⁶⁹ This was the first indication that the presence of two basic groups separated by a distance could be a correlate of high binding affinity.

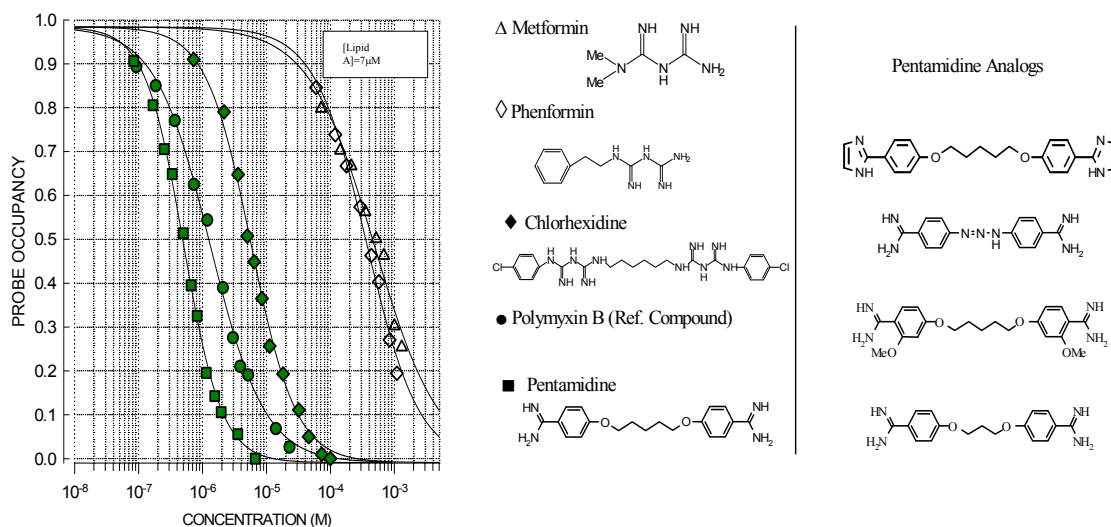


Figure 6. Left: Affinity of cationic amphiphilic drugs toward lipid A measured by DC displacement. Legends (and corresponding structures) are shown right of graph. **Right:** Analogs of pentamidine: imidazolino-pentamidine, berenil, methoxy-pentamidine, propamidine (top to bottom). The affinity of all these analogs was identical to that of pentamidine.

1.4 Structural Correlates of LPS Binding and Neutralization.

1.4.1 Elucidation of the pharmacophore for lipid A binding: The amidinium (pentamidine) and guanidinium (chlorhexidine) groups are also strongly basic protonatable functions (see **Figure 6**) and it was therefore of interest to systematically examine the effect of varying inter-cationic distance and basicity (pK) of the cationic

groups in model dicationic molecules.⁷⁰ α, ω -Diaminoalkanes, the polyamines spermidine and spermine and their derivatives constituted a set of simple, linear molecules with inter-NH₂ distances ranging between 5-16 Å (obtained by molecular modeling assuming extended conformations); N¹- and N⁸-monoacetylated spermidine, and N⁴-benzylspermidine were used to test the importance of two cationic functions, and the possible role of bulky, hydrophobic nonterminal substituents, respectively. Comparisons of spermidine and N¹, N⁸-diguanospermidine (synthesized from spermidine using *O*-methylisourea) allowed the exploration of the hypothesis that basicity impacted upon augmented binding affinity. Pentamidine analogs shown in **Figure 6** constituted another set of molecules with varying inter-cationic distance (Berenil: 12.82 Å - Pentamidine: 19.56 Å). The electron-donating methoxy group *ortho* to the amidinium function decreases its pK, and the imidazolino group is considerably less basic than the amidinium group (**Figure 6**). In brief, the findings were: (a) The affinities of N¹- or N⁸-monoacetylated spermidine were about 1/80th of spermidine, indicating that the presence of two cationic functions corresponded to enhanced affinity; (b) the affinity of 4-benzylspermidine toward lipid A is about 2.4 times less than that of spermidine suggesting that nonterminal bulky "pendant" groups may sterically hinder complexation; (c) a distinct sigmoidal relationship between intercationic distance and affinity toward lipid A was observed, with a sharp increase from 11Å, leveling off at about 13Å (**Figure 7**). This coincides, within experimental error, to the inter-phosphate distance in energy-minimized models of lipid A, and in the crystal

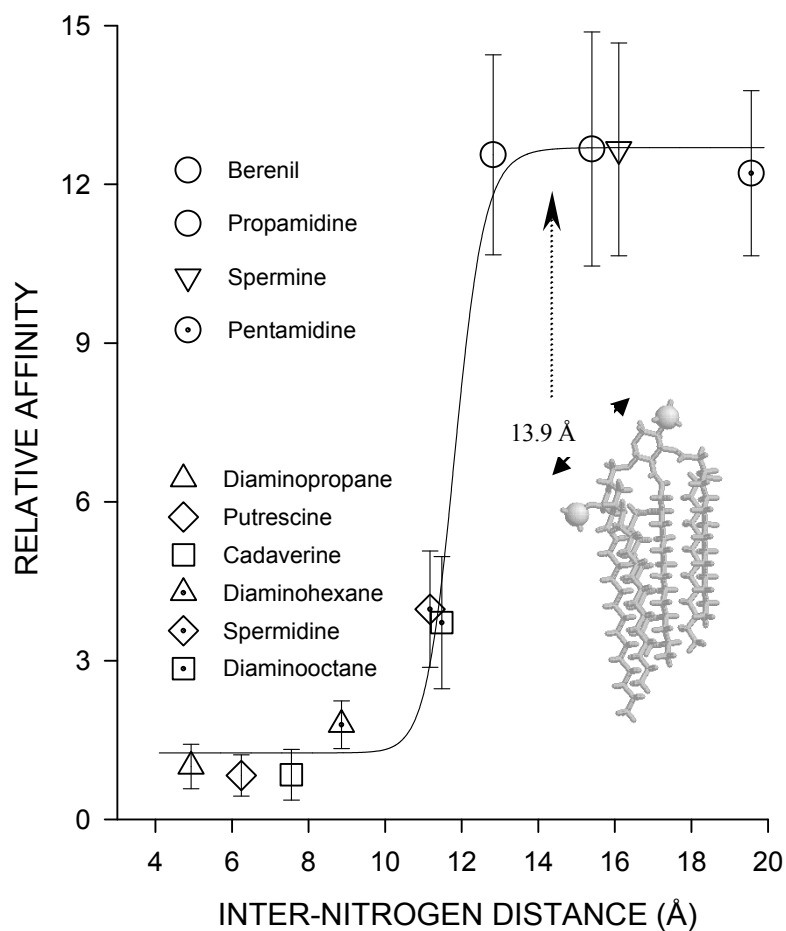


Figure 7. Relationship between inter-nitrogen distance of α,ω -diaminoalkanes, polyamines, and bisamidines, and binding affinity to lipid A. The inflection point of the sigmoidal curve coincides with the inter-phosphate distance of lipid A (inset). Relative affinity is represented as fold affinity w.r.t. diaminopropane.

structure of LPS (13.9Å); (d) pentamidine, and its methoxy- and imidazolino-analogs bound lipid A with identical affinity, as did spermidine and N¹, N⁸-diguanidospermidine, indicating that the pK of the terminal cationic function is not critical in determining binding affinity. However, the electrostatic interactions of cationic ligands with lipid A or LPS appear to mandatorily require the formation of

ionic H-bonds (salt-bridges) since several compounds with quaternized polyamidinium functionalities did not bind endotoxin (data not shown).

The pseudo-bichromophoric nature of pentamidine (see structure in **Figure 6**) ascribes unique photophysical properties, which were exploited in characterizing the mode of binding and nature of the drug-lipid A complex.⁷⁰ Upon binding of pentamidine to lipid A [and not to other polyanions such as DNA⁷¹ that the drug is known to bind to], a unique emission band appears in the fluorescence spectrum which was ascertained to be due to inter-molecular excimer formation⁷⁰, a consequence of the unique geometry and orientation of the chromophores in the pentamidine-lipid A complex. Under conditions when lipid A is completely monomeric (in CHCl₃/MeOH) pentamidine binds specifically to diphosphoryl, and not to monophosphoryl lipid A, with a 1:1 stoichiometry, indicating the bisamidine simultaneously recognizes the two anionic phosphates on the ends of the glycosidic backbone of lipid A⁷⁰ (data not shown). The recognition of the phosphate group by the amidine is not sensitive to the specific orientation of the glycosidic 1-phosphate (which is thought to be an important determinant of biological activity of lipid A)⁸ since both the α - and β -anomeric forms of phosphonoxyethyl analogs of synthetic lipid A [provided by S. Kusumoto⁷²] are bound by pentamidine (data not shown). The interaction of the drug with the toxin is almost exclusively electrostatically driven, with negligible hydrophobic components, and is dependent on the ionization state of both the amidine and the phosphate, since protonation of either the lipid A phosphates (pH<5) or deprotonation of the amidinium groups of the drug (pH>10) results in

destabilization of the complex (data not shown). An energy-minimized model of the pentamidine: lipid A complex, derived from extensive biophysical characterization of the interactions is represented in **Figure 8**, showing the orientation of the drug with respect to lipid A, and the salt-bridges between the lipid A phosphate and the amidines. The model facilitates the consideration of possible sites of introducing sterically favorable hydrophobic groups that would be expected to enhance the entropic contributions of the free energies of interaction.

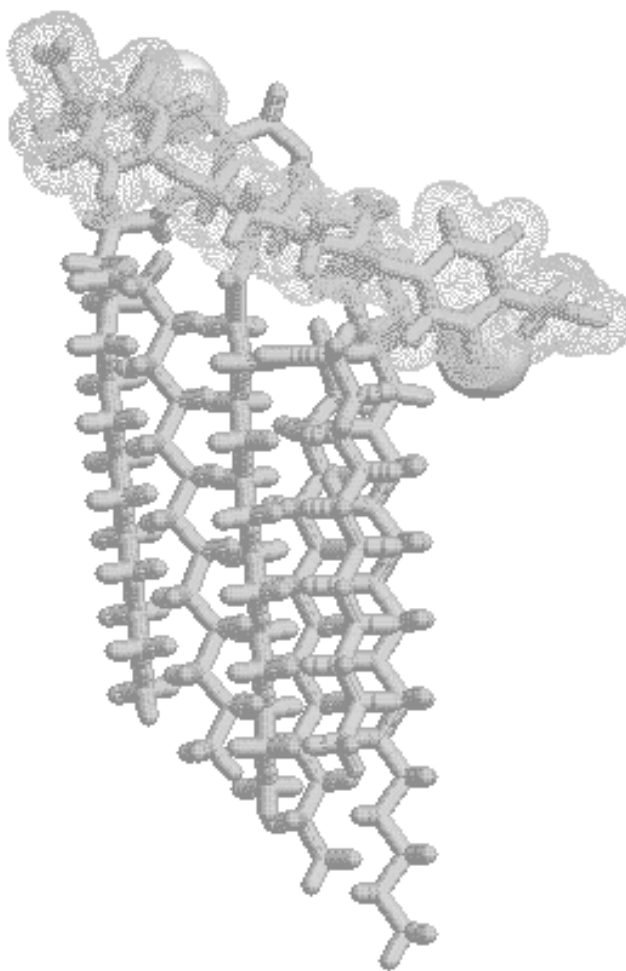


Figure 8. Model of the pentamidine (van der Waals surface): *bis*-phosphoryl lipid-A complex (sticks). The P atoms of lipid A are space-filled.

1.4.2 Lipid A binding is necessary, but not sufficient for LPS neutralization: That the recognition of LPS and subsequent binding by LPS-binding molecules does not necessarily result in inhibition of endotoxic activity can be adduced from the literature. For instance, LPS-binding protein (LBP)²⁷, an acute phase-reactant plasma protein synthesized by the liver under conditions of stress⁷³, and the neutrophil granule-derived bactericidal/permeability increasing protein (BPI) are highly homologous in their sequences^{74;75} and bind LPS competitively⁷⁶ with comparable affinities. Yet, whereas LBP "opsonizes" LPS⁷⁷, and presents it to CD14^{78;79} initiating LPS-induced cellular activation processes⁸⁰, the binding of BPI to LPS results in neutralization of endotoxic activity.^{81;82} Attempts at understanding the structural basis of this important functional difference led to the elucidation of high-resolution crystal structures of BPI⁸³ and a *Limulus* (horseshoe crab) endotoxin binding protein⁸⁴ (ENP).^{85;86} Another pertinent example is that of polymyxin B (PMB). It has been known for about a decade⁸⁷ that polymyxin nonapeptide (PMN), with a single fatty acyl-Dab residue removed from its decapeptide parent molecule is virtually bereft of endotoxin-neutralization activity. PMB and PMN bind lipid A and LPS with identical affinities, and behave indistinguishably in a variety of spectroscopic assays designed to probe ligand-induced fluidity changes of the acyl domains of lipid A, bilayer-to-nonlamellar phase transitions, and neutralization of the electrostatic double layer of lipid A or LPS aggregates.⁸⁸ These data, taken together, point to the importance of stabilization of ligand-LPS complexes by hydrophobic interactions, a premise which has been examined for PMB using techniques such as surface plasmon resonance⁸⁹

and titration calorimetry.⁹⁰ The lack of comparison, however, for PMB and PMN in these studies^{90;91} has not yet permitted a complete and formal verification.

Pentamidine is an excellent case in point illustrating the binding is necessary, but not sufficient for neutralization. Whereas it binds LPS with an affinity even greater than that of PMB, only feeble inhibition of cytokine (Tumor Necrosis Factor- α ; TNF- α) release from LPS-stimulated human mononuclear cells was observed (**Figure 9**) and did not protect mice against lethal doses of LPS.

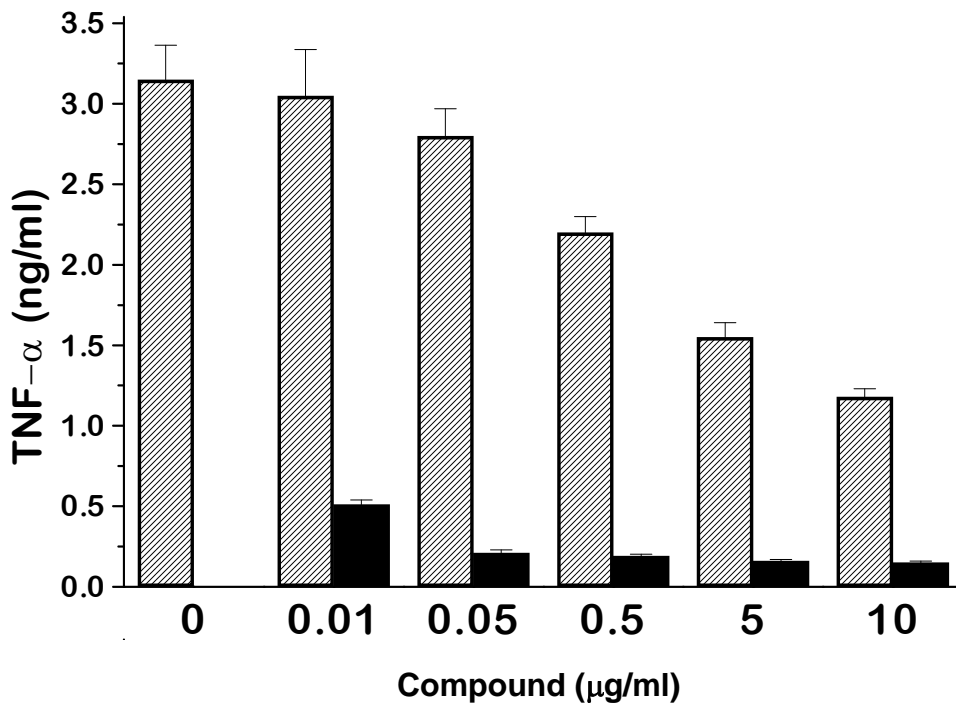


Figure 9. Inhibition of TNF- α in LPS (10 ng/mL)-stimulated human PBMC by pentamidine (hatched bars) and polymyxin B (solid bars). Note that inhibition by pentamidine is partial even at the highest concentration (10 μ g/ml)

1.4.3 Structural correlates of neutralization of endotoxicity. The obligatory requirement of a hydrophobic moiety: Having identified that the presence of two protonatable cationic groups positioned about 14 Å apart in a linear molecule was sufficient to ascribe high-affinity binding to LPS, and an additional hydrophobic moiety was necessary for the binding to result in neutralization of endotoxic activity (sequestration), experiments using the polyamines, spermidine (~ 11 Å; sub-optimal length), spermine (~16 Å, optimal length), and their monoacylated analogs⁹² (**Figure 10**) were performed. Spermine was inactive while the acylated polyamines inhibited TNF- α release in a dose-dependent manner, the longer homologated spermine analog (Compound **B**) being more active than the monoacylated spermine analog [one terminal protonatable amine function is lost] (Compound **A**, **Figure 10**) confirming the necessity of optimal intercationic distance (see **Figure 7**). These results provided

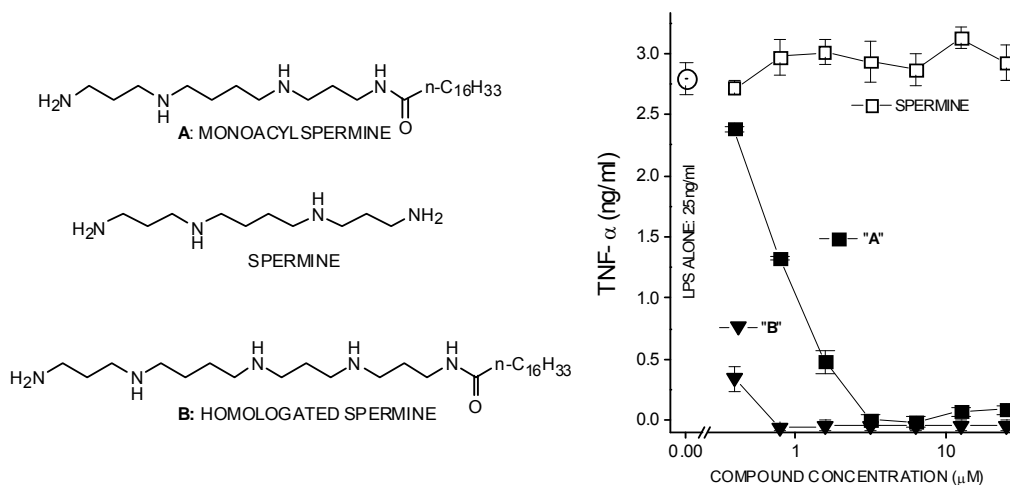


Figure 10. Structures of acylpolyamines (left), and inhibition of TNF- α induction in J774 cells stimulated with 25 ng/mL LPS (right). Essentially identical results were obtained with RAW cells. Similar inhibition profiles were obtained in nitric oxide (measured as nitrite) assays.

clear structural leads in efforts to recognize simple molecules that would behave as endotoxin sequestrants, and importantly, led to the identification of the pharmacophore for LPS-sequestration.

1.5 Lipopolyamines as Lead Compounds for Development of LPS Sequestrants.

The structural features that we had identified to be important in conferring LPS-sequestering properties are to be found in lipopolyamines, members of a burgeoning class of cationic lipid molecules designed to facilitate transfection of DNA into eukaryotic cells, now receiving increasing attention because of interest in human gene therapy.^{93-94;95} These molecules are of particular interest since they are designed to be of low toxicity to mammalian cells, and are being approved by the FDA for human use as safe alternatives to viral vectors.^{96-97;98}

Our proposal of evaluating lipopolyamines as potential endotoxin sequestering molecules was based on two simple heuristics which had been experimentally validated:

Heuristic 1: An optimal distance of ~ 14 Å is necessary between protonatable functions in *bis*-cationic molecules for simultaneous ionic interactions with the glycosidic phosphates on lipid A, it is the *bis*-cationic scaffold that is the principal determinant of binding affinity (**Figure 7**).^{99;100}

Heuristic 2: Binding is necessary, but not sufficient for activity, and an additional, appropriately positioned hydrophobic group is obligatory for the interaction to manifest in neutralization of endotoxicity.^{101;102}

For the sake of brevity, salient aspects of key structure-activity relationships in one homologous series of twelve mono- and *bis*-acyl homologated spermine analogs (**Figure 11**) will be first discussed.¹⁰³

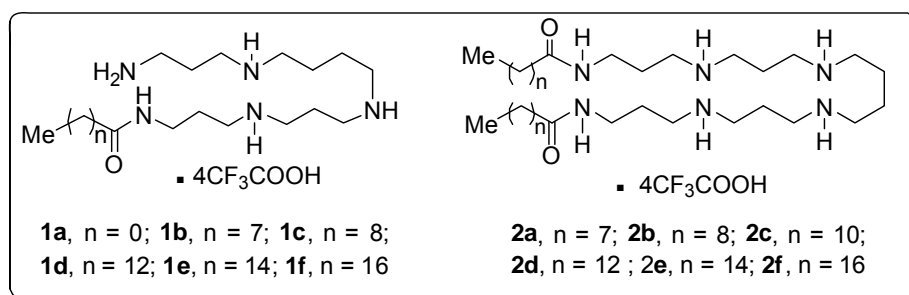


Figure 11. Structures of mono- and *bis*-acyl polyamine analogs.¹⁰⁵

Two questions were addressed in this study: (i) what is the optimal hydrophobic chain length for effective anti-endotoxic activity, (ii) are symmetrical *bis*-acyl spermines more effective than mono-acyl compounds. It was found that a carbon number of 14-16 was optimal in mono-acyl spermines (**Figure 12**) which were in general, as potent as their *bis*-homologs and, in addition, showed lower surface activity (lower nonspecific cytotoxicity).

In comparing the NO and TNF- α inhibition profiles with the LPS-binding affinities for this congeneric series, with the exception of **1a**, all of the other mono-acyl compounds bound LPS with ED₅₀ values between ~1-2 μ M, while only the longer acyl chain compounds (**1d-f**) were biologically active (**Figure 12**). This result emphasized the necessity of employing a biological primary screen in tandem with the displacement assay in order to derive reliable structure-activity relationships in

LPS-sequestering compounds. The apparent inverse correlation between ED_{50} and neutralization potency for the *bis*-acyl **2** series was simply a consequence of the poor solubility of these homologues. Free aqueous concentrations of the *bis*-acyl compounds were progressively retarded with increasing chain length, diminishing binding and, consequently, neutralization (**Figure 12**). The protective effects of **1e** (the most potent compound in the human TNF- α inhibition assay), **2a** (most active in inhibiting NO release in J774A.1 cells), and **2c** (which was of lower potency than either **1e** or **2a** in both assays) were characterized in a murine model of endotoxemic

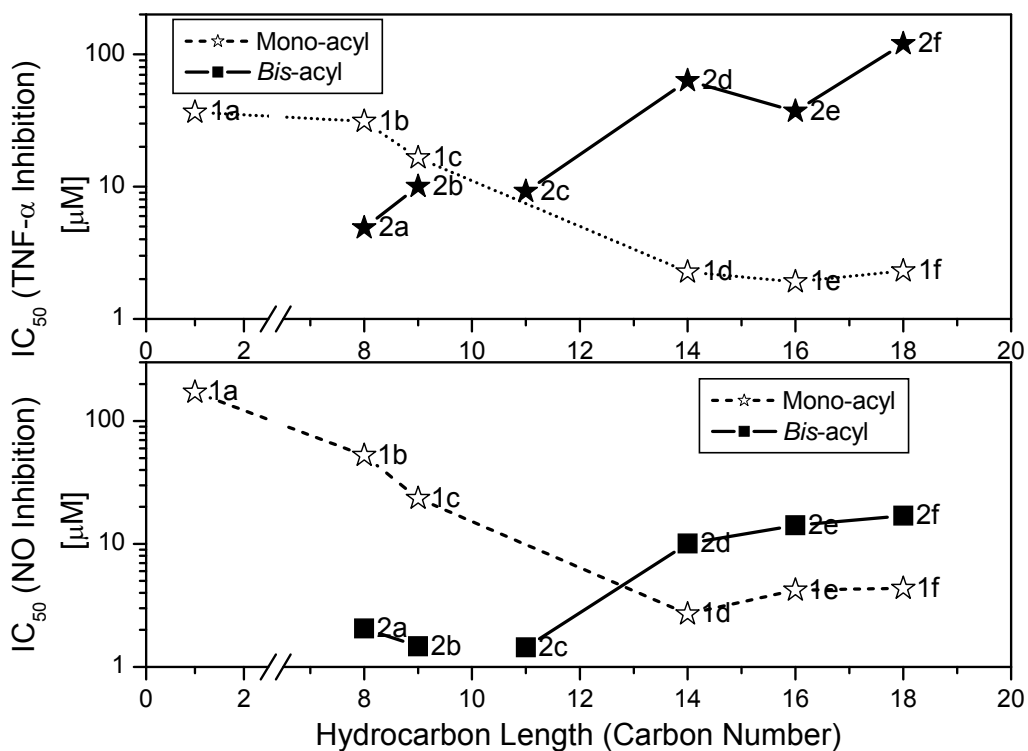


Figure 12. Correlation between carbon number of the hydrocarbon group in mono- (open stars, dotted line) and *bis*-acyl (closed stars, solid line) and TNF- α inhibition in human blood (top) and NO inhibition in murine J774A.1 cells (bottom). Data represent means of duplicate values obtained from a representative experiment.

sepsis. A supralethal dose (2X the dose causing 100% lethality) of 200 ng/mouse of LPS was administered intraperitoneally (i.p.) and separate i.p. injections of graded doses of compound were injected, and lethality was observed at 24 h. As is evident from **Table 1**, a clear dose-response was observed, with **1e** affording complete protection at the 100 or 200 $\mu\text{g}/\text{mouse}$ dose, and partial protection at the 50 μg dose. Both the *bis*-compounds were found to be inferior to **1e**, suggesting that *in vitro* inhibition of TNF- α was correlated better with outcomes in *in vivo* animal models of sepsis.

Compound Dose (μg / mouse)	Compound		
	1e	2a	2c
200	0/5*	1/5*	1/5*
100	0/5*	4/5	2/5
50	2/5	5/5	4/5
10	5/5	5/5	4/5
0	5/5	5/5	5/5

Table 1. Dose-dependent protection of CF-1 mice challenged with a supralethal dose of 200 ng/mouse of LPS (LD_{100} = 100 ng) by the acylhomospermines in cohorts of five animals. Lethality was recorded at 24 h post-challenge. Ratios denote dead/total. Asterisks indicate statistically significant values, $p < 0.05$.

Chapter 2

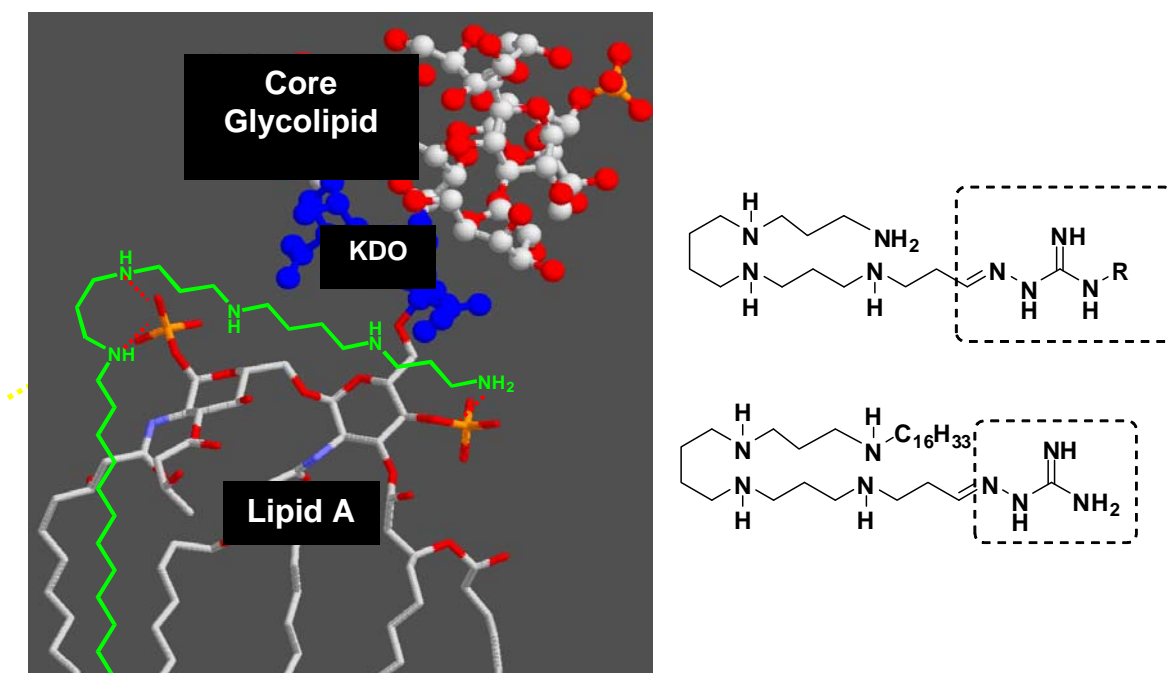
Structure-Activity Relationships of Lipopolysaccharide Sequestration in Guanyldiazide-bearing Lipopolyamines

2.1 Introduction and Rationale.

Our identification of the lipopolyamines as potential endotoxin-sequestering molecules was based on two simple heuristics that have been experimentally tested and validated^{99;100;103-106}: (a) an optimal distance of ≈ 14 Å is necessary between protonatable functions in linear *bis*-cationic molecules for simultaneous ionic interactions with the anionic phosphates on lipid A (**Figure 13**), and (b) additional, appropriately positioned hydrophobic group(s) are obligatory for the interaction to manifest in neutralization of endotoxicity. Leads obtained from high-throughput screening on focused libraries¹⁰⁷⁻¹⁰⁹ as well as from molecular modeling and *in silico* docking studies¹¹⁰ suggested that a long-chain alkyl, rather than an acyl group that we had previously characterized¹⁰³ may allow for more favorable electrostatic interactions with the lipid A phosphate groups. Independent SAR leads obtained in iterative rounds of screening focused libraries^{104;108;111-115} have all converged on molecules bearing a homologated spermine (homospermine) scaffold. However, we had identified in such screens several guanyldiazides as potent LPS binders.¹⁰⁸ We were desirous of (i) determining if the SAR pertaining to the hydrophobic substituent derived for the acylpolyamines¹⁰³ would also hold for molecules with similar

homospermine scaffolds grafted with guanyldrazone functionalities, (ii) if the presence of the guanyldrazone functionality would afford greater LPS sequestration potency owing to reasons mentioned earlier, and (iii) if *N*-alkyl versus unsubstituted guanyldrazone compounds would manifest in differential endotoxin neutralization activities due to possible steric effects. In order to examine these questions, I synthesized a congeneric set of guanyldrazone analogues (**Figure 13**).

Figure 13. *Left:* Molecular model of a mono-homologated, mono-alkyl polyamine docked on LPS, showing bidentate ionic H-bonds with the lipid A phosphate groups and the external amines, as well as the carboxylates of the KDO sugars of the core-glycolipid, with the internal amines. *Right:* Structures of designed series of compounds bearing guanyldrazone functionalities.



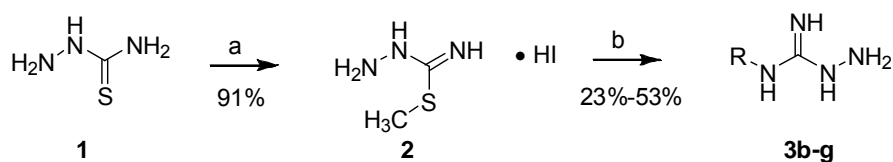
2.2 Syntheses of Compounds Bearing Alkylguanylhydrazone on One End and a Free Amino Groups at the Other Terminus.

The syntheses of the **8** series involved a straightforward condensation of either commercially-available aminoguanidine **3a** or *N*-alkylhydrazinecarboximidamides **3b-g** with the *N*¹,*N*²,*N*³,*N*⁴-tetraBoc-protected spermine-propanal precursor (**6**). *N*-alkylhydrazinecarboximidamides were synthesized via *S*-methylation of hydrazinecarbothiamide, followed by displacement with the corresponding alkylamine (**Scheme 1**). *N*¹,*N*²,*N*³-triBoc-protected spermine **4**, synthesized as reported earlier^{103;113;114} was *N*-alkylated with 3-bromopropan-1-ol, and the secondary amine was Boc-protected in a one-pot procedure. The alcohol **5** was then oxidized to the corresponding aldehyde **6**. The protected guanylhydrazone derivatives **7a-g** were obtained in good yields via condensation of **6** with **3a** (aminoguanidine) or **3b-g**. The Boc groups were finally deprotected with TFA to afford the target compounds as orangish-yellow solids (**Scheme 2**).

2.3 Synthesis of Analog Bearing an *N*-alkyl Substituent on One End and an Unsubstituted Guanylhydrazone at the Other Terminus.

The synthesis of **14** (**Scheme 3**), bearing an *N*-alkyl substituent on one end and an unsubstituted guanylhydrazone on the other terminus was carried out starting from *N*¹,*N*²,*N*³,*N*⁴-tetraBoc-protected spermine (**9**). *N*-Alkylation with *n*-C₁₆H₃₃I was carried out in the presence of NaH; the mono *N*-alkylated precursor **10** was isolated and subjected to *N*-alkylation on the other terminus with 3-bromopropoxy-*tert*-

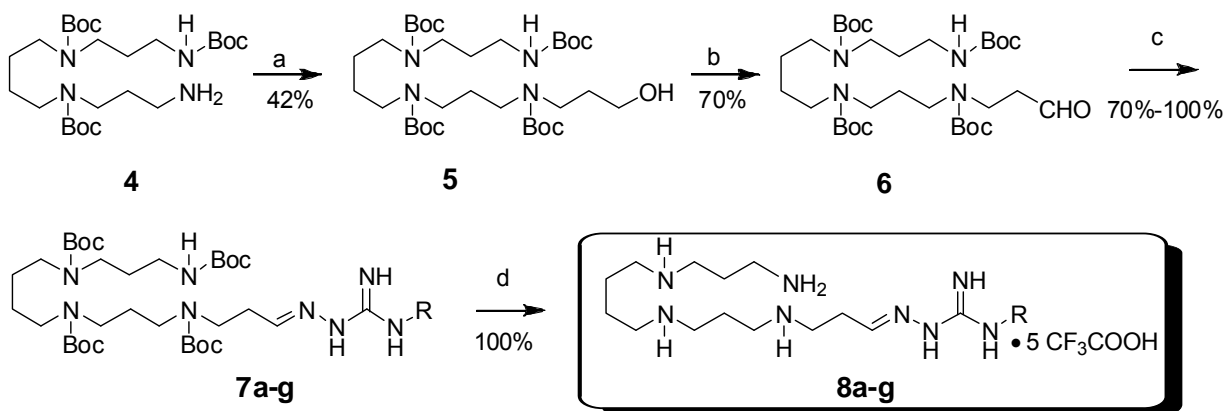
Scheme 1



Reagents and conditions: a. MeI, EtOH, 60 °C, 30 min;
 b. R-NH₂, EtOH, reflux, 1.5 h.

R= H	3a (commercially available)
R= C ₈ H ₁₇	3b
R= C ₁₀ H ₂₁	3c
R= C ₁₂ H ₂₅	3d
R= C ₁₄ H ₂₉	3e
R= C ₁₆ H ₃₃	3f
R= C ₁₈ H ₃₇	3g

Scheme 2



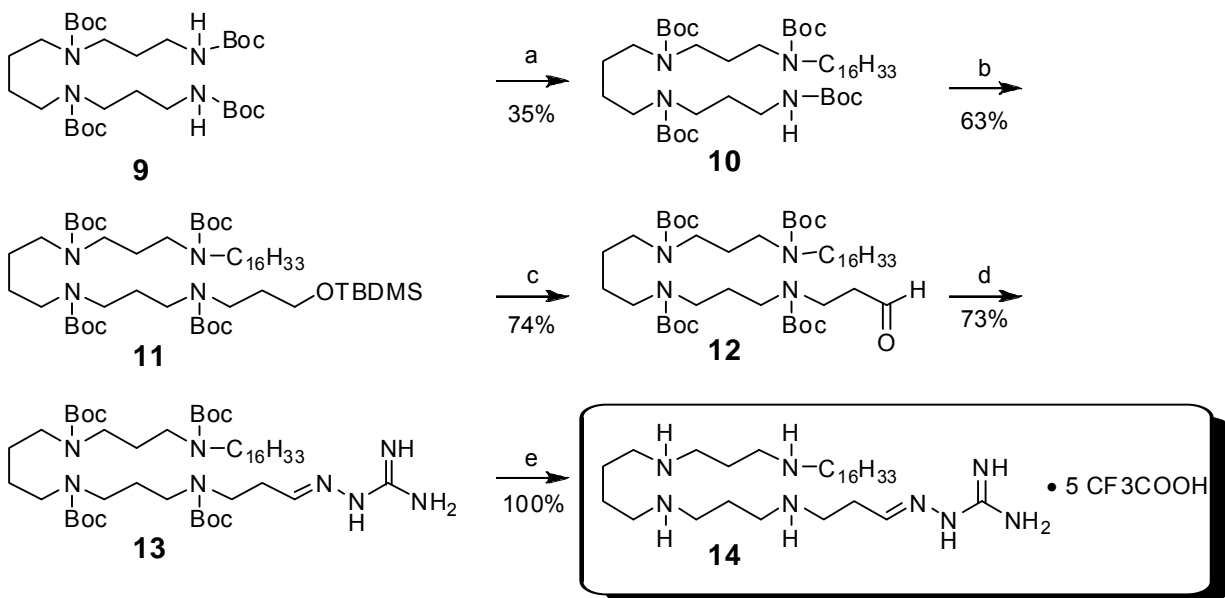
R= H	7a
R= C ₈ H ₁₇	7b
R= C ₁₀ H ₂₁	7c
R= C ₁₂ H ₂₅	7d
R= C ₁₄ H ₂₉	7e
R= C ₁₆ H ₃₃	7f
R= C ₁₈ H ₃₇	7g

R= H	8a
R= C ₈ H ₁₇	8b
R= C ₁₀ H ₂₁	8c
R= C ₁₂ H ₂₅	8d
R= C ₁₄ H ₂₉	8e
R= C ₁₆ H ₃₃	8f
R= C ₁₈ H ₃₇	8g

Reagents and conditions: a. (i) 3-bromopropan-1-ol, K₂CO₃, DMF, 60 °C, 24 h;
 (ii) Boc₂O (excess), MeOH, r.t., 12 h;
 b. PCC, DCM, r.t., 4.5 h;
 c. aminoguanidine (**3a**) or **3b-3g**, CH₃COOH (cat.), EtOH, 85 °C, 2 h;
 d. CF₃COOH, r.t., 30 min. The pentatrifluoroacetate salt form is assumed.

butyldimethylsilane. Sequential deprotection of the TBDMS (*tert*-butyldimethylsilyl) group, oxidation of the resultant alcohol to the aldehyde, condensation with aminoguanidine and finally, deprotection with TFA yielded **14** in 12% overall yield.

Scheme 3



Reagents and conditions: a. $C_{16}H_{33}I$, NaH, DMF, 0 °C-r.t., 20 h;
 b. 3-bromopropoxy-*tert*-butyl-dimethylsilane (excess), NaH, DMF, 0 °C-r.t., 20 h;
 c. (i) TBAF (1 M in THF), 2 h; (ii) PCC, DCM, r.t., 4.5 h;
 d. **3a** (aminoguanidine), CH_3COOH (cat.), EtOH, 85 °C, 2 h;
 e. CF_3COOH , r.t., 30 min. The pentatrifluoroacetate salt form is assumed.

2.4 LPS Sequestration Activities of the Guanylhydrazone Compounds.

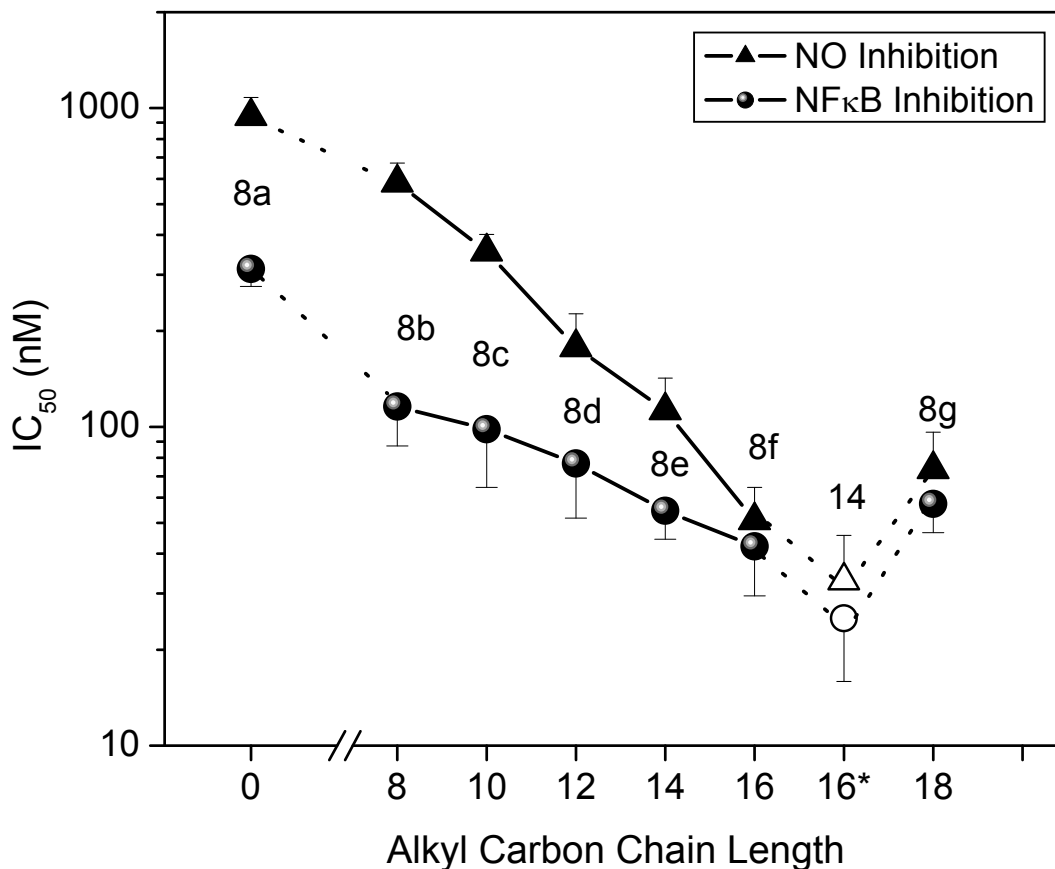


Figure 14. Comparison of activities of the guanylhydrazone compounds according to the IC₅₀ of NF-κB and NO inhibition.

As mentioned earlier, several guanylhydrazones had been identified in rapid-throughput screens in focused libraries as potent LPS binders.^{108;116} Guanidines and, by extension, guanylhydrazones, are thought to interact with phosphate groups very favorably via bidentate H-bonds by virtue of their planar geometry and multiple H-bond donor N-atoms (the ‘arginine fork’ principle¹¹⁷), which is not possible in the case of simple primary amines that constitute the cationic termini of the compounds

that we have hitherto characterized.^{103;104;113;114;118} Since virtually all of our screening results point to superior LPS recognition by homospermine scaffolds, one of the research objectives was to ‘graft’ guanylhydrazone functionalities on such a scaffold. It was of interest to examine if substantial differences in activities would be apparent in compounds with an *N*-alkylated guanylhydrazone functional group on one end and a free primary amine on the other or, conversely, an unsubstituted guanylhydrazone on one terminus, and an *N*-alkylated secondary amine on the other.

In the NF- κ B reporter gene assay performed in TLR4-expressing HEK cells, a distinct enhancement in LPS-neutralizing potency with increasing alkyl chain lengths in the **8** series of compounds was observed, with the optimal chain length being hexadecyl (**8f**); this SAR is virtually identical to that observed with the acylhomospermine compounds that we had examined earlier,¹⁰³ which suggests that a C₁₆ hydrocarbon chain is optimal for maximal interactions with the polyacyl domain of lipid A.¹¹⁹ The activity of compound **14**, also with a hexadecyl substituent on the terminal amine rather than on the guanylhydrazone, was no different than that of **8f** within the limits of statistical significance (**Figure 14**). This would appear to indicate that long-chain substituents on the cationic termini do not adversely affect Coulombic interactions with the lipid A phosphates.

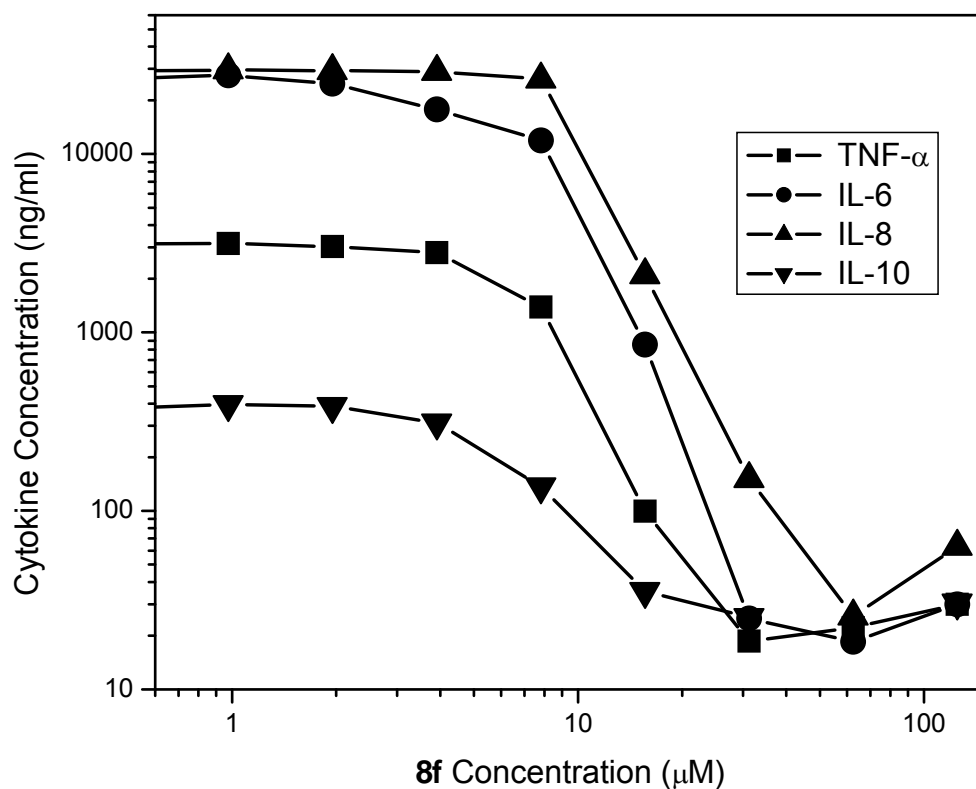


Figure 15. Inhibition by **8f** of LPS-induced proinflammatory cytokine production in human blood measured by multiplexed cytometric bead array assay. Results of a single representative experiment is shown.

8f Dose (μg / mouse)	Lethality in CF-1 Mice (alive/total)
200	0/5*
100	1/5*
50	2/5
0	5/5

Table 2. Dose-dependent mice lethality assay of **8f** on mice.

Given the minor differences in potency between **8f** and **14**, we elected to characterize **8f** in greater detail because of a higher toxicity for **14** in *in vitro* cellular assays (data not shown). As expected, **8f** inhibits, in a dose-dependent manner, LPS-induced proinflammatory cytokine production in whole human blood *ex vivo* (**Figure 15**); the IC₅₀ values in human blood are considerably higher than in the NF-κB assay perhaps due to the fact that these compounds are bound to albumin strongly (work in progress) and albumin concentrations abound in the milieu of whole blood. Compound **8f** also affords dose-dependent protection against lethal endotoxemic challenge in a murine model (**Table 1**), as we have observed with acylhomospermines.¹⁰³

2.5 Conclusions.

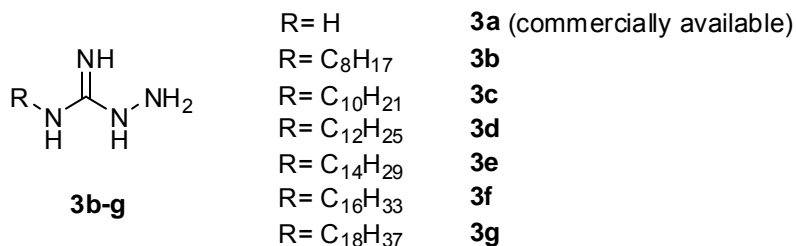
We find that, as for the acylhomospermine compounds, the C₁₆ alkyl chain is optimal in the *N*-alkylguanyldrazone series; a homospermine analogue with the terminal amine *N*-alkylated with a C₁₆ chain with the other terminus of the molecule bearing an unsubstituted guanyldrazone moiety is marginally more active suggesting very slight, if any, steric effects. Neither C₁₆ analogue is significantly more active than the *N*-C₁₆-alkyl¹¹⁴ or *N*-C₁₆-acyl¹⁰³ compounds that we had characterized earlier, indicating that a primary amine serves just as well as a guanyldrazone in recognizing the lipid A phosphate groups.

It was of particular interest to examine if **8f** with its considerably higher pKa than an amine, planar geometry and multiple H-bond donor atoms, would be more potent than the *N*-acyl¹⁰³- and *N*-alkyl¹¹⁴ homospermine leads that are currently in preclinical development. Although much to our disappointment, no discernible differences in potency between these compounds in a battery of *in vitro* as well as animal experiments (data not shown) were observed, these results are, nonetheless, instructive in that they indicate that basicity of the terminal cationic functionality, *per se*, is not a determinant of LPS-sequestering activity, and that no increments in activity are to be gained by incorporating strongly basic functional groups. Indeed, preliminary acute toxicity studies in rodents indicate that **8f** is considerably more toxic than the aforementioned homospermine leads. These data, collectively, have now led us to consider the exploration of analogues with multiple electron-donating groups placed adjacent to the amines on the scaffold; such compounds are expected to be considerably less basic.

2.6 Experimental Data.

2.6.1 Experimental Procedures

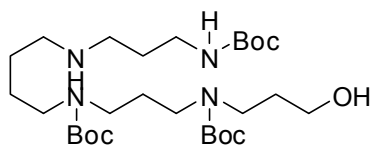
2.6.1.1 Syntheses of compounds bearing alkylguanylylhyrazone on one end and a free amino group at the other terminus:



General Procedure for the Syntheses of Compounds **3b-g**.¹²⁰

A solution of hydrazinecarbothioamide (**1**; 20.0 g, 219.4 mmol) in anhydrous ethanol (200 mL) was brought to 60 °C and methyl iodide was added. After stirring for 30 min, the reaction suspension was filtered and white solid was yielded as compound **2**. The white solid was washed with ether (46.9 g, 91%). A solution of compound **2** (1.0 eq.) and the corresponding amine (1.0 eq.) in ethanol was heated under reflux for 1.5 h. The solution was cooled and diluted with ether, giving a gummy pink precipitate. The crude product was extracted with hot ethanol and concentrated under reduced pressure and the residue was recrystallized from CH₃NO₂ to yield compound **3b-g** (23-53%). Representative data for the series are given below. **3b**: ¹H NMR (400 MHz, MeOD) δ3.17-3.25 (m, 2H) , 1.55-1.66 (br m, 2H) , 1.26-1.45 (m, 10H), 0.86-0.97 (m, 3H). ¹³C NMR (126 MHz, MeOD) δ159.68, 42.96, 42.18, 32.96, 30.34, 27.72, 23.71, 14.43. MS (ESI) calculated for C₉H₂₂N₄ *m/z* 186.18 found 187.22

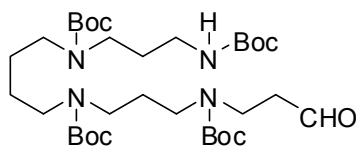
(MH⁺). **3g**: ¹H NMR (400 MHz, MeOD) δ 4.51 (br s, 1H), 3.03-3.14 (m, 1H), 2.76-2.85 (m, 1H), 1.44-1.61 (m, 2H), 1.04-1.36 (m, 30H), 0.80 (s, *J* = 7.0 Hz, 3H). ¹³C NMR (126 MHz, MeOD) δ 152.67, 42.17, 40.79, 33.09, 30.79, 30.52, 30.39, 30.13, 28.63, 27.72, 27.46, 23.75, 14.45. MS (ESI) calculated for C₁₉H₄₂N₄ *m/z* 326.34, found 327.36 (MH⁺).



5

Synthesis of **5**.

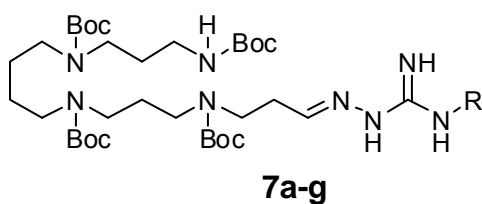
To a solution of **4** (930 mg, 1.85 mmol) in anhydrous DMF (8 mL) was added K₂CO₃ (768 mg, 5.55 mmol), followed by 3-bromopropanol (194 μL, 2.22 mmol). The reaction mixture was stirred at 60 °C for 18 h. The reaction mixture was diluted with DCM and the resultant solution was successively washed with water (2X), brine (1X) and dried over Na₂SO₄. After removal of solvent under vacuum, the residue was purified by flash column chromatography (hexane:EtOAc = 7:3) to afford the title compound **5** as a viscous oil (514 mg, 42%). ¹H NMR (400 MHz, CDCl₃) δ 4.89 (br s, 3H), 3.55-3.79 (m, 7H), 3.09-3.40 (m, 11H), 1.57-1.77 (m, 8H), 1.44 (br s, 36H). ¹³C NMR (126 MHz, CDCl₃) δ 156.20, 78.60, 58.16, 35.86, 31.81, 27.42, 27.34; MS (ESI) calculated for C₃₃H₆₄N₄O₉ *m/z* 660.46, found 683.49 (M+Na⁺).



6

Synthesis of **6**.

To a solution of **5** (500 mg, 0.76 mmol) in anhydrous DCM (20 mL) was added pyridinium chlorochromate (PCC; 245 mg, 1.14 mmol) and the solution was stirred at ambient temperature for 4.5 h. After removal of solvent under high vacuum, the residue was purified by flash column chromatography (hexane:EtOAc = 3:1) to afford the title compound **6** as a viscous oil (349 mg, 70%). ¹H NMR (400 MHz, CDCl₃) δ 9.81 (s, 1H), 3.48-3.56 (m, 2H), 3.07-3.32 (m, 11H), 2.66-2.77 (m, 2H), 1.61-1.82 (m, 5H), 1.40-1.55 (m, 36H). ¹³C NMR (126 MHz, CDCl₃) δ 199.95, 155.09, 154.42, 78.93, 78.37, 45.80, 45.51, 44.76, 44.15, 43.61, 43.12, 42.64, 42.29, 40.05, 36.28, 27.87, 27.46, 27.42, 27.39, 27.26, 25.00, 24.55. MS (ESI) calculated for C₃₃H₆₂N₄O₉ *m/z* 658.45, found 681.37 (M+Na⁺).



R= H	7a
R= C ₈ H ₁₇	7b
R= C ₁₀ H ₂₁	7c
R= C ₁₂ H ₂₅	7d
R= C ₁₄ H ₂₉	7e
R= C ₁₆ H ₃₃	7f
R= C ₁₈ H ₃₇	7g

General Procedure for the Syntheses of Compounds **7a-g**.

To a solution of **6** (100 mg, 0.15 mmol) in anhydrous EtOH (5 mL) was added compound **3a-g** (1.3 eq.) followed by catalytic amount of AcOH. The solution was refluxed at 85 °C for 2 h. After removal of solvent under high vacuum, the residue was purified by flash column chromatography (DCM: MeOH = 9:1) to afford **7a-g** as yellow viscous oils (70% - 100%).

7a: yield 80%; ¹H NMR (400 MHz, CDCl₃) δ 7.32-7.63 (m, 3H) , 3.34-3.62 (m, 3H) , 2.97-3.33 (m, 11H) , 2.39-2.61 (m, 2H) , 1.56-1.91 (m, 5H), 1.35-1.52 (m, 36H). ¹³C NMR (126 MHz, CDCl₃) δ 156.23, 156.10, 155.86, 155.50, 80.24, 80.00, 79.79, 79.50, 79.18, 78.98, 65.86, 53.45, 46.81, 46.52, 44.72, 44.21, 43.76, 43.07, 37.71, 37.38, 28.50, 28.46, 28.29, 28.05, 27.98, 27.63, 27.08, 26.03, 25.52, 15.27. MS (ESI) calculated for C₃₄H₆₆N₈O₈: *m/z* 714.50, found 715.48 (MH⁺).

7b: yield 100%; ¹H NMR (400 MHz, CDCl₃) δ 7.63 (br s, 1H) , 6.69-7.21 (br m, 1H) , 2.96-3.56 (m, 16H) , 2.49 (br s, 2H) , 1.55-1.82 (m, 6H) , 1.16-1.54 (m, 52H), 0.80-0.90 (m, 3H). ¹³C NMR (126 MHz, CDCl₃) δ 156.26, 156.12, 155.53, 154.46, 154.38, 80.14, 79.95, 79.55, 79.47, 79.24, 79.04, 53.50, 46.57, 46.40, 44.94, 44.25, 42.25, 37.70, 37.41, 31.75, 28.71, 28.45, 26.66, 25.55, 22.61, 14.10. MS (ESI) calculated for C₄₂H₈₂N₈O₈ *m/z* 826.63, found 827.66 (MH⁺).

7c: yield 73%; ¹H NMR (400 MHz, CDCl₃) δ 7.63 (br s, 1H) , 6.69-7.20 (br m, 1H) , 2.99-3.53 (m, 16H) , 2.49 (br s, 2H) , 1.55-1.80 (m, 6H) , 1.14-1.56 (m, 56H), 0.87 (t, *J* = 6.8 Hz, 3H). ¹³C NMR (126 MHz, CDCl₃) δ 155.25, 155.21, 155.13, 154.57, 154.51, 78.96, 78.92, 78.85, 78.83, 78.52, 64.84, 52.45, 45.83, 45.46, 43.89, 43.26,

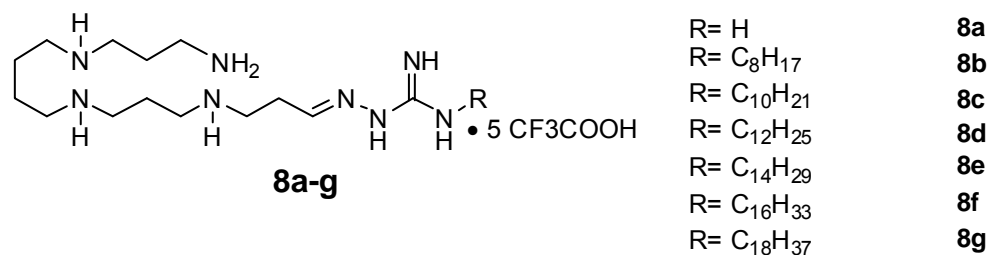
41.17, 36.69, 36.42, 36.40, 30.84, 27.43, 24.57, 21.64, 14.25, 13.10. MS (ESI) calculated for $C_{44}H_{86}N_8O_8$ m/z 854.66, found 855.70 (MH^+).

7d: yield 80%; 1H NMR (400 MHz, $CDCl_3$) δ 7.66 (br s, 1H), 6.70-7.22 (br m, 2H), 3.03-3.53 (m, 16H), 2.50 (br s, 2H), 1.59-1.81 (m, 6H), 1.20-1.54 (m, 60H), 0.87 (t, $J = 6.8$ Hz, 3H). ^{13}C NMR (126 MHz, $CDCl_3$) δ 156.24, 156.11, 156.06, 155.50, 155.31, 155.27, 80.15, 80.11, 80.00, 79.89, 79.54, 79.37, 79.06, 79.02, 65.86, 45.00, 44.96, 44.91, 44.83, 44.69, 44.26, 43.79, 42.23, 37.69, 37.53, 37.42, 29.64, 29.59, 29.34, 28.69, 28.51, 26.69, 22.68, 15.27, 14.13. MS (ESI) calculated for $C_{46}H_{90}N_8O_8$ m/z 882.69, found 883.72 (MH^+).

7e: yield 75%; 1H NMR (400 MHz, $CDCl_3$) δ 7.61 (br s, 1H), 6.67-7.19 (br m, 2H), 2.97-3.55 (m, 16H), 2.49 (br s, 2H), 1.55-1.79 (m, 6H), 1.14-1.56 (m, 64H), 0.85 (t, $J = 6.8$ Hz, 3H). ^{13}C NMR (126 MHz, $CDCl_3$) δ 156.25, 156.12, 156.06, 155.51, 154.53, 153.98, 153.92, 80.13, 80.07, 79.90, 79.83, 79.53, 79.37, 79.02, 46.85, 46.40, 45.02, 44.97, 44.94, 44.70, 44.24, 43.78, 42.73, 42.70, 42.29, 37.70, 37.42, 31.91, 29.69, 29.1, 26.689, 22.68, 14.13. MS (ESI) calculated for $C_{48}H_{94}N_8O_8$ m/z 910.72, found 911.75 (MH^+).

7f: yield 71%; 1H NMR (400 MHz, $CDCl_3$) δ 7.66 (br s, 1H), 6.67-7.19 (br m, 2H), 2.97-3.58 (m, 16H), 2.50 (br s, 2H), 1.58-1.81 (m, 6H), 1.15-1.58 (m, 68H), 0.86 (t, $J = 6.8$ Hz, 3H). ^{13}C NMR (126 MHz, $CDCl_3$) δ 155.25, 155.10, 154.52, 148.09, 147.00, 79.12, 78.83, 78.53, 78.36, 78.03, 52.46, 45.53, 44.50, 43.90, 43.22, 41.20, 36.69, 36.42, 30.90, 28.68, 28.18, 27.43, 25.68, 24.54, 21.66, 13.11. MS (ESI) calculated for $C_{50}H_{98}N_8O_8$ m/z 938.75, found 939.78 (MH^+).

7g: yield 70%; ^1H NMR (400 MHz, CDCl_3) δ 7.61 (br s, 1H), 6.72-7.23 (br m, 2H), 2.97-3.54 (m, 18H), 2.49 (s, 1H), 1.59-1.78 (br s, 8H), 1.17-1.57 (m, 70H), 0.89 (t, J = 6.6 Hz, 3H). ^{13}C NMR (126 MHz, CDCl_3) δ 169.20, 153.62, 131.75, 126.97, 74.42, 68.85, 64.98, 64.20, 62.76, 62.59, 62.23, 45.96, 42.33, 40.82, 40.61, 38.94, 32.19, 30.83, 25.65, 23.32, 14.12, 14.07, 13.96, 8.59. MS (ESI) calculated for $\text{C}_{52}\text{H}_{102}\text{N}_8\text{O}_8$ m/z 966.78, found 967.77 (MH^+).



General Procedure for the Syntheses of Compounds **8a-g**.

The resultant **7a-g** was dissolved in excess dry trifluoroacetic acid (TFA) and stirred at r.t. for 30 min. TFA was removed by purging nitrogen and the residue was thoroughly washed with diethyl ether to obtain the title compounds as yellow flaky solids **8a-g** (~100%).

8a: ^1H NMR (500 MHz, MeOD) δ 7.54 (t, J = 4.1 Hz, 1H), 3.40 (t, J = 7.1 Hz, 2H), 3.05 (m, 12H), 2.75-2.84 (m, 2H), 2.06-2.23 (m, 4H), 1.78-1.90 (br s, 4H), 1.17-1.36 (m, 2H). ^{13}C NMR (126 MHz, MeOD) δ 155.70, 147.12, 117.75, 115.43, 46.80, 44.59, 44.42, 44.39, 43.55, 36.38. MS (ESI) calculated for $\text{C}_{14}\text{H}_{34}\text{N}_8$ m/z 314.29, found 158.17 ($\text{MH}^+\text{+H}^+$ [doubly-charged species]), 315.33 (MH^+).

8b: ^1H NMR (400 MHz, MeOD) δ 7.31-7.82 (m, 1H), 3.36-3.43 (m, 15H), 3.06-3.31 (m, 15H), 2.74-2.85 (m, 2H), 2.03-2.28 (m, 4H), 1.76-1.94 (m, 4H), 1.27-1.48 (m, 10H), 0.85-0.97 (m, 3H). ^{13}C NMR (126 MHz, MeOD) δ 161.86, 161.59, 117.86, 115.55, 46.81, 43.71, 41.14, 36.41, 31.54, 28.53, 26.28, 23.97, 22.81, 22.70, 22.29, 13.01. MS (ESI) calculated for $\text{C}_{22}\text{H}_{50}\text{N}_8$ m/z 426.42, found 214.22 ($\text{MH}^+\text{+H}^+$), 427.42 (MH^+).

8c: ^1H NMR (400 MHz, MeOD) δ 7.37-7.67 (m, 1H), 3.35-3.43 (m, 4H), 3.05-3.31 (m, 14H), 2.76-2.83 (m, 2H), 2.05-2.25 (m, 4H), 1.75-1.93 (m, 4H), 1.59-1.70 (br m, 2H), 1.23-1.47 (m, 14H), 0.83-1.00 (m, 3H); ^{13}C NMR (126 MHz, MeOD) δ 154.36, 146.54, 146.49, 146.44, 44.58, 44.43, 44.40, 43.71, 41.14, 36.40, 31.64, 26.28, 23.98, 22.81, 22.70, 22.32, 13.03. MS (ESI) calculated for $\text{C}_{24}\text{H}_{54}\text{N}_8$ m/z 454.45, found 228.23 ($\text{MH}^+\text{+H}^+$), 455.45 (MH^+).

8d: ^1H NMR (400 MHz, MeOD) δ 7.40-7.67 (m, 1H), 3.40 (t, $J = 7.1$ Hz, 2H), 3.05-3.31 (m, 14H), 2.74-2.84 (m, 2H), 2.05-2.25 (m, 4H), 1.77-1.90 (br m, 4H), 1.58-1.70 (m, 2H), 1.24-1.46 (m, 18H), 0.92 (t, $J = 6.8$ Hz, 3H). ^{13}C NMR (126 MHz, MeOD) δ 154.37, 146.62, 146.57, 146.54, 117.47, 115.46, 115.43, 44.59, 44.43, 44.40, 43.71, 41.13, 36.40, 31.67, 29.34, 29.25, 29.07, 28.57, 28.40, 26.29, 23.97, 22.81, 22.70, 22.33, 13.03. MS (ESI) calculated for $\text{C}_{26}\text{H}_{58}\text{N}_8$ m/z 482.48, found 242.25 ($\text{MH}^+\text{+H}^+$), 483.49 (MH^+).

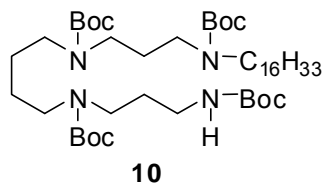
8e: ^1H NMR (400 MHz, MeOD) δ 7.46-7.64 (m, 1H), 3.40 (t, $J = 7.1$ Hz, 2H), 3.04-3.30 (m, 14H), 2.73-2.84 (m, 2H), 2.04-2.25 (m, 4H), 1.78-1.89 (br m, 4H), 1.58-1.70 (m, 2H), 1.25-1.42 (m, 22H), 0.92 (t, $J = 6.8$ Hz, 3H). ^{13}C NMR (126 MHz,

MeOD) δ 154.37, 146.60, 146.59, 117.74, 115.44, 44.59, 44.43, 44.40, 43.71, 41.15, 36.41, 31.67, 28.96, 26.29, 23.97, 22.81, 22.70, 22.33, 13.03. MS (ESI) calculated for $C_{28}H_{62}N_8$ m/z 510.51, found 256.31 ($MH^+ + H^+$), 511.60 (MH^+).

8f: 1H NMR (400 MHz, MeOD) δ 7.51-7.56 (m, 1H), 3.40 (t, $J = 7.1$ Hz, 2H), 3.05-3.31 (m, 13H), 2.75-2.84 (m, 2H), 2.05-2.24 (m, 4H), 1.79-1.91 (br m, 4H), 1.58-1.69 (m, 2H), 1.26-1.46 (m, 26H), 0.92 (t, $J = 6.8$ Hz, 3H). ^{13}C NMR (126 MHz, MeOD) δ 154.36, 146.63, 146.59, 146.55, 117.81, 115.47, 44.60, 44.44, 44.41, 43.72, 41.15, 36.41, 31.67, 28.57, 26.29, 23.96, 22.81, 22.70, 13.05, 22.33. MS (ESI) calculated for $C_{30}H_{66}N_8$ m/z 538.54, found 270.28 ($MH^+ + H^+$), 539.56 (MH^+).

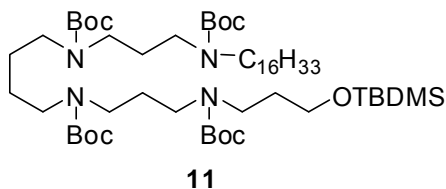
8g: 1H NMR (400 MHz, MeOD) δ 7.51 (br s, 1H), 3.40 (t, $J = 7.0$ Hz, 2H), 3.04-3.30 (m, 14H), 2.73-2.86 (m, 2H), 2.05-2.24 (m, 4H), 1.77-1.88 (br m, 4H), 1.58-1.69 (m, 2H), 1.21-1.47 (m, 29H), 0.91 (t, $J = 6.7$ Hz, 3H). ^{13}C NMR (126 MHz, MeOD) δ 154.781, 147.09, 147.03, 45.02, 44.86, 44.84, 44.14, 41.57, 36.83, 32.09, 28.85, 26.71, 24.38, 23.23, 23.12, 22.75, 13.47. MS (ESI) calculated for $C_{32}H_{70}N_8$ m/z 566.574, found 284.31 ($MH^+ + H^+$), 567.58 (MH^+).

2.6.1.2 Synthesis of analog bearing an *N*-alkyl substituent on one end and an unsubstituted guanylhydrazone at the other terminus:



Synthesis of 10.

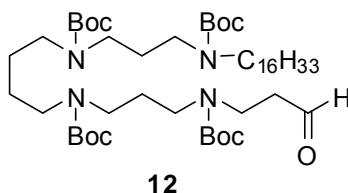
Compound **9** (2.4 g, 3.98 mmol) was added to the suspension of NaH (30 eq.) in DMF at 0 °C. After the reaction suspension was stirred at 0 °C for 30 min, 1-iodohexadecane (1.68 g, 1.0 eq.) which was dissolved in 5 mL DMF was added to the reaction. The mixture was then stirred at r.t. for 24 h. The reaction solution was quenched with 1 M HCl and extracted with DCM (3X). The extracted DCM layers were washed with brine (1X) and dried over Na₂SO₄. After removal of the solvent under reduced pressure, the desired compound **10** was isolated at 16% EtOAc/hexane by flash column chromatography (35%). ¹H NMR (500 MHz, CDCl₃) δ 3.01-3.33 (br m, 14H), 1.61-1.78 (m, 4H), 1.37-1.54 (m, 40H), 1.25 (s, 27H), 0.88 (t, *J* = 7.0 Hz, 3H). ¹³C NMR (126 MHz, CDCl₃) δ 156.11, 155.95, 155.48, 79.27, 79.12, 47.10, 46.80, 46.63, 46.52, 44.90, 44.66, 44.60, 44.18, 43.68, 37.66, 37.29, 31.93, 29.70, 29.36, 28.45, 26.87, 25.95, 25.89, 25.55, 22.69, 14.13. MS (ESI) calculated for C₄₆H₉₀N₄O₈ *m/z* 826.68, found 849.71 (M+Na⁺).



Synthesis of **11**:

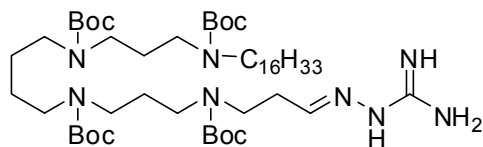
To a solution of *tert*-butyl dimethylsilylchloride (TBDMSCl; 1.2 eq.) and imidazole (1.3 eq.) in anhydrous DMF was added 3-bromopropanol (1.0 eq.) at 0 °C.¹²¹ After 1 h, the reaction mixture was brought to r.t. and stirred for 8 h. The reaction solution was then diluted with ether and the ethereal layer was washed with sat. NaHCO₃ solution (1X) and 10% HCl and dried over Na₂SO₄. Compound **10** (670 mg, 0.81 mmol) was added to a suspension of NaH (40 eq.) in DMF at 0 °C. After the reaction suspension was stirred at 0 °C for 30 min, an excess of freshly prepared 3-bromopropoxy-*tert*-butyl-dimethylsilane (8.1 mmol) was added to the reaction and the solution stirred at r.t. for 20 h. The reaction solution was quenched with 1 M HCl and extracted with DCM (3X). The extracted DCM layers were washed with brine (1X) and dried over Na₂SO₄. After removal of the solvent under reduced pressure, the desired compound **11** (510 mg, 63%) was isolated at 13% EtOAc/hexane by flash column chromatography. ¹H NMR (500 MHz, CDCl₃) δ 3.52-3.64 (br m, 2H), 3.03-3.25 (br m, 16H), 1.64-1.78 (br m, 6H), 1.41 (s, 40H), 1.14-1.32 (m, 28H), 0.82-0.89 (m, 12H), 0.01 (s, 6H). ¹³C NMR (126 MHz, CDCl₃) δ 155.44, 79.20, 60.78, 47.08, 46.83, 46.65, 44.89, 44.62, 44.34, 31.93, 29.70, 29.37, 28.49, 26.88, 25.93, 22.69,

18.27, 14.13. MS (ESI) calculated for $C_{55}H_{110}N_4O_9Si$ m/z 998.80, found 1021.94 (M+Na⁺).



Synthesis of **12**.

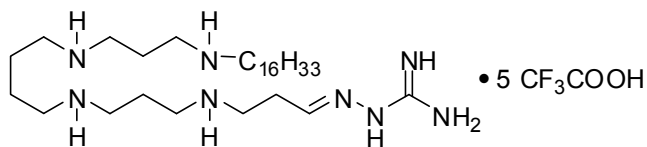
To a solution of **11** (400 mg, 0.40 mmol) in anhydrous THF (20 mL) was added tetra-n-butyl-ammonium fluoride (TBAF; 1 M in THF, 174 μ L, 0.17 mmol) and the solution was stirred at ambient temperature for 2 h. After removal of solvent under high vacuum, the residue was dissolved in 10 mL anhydrous DCM and PCC (130 mg, 0.60 mmol) was added. The reaction mixture was stirred at r.t. for 4.5 h. After removal of solvent under high vacuum, the residue was purified by flash column chromatography (hexane:EtOAc = 3:1) to afford the title compound **12** as a viscous oil (260 mg, 74 %). ¹H NMR (500 MHz, CDCl₃) δ 9.79 (s, 1H), 3.51 (br s, 2H), 3.16 (br s, 14H), 2.70 (br s, 2H), 1.73 (br s, 5H), 1.45 (br s, 41H), 1.25 (br s, 27H), 0.88 (t, J = 6.9 Hz, 3H). ¹³C NMR (126 MHz, CDCl₃) δ 200.99, 155.47, 79.93, 79.34, 79.25, 79.11, 47.08, 46.86, 46.84, 46.78, 46.62, 45.80, 44.69, 44.61, 43.63, 43.32, 41.12, 41.09, 31.93, 30.95, 29.66, 29.37, 28.32, 27.52, 26.88, 25.95, 25.60, 22.69, 14.13. MS (ESI) calculated for $C_{49}H_{94}N_4O_9$ m/z 882.70, found 905.68 (M+Na⁺).



13

Synthesis of **13**.

To a solution of **12** (100 mg, 0.11 mmol) in anhydrous EtOH (5 mL) was added compound **3a** (1.3 eq) followed by catalytic amount of AcOH. The solution was refluxed at 85 °C for 2 h. After removal of solvent under high vacuum, the residue was purified by flash column chromatography (DCM:MeOH = 19:1) to afford the title compound **13** as a yellow viscous oil (73%). ¹H NMR (500 MHz, CDCl₃) δ 7.48 (br s, 3H), 3.05-3.32 (br m, 2H), 3.16 (br s, 14H), 2.43-2.56 (br m, 2H), 1.73 (br s, 4H), 1.45 (br s, 41H), 1.25 (br s, 27H), 0.88 (t, *J* = 6.9 Hz, 3H). ¹³C NMR (126 MHz, CDCl₃) δ 155.96, 155.51, 79.97, 79.45, 79.29, 53.44, 47.12, 46.73, 46.61, 44.71, 43.08, 42.98, 31.92, 31.10, 30.95, 29.69, 29.66, 29.61, 29.42, 29.36, 28.50, 28.47, 27.59, 27.51, 26.87, 25.97, 25.86, 25.59, 25.55, 22.69, 14.13. MS (ESI) calculated for C₅₀H₉₈N₈O₈ *m/z* 938.75, found 939.75 (MH⁺).



14

Synthesis of **14**:

The resulting compound **13** was dissolved in excess dry TFA and stirred at r.t. for 30 min. Excess solvent was removed by purging nitrogen and the residue was thoroughly washed with diethyl ether to obtain a white solid **14** (~100%). ¹H NMR (500 MHz, DMSO-d₆) δ 12.01 (s, 1H), 8.64-8.95 (m, 6H), 7.61-7.96 (br m, 3H), 7.49 (t, *J* = 4.0, 1H), 3.19-3.27 (m, 2H), 2.83-3.06 (m, 13H), 2.62-2.69 (m, 2H), 1.89-2.01 (br m, 4H), 1.51-1.69 (br m, 6H), 1.18-1.34 (m, 24H), 0.85 (t, *J* = 6.9 Hz, 3H). ¹³C NMR (126 MHz, DMSO) δ 155.20, 147.44, 118.18, 115.80, 46.71, 46.10, 44.01, 43.86, 43.79, 42.87, 31.25, 29.00, 28.33, 25.83, 25.37, 22.64, 22.34, 22.32, 22.05, 13.92. MS (ESI) calculated for C₃₀H₆₆N₈ *m/z* 538.54, found 270.30 (MH⁺+H⁺), 539.54 (MH⁺).

2.6.2 Materials and Methods

2.6.2.1 Chemistry: All of the solvents and reagents used were obtained commercially and used as such unless noted otherwise. Moisture or air-sensitive reactions were conducted under argon atmosphere in oven-dried (120°C) glass apparatus. Solvents were removed under reduced pressure using standard rotary evaporators. Flash column chromatography was carried out using silica gel 635 (60-100 mesh), while thin-layer chromatography was carried out on silica gel CCM pre-coated aluminum sheets. All yields reported refer to isolated material judged to be homogenous by TLC, NMR spectroscopy and mass spectrometry.

2.6.2.2 Assays

NF- κ B inhibition: The inhibition of NF- κ B (a key transcriptional activator of the innate immune system) was quantified using HEK-Blue-4TM cells. Stable expression of secreted alkaline phosphatase (sAP) under control of NF- κ B/AP-1 promoters is inducible by LPS, and extracellular sAP in the supernatant is proportional to NF- κ B induction. HEK- Blue-4TM cells were incubated at a density of $\sim 10^6$ cells/ml in a volume of 80 μ l/well, in 384-well, flat-bottomed, cell culture-treated microtiter plates until confluency was achieved, and subsequently graded concentrations of stimuli were added to the cells. sAP was assayed spectrophotometrically using an alkaline phosphatase-specific chromogen (present in HEK-detection medium as supplied by the vendor) at 620 nm.

Nitric Oxide Assay: Nitric oxide production was measured as total nitrite in murine macrophage J774A.1 cells using the Griess assay¹²² as described in the literature.¹⁰⁶ J774A.1 cells were plated at $\sim 10^6$ /ml in a volume of 40 μ l/well, in 384-well, flat-bottomed, cell culture treated microtiter plates and subsequently stimulated with 10 ng/ml lipopolysaccharide (LPS). Concurrent to LPS stimulation, serially diluted concentrations of test compounds were added to the cell medium and left to incubate overnight for 16 h. Polymyxin B was used as reference compound in each plate. Positive- (LPS stimulation only) and negative-controls (J774A.1 medium only) were included in each experiment. Nitrite concentrations were measured by adding 40 μ l of supernatant to equal volumes of Griess reagents (50 μ l/well; 0.1% NED solution in

ddH₂O and 1% sulfanilamide, 5% phosphoric acid solution in ddH₂O) and incubating for 15 minutes at room temperature in the dark. Absorbance at 535 nm was measured using a Molecular Devices Spectramax M2 multifunction plate reader (Sunnyvale, CA). Nitrite concentrations were interpolated from standard curves obtained from serially diluted sodium nitrite standards.

Multiplexed cytokine assay *ex vivo* in human blood: 100 µl aliquots of fresh whole blood, anticoagulated with heparin, obtained by venipuncture from healthy human volunteers with informed consent and as per guidelines approved by the Human Subjects Experimentation Committee, was exposed to an equal volume of 100 ng/ml of *E. coli* 0111:B4 LPS, with graded concentrations of test compounds diluted in saline for 4 h in a 96-well microtiter plate.^{123;124} The effect of the compounds on modulating cytokine production was examined using a FACSArray multiplexed flow-cytometric bead array (CBA) system (Becton-Dickinson-Pharmingen, San Jose, CA). The system uses a sandwich ELISA-on-a-bead principle,^{125;126} and is comprised of 6 populations of microbeads that are spectrally unique in terms of their intrinsic fluorescence emission intensities (detected in the FL3 channel of a standard flow cytometer). Each bead population is coated with a distinct capture antibody to detect six different cytokines concurrently from biological samples (the human inflammation CBA kit includes TNF- α , IL-1 β , IL-6, IL-8, IL-10, and IL-12p70). The beads are incubated with 30 µl of sample, and the cytokines of interest are first captured on the bead. After washing the beads, a mixture of optimally paired second

antibodies conjugated to phycoerythrin is added which then forms a fluorescent ternary complex with the immobilized cytokine, the intensity (measured in the FL2 channel) of which is proportional to the cytokine concentration on the bead. The assay was performed according to protocols provided by the vendor. Standard curves were generated using recombinant cytokines provided in the kit. The data were analyzed in the CBA software suite that is integral to the FACSArray system.

Mouse lethality experiments: Female, outbred, 9- to 11-week-old CF-1 mice (Charles River, Wilmington, MA) weighing 22-28 g were used as described elsewhere.^{104;106;113;114} The animals were sensitized to the lethal effects of LPS by D-galactosamine.^{125;127;128} The lethal dose causing 100% mortality (LD₁₀₀) dose for the batch of LPS used (*E. coli* 0111:B4; procured from Sigma) was first determined by administering D-galactosamine (800 mg/kg) and LPS (0, 50, 100, 200 ng/mouse) as a single injection intraperitoneally (i.p.) in freshly prepared saline to cohorts of five animals in a volume of 0.2 mL. Mice received graded doses of compound diluted in saline, i.p. in one flank, immediately before a supralethal (200 ng) LPS challenge, which was administered as a separate i.p. injection into the other flank. Lethality was determined at 24 h post LPS challenge.

Chapter 3

Toll-like Receptors (TLRs) and TLR2

3.1 Background.

Toll-like receptors (TLRs) are pattern recognition receptors present on diverse cell types that recognize specific molecular patterns present in molecules that are broadly shared by pathogens but distinguishable from host molecules, collectively referred to as pathogen-associated molecular patterns (PAMPs).^{129;130} There are 10 TLRs in the human genome; these are trans-membrane proteins with an extracellular domain having leucine-rich repeats (LRR) and a cytosolic domain called the Toll/IL-1 receptor (TIR) domain.¹³⁰ The ligands for these receptors are highly conserved microbial molecules such as lipopolysaccharides (LPS) (recognized by TLR4), lipopeptides (TLR2 in combination with TLR1 or TLR6), flagellin (TLR5), single stranded RNA (TLR7 and TLR8), double stranded RNA (TLR3), CpG motif-containing DNA (recognized by TLR9), and profilin present on uropathogenic bacteria (TLR 11).^{131;132} The activation of TLRs by their cognate ligands leads to production of inflammatory cytokines, and up-regulation of MHC molecules and co-stimulatory signals in antigen-presenting cells as well as activating natural killer (NK) cells [innate immune response], in addition to priming and amplifying T-, and B-cell effector functions¹³³⁻¹³⁶ [adaptive immune responses]. Thus, TLR stimuli serve to link innate and adaptive immunity¹³⁴ and can therefore be exploited as powerful adjuvants in eliciting both primary and anamnestic immune responses. TLR1, -2, -4, -5, and -6

respond to extracellular stimuli, while TLR3, -7, -8 and -9 respond to intracytoplasmic PAMPs, being associated with the endolysosomal compartment.¹³⁰

3.2 TLR1/TLR2/TLR6 Agonistic Bacterial Lipoteichoic Acid and Lipopeptides.

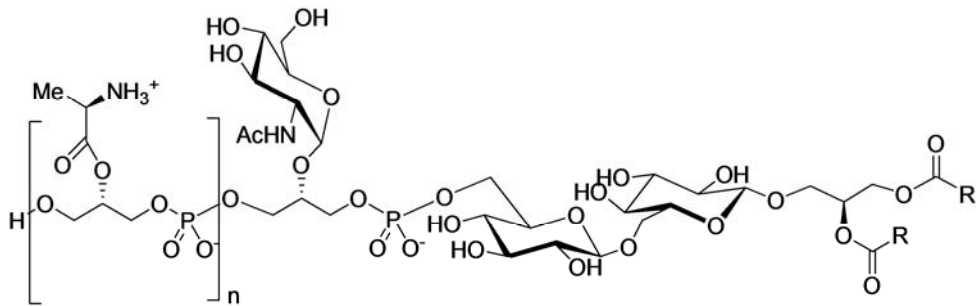


Figure 16. Structure of lipoteichoic acid (LTA), a constituent of the cell envelope of Gram-positive organisms.

The exoskeleton of the Gram-positive organism, similar to that of Gram-negative bacteria, is comprised of underlying peptidoglycan (PGN), a super-sized polymer of β -1 \rightarrow 4-linked *N*-acetylglucosamine-*N*-acetylmuramic acid glycan strands that are cross-linked by short peptides.¹³⁷ Unlike in Gram-negative bacteria which bear LPS on the outer leaflet of the outer membrane, the external surface of the peptidoglycan layer is decorated with lipoteichoic acids (LTA; **Figure 16**),¹³⁸ which are anchored in the peptidoglycan substratum via a diacylglycerol moiety and bear a surface-exposed, polyanionic, 1–3-linked polyglycerophosphate appendage which varies in its subunit composition in LTAs from various Gram-positive bacteria; in *S. aureus*, the repeating subunit contains D-alanine and α -D-*N*-acetylglucosamine.¹³⁹

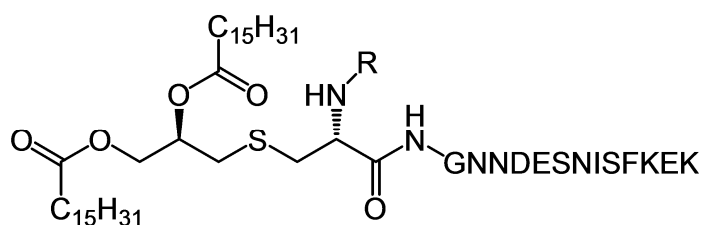


Figure 17. Structure of MALP-2, the first TLR2 agonistic, immunostimulatory lipopeptide identified. The lipopeptide comprises of a diacylthioglycerol unit (yellow) in thioether linkage (purple) with cysteine (red). The α -amino group of cysteine is acylated (R = palmitoyl) in triacyl lipopeptides. The peptide unit (green) can be variable, and does not appear to be a determinant of immunostimulatory activity.

Lipoproteins are found in the bacterial cytoplasmic membrane and are also common constituents of the cell wall of both Gram-negative and Gram-positive bacteria.¹⁴⁰ The free amine of the N-terminus of lipoproteins is acylated with a *S*-(2,3-diacyloxypropyl)cysteiny residue which constitutes the immunostimulatory moiety¹⁴¹ as shown by studies on synthetic peptides containing the diacylthioglycerol unit (see below).¹³⁹ In contradistinction to enterobacterial LPS which is recognized by Toll-like receptor-4 (TLR4), PGN,¹⁴² LTA,¹⁴³ lipopeptides,¹⁴⁴ as well as some non-enterobacterial LPS¹⁴⁵ signal via TLR2. One of the earliest reports on bacterial components other than LPS was the study by Melchers *et al.*,¹⁴⁶ showing that purified lipoprotein from the outer membrane of *E. coli* was a B-lymphocyte mitogen, expressing activity in LPS-nonresponder C3H/HeJ mice. Lipoprotein fractions isolated from Gram-positive organisms as well as mycoplasmal cultures indicated potent macrophage-activating and CTL-inducing properties.¹⁴⁷⁻¹⁵⁰ A lipopeptide fraction termed mycoplasma associated lipopeptide-2kDa (MALP-2; **Figure 17**) was

subsequently isolated and structurally characterized,¹⁴¹ leading to the identification of *S*-(2,3-dihydroxypropyl)cysteine as the structural core of MALP-2.¹⁵¹ Recent structure-activity relationships have sought to examine the stereochemistry, acylation pattern, and the contributions of the peptide unit.¹⁵²⁻¹⁵⁵ In contradistinction to Gram-negative LPS which is recognized by Toll-like receptor-4 (TLR4),^{136;156-161} the lipopeptides signal via TLR2.^{144;152;154;162} Although diacyl lipopeptides have been reported to be agonists of heterodimers of TLR2/TLR6^{153;163;164} and triacylated species were thought to signal via TLR2/TLR1,^{144;154;162} the recognition of the lipopeptides by TLR2 has been recently shown to be relatively independent of TLR1 and TLR6, and are mediated predominantly via TLR2.^{165;166}

3.2.1 Structural basis for the interactions of PAM₂CSK₄ with TLR2 and PAM₃CSK₄ with TLR2/TLR1: The crystal structures of both PAM₂CSK₄ and PAM₃CSK₄ with TLR1-TLR2 heterodimers have recently been determined (**Figure 18**).¹⁶⁷ This not only provides a structural basis for differential recruitment of TLR6 and TLR1 to heterodimerize with TLR2 by diacyl and triacyl lipopeptides, but also allows, for the first time, a rational, structure-based template for the *ab initio* design of novel analogues of TLR2. The *N*-acyl group of the triacyl PAM₃CSK₄ interacts with a hydrophobic groove in TLR1, driving the formation of an ‘*m*’ shaped TLR2-TLR1 dimer (**Figure 18**), whereas both ester-linked acyl groups of the diacyl PAM₂CSK₄ are inserted into a hydrophobic pocket in TLR2, rendering the diacyl lipopeptide a pure TLR2 ligand.¹⁶⁷ The correct stereoisomer is necessary for the

appropriate orientation of the ester-linked acyl groups in the hydrophobic pocket of TLR2. The external tetralysine peptide unit is almost fully solvent-exposed and does not participate in significant interactions with TLR2, which is consistent with our observation that the PAM₂CS unit is sufficient to confer full TLR-agonistic activity.

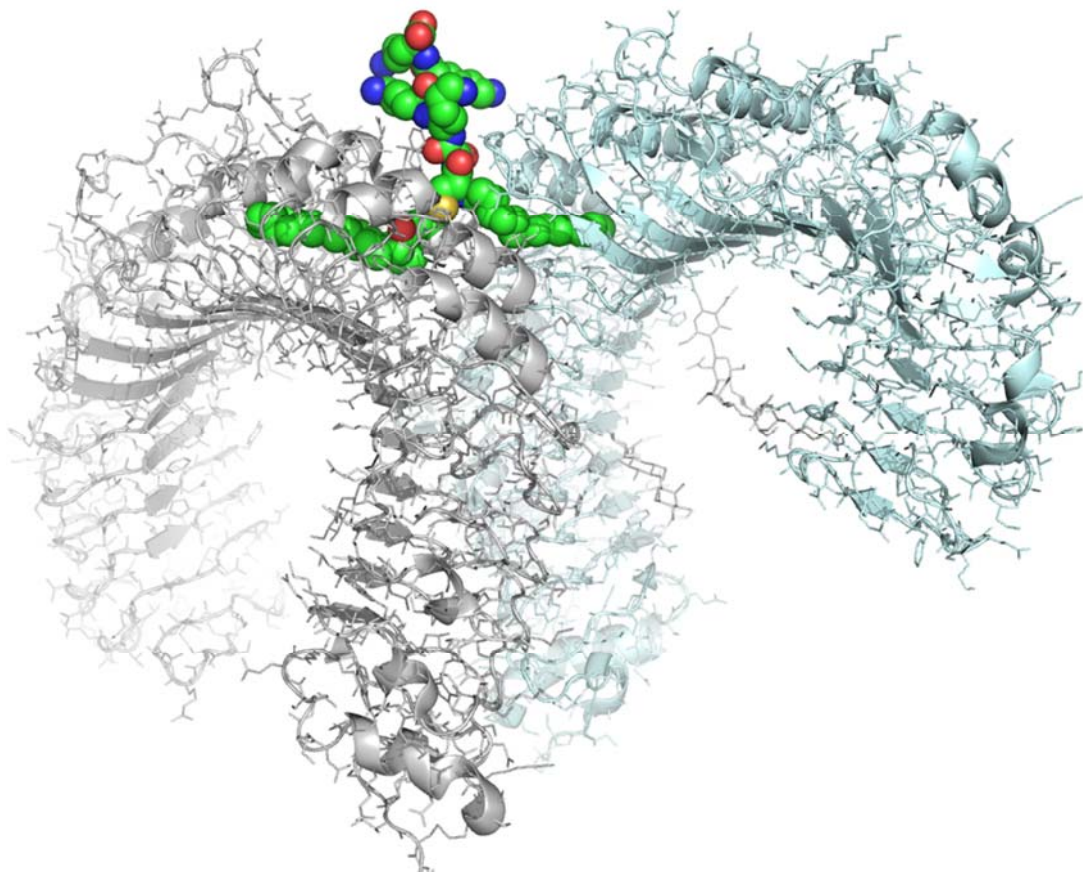


Figure 18. Crystal structure of PAM₃CSK₄ (shown in spacefill) bound to a heterodimer of TLR1 and TLR2 (PDB: 2Z7X).

3.2.2 Effects of the TLR2 agonistic lipopeptides on professional antigen presenting cells and effector lymphocytes: The exposure of bone marrow-derived dendritic cells of C57/BL6 mice to the lipopeptide FSL-1 has been shown to result in a TLR2-dependent upregulation of MHC Class II and CD80/CD86 co-stimulatory molecules, with enhanced expression of CD11b and CD11c, associated with the production of TNF- α and IL-12.¹⁶⁸ It is noteworthy that, in this study, whereas LPS also induced IL-10 production, FSL-1 only induced a pro-T_H1-type cytokine response.¹⁶⁸ These results have been independently confirmed in BALB/c mice using MALP-2, and extended to show that the lipopeptide also upregulates immunoproteasome (LMP2, LMP7 and MECL1) activity in a dose-dependent manner, suggesting that lipopeptides may indirectly enhance MHC Class I-restricted responses by accelerated antigen processing and peptide presentation.¹⁶⁹ Importantly, the effects of lipopeptides on APC maturation and antigen presentation have also been demonstrated in human DCs.¹⁷⁰

MALP-2 directly stimulates murine B lymphocytes without accessory APC help in a TLR2- and dose-dependent fashion. The expansion in the resting CD19⁺ population was accompanied by upregulation of both MHC Class I and II molecules, as well as CD25 (IL2R α), CD40, CD80 and CD86.¹⁷¹ Triacyl PAM₃CSK₄ has been shown to induce IL-6 production in human tonsillar B cells.¹⁷² In addition, PAM₂CSK₄ and MALP-2 induce isotypic switching and differentiation of naïve human B lymphocytes to IgG-secreting plasma cells,¹⁷³ indicating a functional association between BCR stimulation and TLR activation.¹⁷³ Triacyl PAM₃CSK₄ has been shown to

dramatically enhance MHC Class I-restricted CTL proliferation to an immunodominant influenza peptide M_{X58-66} in a human autologous DC/CD8⁺ T cell co-culture model.¹⁷⁴ The peptide-specific CTLs (assessed by tetramer staining) were also found to be strong producers of IFN- γ . Lipopeptide-primed DCs also stimulated the proliferation of allogeneic naïve CD8⁺ CTLs.¹⁷⁴ Intranasal immunization of mice with influenza-specific peptide resulted in greatly enhanced numbers of IFN- γ -secreting CD8⁺ CTLs when lipopeptides were used as adjuvants.¹⁷⁵ Similarly, MALP-2 induces robust, long-lived CTL responses against HIV-1 Tat protein.^{176;177}

These results collectively indicate that the adjuvanticity of the lipopeptides encompasses a strong CTL response. Reports as early as 1997 indicated that PAM₃CSK₄ markedly enhanced the humoral response to haptens conjugated to poly-L-lysine; adjuvanticity was also observed by these authors for the lipopeptide-T_H1 cell epitope conjugates in *in vitro* immunization protocols.¹⁷⁸ It was subsequently shown using human lymphocytes *ex vivo*, that PAM₃CSK₄-dependent CD4⁺ T cell differentiation and proliferation required professional APC, and that naïve CD4⁺ T cell differentiation progressed with faster kinetics in the presence of the adjuvant. The lipopeptide enhanced the frequency of *in vitro* expanded T_H cells specific for tetanus toxoid and hepatitis B surface antigen peptides, with the majority of the expanded CD3⁺/CD4⁺ cells being positive for IFN- γ .¹⁷⁹ A recent study indicates that the lipopeptides lower the threshold for T_H1 responses by TLR2-dependent secretion of IL-12p70 by DC.¹⁸⁰

Chapter 4

Structure-Activity Relationships in TLR2-Agonistic Diacylthioglyceryl

Lipopeptides

4.1 Introduction and Rationale.

The link between immune stimulation resulting from acute infection and the resolution of tumors has long been recognized,¹⁸¹ and the phenomenon of infection-related "spontaneous regression" of cancer has been documented throughout history, beginning as early as 2600 B.C..^{182;183} The foundations of modern immunotherapy for cancer were laid in 1891 by William B. Coley, who injected live streptococcal organisms into a long-bone sarcoma lesion and observed shrinkage of the tumor.¹⁸⁴ More than a century has elapsed since Coley's empirical findings were first reported, but the active principle(s) in Coley's toxin remain undetermined. This long lag-period is perhaps not altogether surprising because the recognition of innate immune system is, in itself, recent,¹⁸⁵⁻¹⁸⁷ and our understanding of the structure and function of the family of Toll-like receptors (TLRs)^{159;188} that recognize "pathogen-associated molecular patterns (PAMPs)",¹⁸⁹ and the effector mechanisms that mediate innate immune responses^{129;190;191} are yet nascent. Nonetheless, there exists considerable potential in harnessing innate immune responses in a wide range of disease states, notably cancer, as evidenced by the number of TLR agonists already in clinical trials,¹⁹² and the resurgence of interest in the immunotherapy of neoplastic states.¹⁹³⁻

In comparing the various constituents of the Gram-positive cell, we have found lipopeptides to be extremely potent TLR2 agonists, and yet without apparent toxicity in animal models.¹⁹⁶ In murine cells, PAM₂CSK₄ (*S*-[2,3-*bis*(palmitoyloxy)-(2*RS*)-propyl]-*R*-cysteinyl-*S*-seryl-*S*-lysyl-*S*-lysyl-*S*-lysyl-*S*-lysine), a commercially-available, synthetic model lipopeptide (**Figure 19**), was equipotent in its NF-κB inducing activity relative to LPS, but elicited much lower proinflammatory cytokines, while both LPS and the lipopeptide potently induced the secretion of a similar pattern of chemokines suggestive of the engagement of downstream TRIF pathways.¹⁹⁶ Furthermore, we have found that while LPS, as expected, elicited a robust fever response in rabbits at a dose of 200 ng/kg, a 200 μg/kg dose (1000X) of the lipopeptide (PAM₂CSK₄) was without any discernible pyrogenic or other apparent acute toxic effect (**Figure 20**). In the following assay of induction of cytokines in human blood (The most representative data [TNF-α, IL-β, IL-6] was shown here, **Figure 21**), it was proved that PAM₂CSK₄ might be not proinflammatory. Shown from the assay, PAM₂CSK₄ did not trigger any release of cytokines while LPS showed a strong proinflammatory effect. However, PAM₂CSK₄ does stimulate the production of nitric oxide (NO) in murine Mφ and the phosphorylation of p38MAPK in human blood, both of which serve as indicators for immunostimulation (**Figure 22**). It was also discovered that PAM₂CSK₄, like LPS, stimulates natural killer (NK) cells (**Figure 23**). These observations all suggest that the lipopeptides may be remarkably potent, yet nontoxic immunotherapeutic agents. Indeed, in a Phase I/Phase II clinical trial¹⁹⁷ on a single, intraoperative 20-30 μg intratumoral injection

of MALP-2¹⁴¹ (a diacyl lipopeptide similar in its core structure to PAM₂CSK₄) in patients with inoperable carcinoma of the pancreas, the lipopeptide was well-tolerated and proved efficacious in prolonging survival.¹⁹⁷

Considerable structure-activity relationships dictating TLR2 binding and subsequent stimulation of innate immune responses have been documented for a range of synthetic lipopeptides. The minimal structure for biological activity is the Cys-Ser lipodipeptide¹⁹⁸ with the lipoaminoacid Cys-OH derivative being almost inactive;¹⁹⁹ the remainder of the peptidic unit appears, in large part, not to be critical for activity since a variety of analogues of different lengths with different amino acid sequences were found to be equipotent.^{198;200-202} The (*R*)-configuration at the asymmetric glyceryl carbon confers maximum activity,^{152;203} and the threshold of the acyl chain length of the two ester-bound fatty acids is 8 carbons, with shorter acyl analogues being inactive.¹⁴⁴ It should be pointed out, however, that the majority of earlier SAR studies had been performed with murine cells, many even before the TLRs had been discovered, and it is now clear that significant species-specific differences exist between human and murine TLR responses^{144;204} as a consequence of subtle structural differences in the ligand binding pocket within TLR2.¹⁶⁷ Furthermore, the recent high-resolution crystal structure of lipopeptides complexed to human- as well as murine-derived TLR1/TLR2 heterodimers¹⁶⁷ raises additional questions since the binding site in TLR2 is highly unusual, being located in the convex region formed at the border of the central and C-terminal domains with the peptidic unit interacting with interfacial residues at the neck region of the binding

pocket.¹⁶⁷ It was of interest to examine whether the chirality of the highly conserved Cys residue (L-Cys versus D-Cys) and the thioether bridge connecting the diacylglycerol unit to the peptide chain are critical determinants of activity, and if the thioether could be bioisosterically substituted by an ether linkage. The importance of the ester-linked palmitoyl groups on the thioglycerol backbone is also not documented, and the effect of replacing them with amide-linked acyl groups remained to be explored. The geometry of the Cys-Ser dipeptide unit also appears to be crucial, in that there are key interactions with conserved Tyr316 and Pro315 residues at the neck of the binding pocket (**Figure 19**) in the crystal structure.¹⁶⁷ I wished to examine the effect of inverting the stereocenters of both residues in the dipeptide unit. It is also to be noted that the carboxylic acid of Cys is in amide linkage with the amine of serine (**Figure 19**), and I wished to test whether inversion of the orientation of Ser, resulting by the coupling the carboxyl group of serine to the amino group of cysteamine could perhaps yield analogues that were TLR2 receptor antagonists.

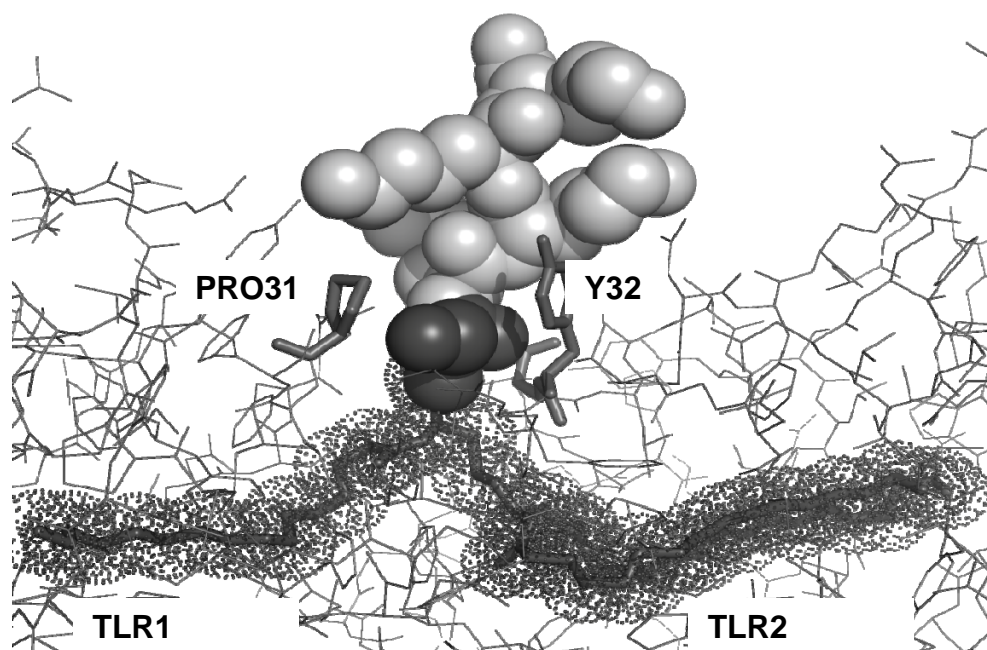
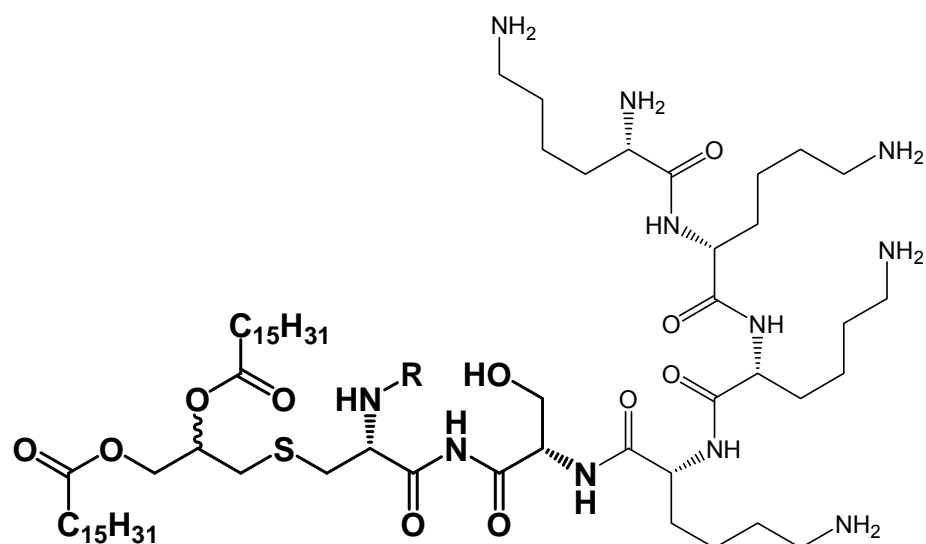


Figure 19. *Top:* The structure of PAM₂CSK₄. R is palmitoyl in PAM₃CSK₄. *Bottom:* The crystal structure of PAM₃CSK₄ bound to a heterodimer of human-derived TLR2 and TLR1 (PDB code: 2z80). The acyl groups are shown in emphasized sticks with van der Waals surfaces represented by dots. The Cys-Ser dipeptide is shown as dark spheres and tetra-lysine as light gray spheres.

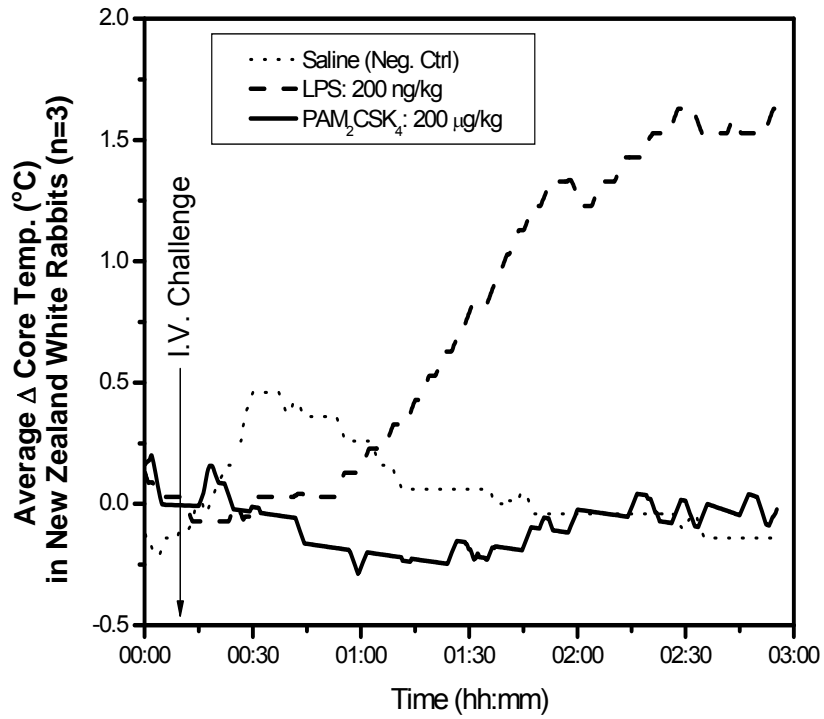


Figure 20. Pyrogenicity responses to LPS and PAM₂CSK₄ in rabbits.

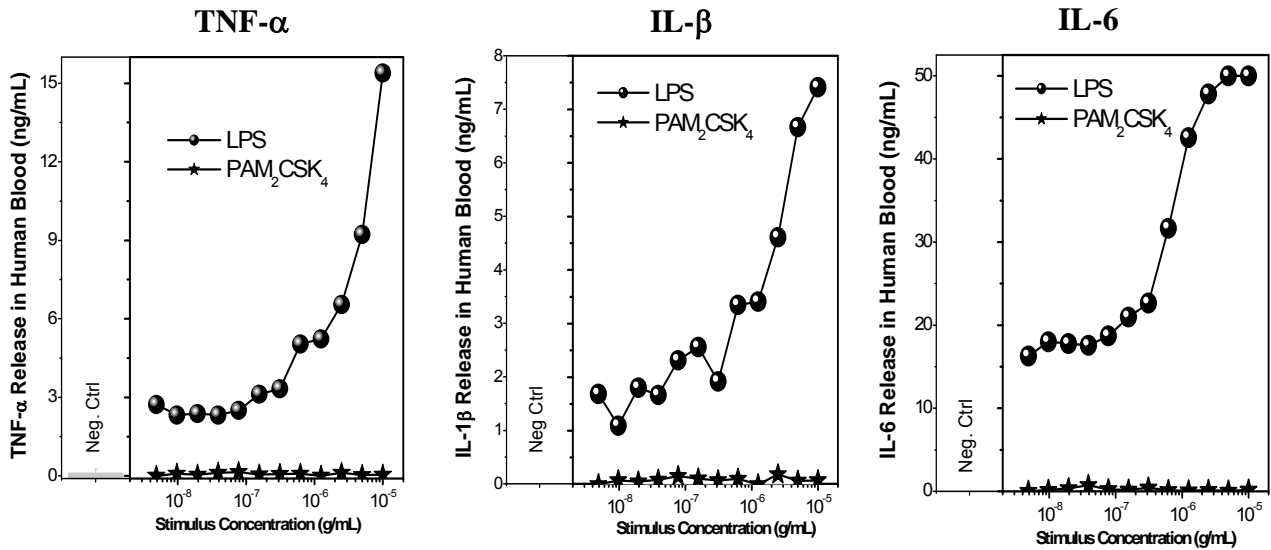
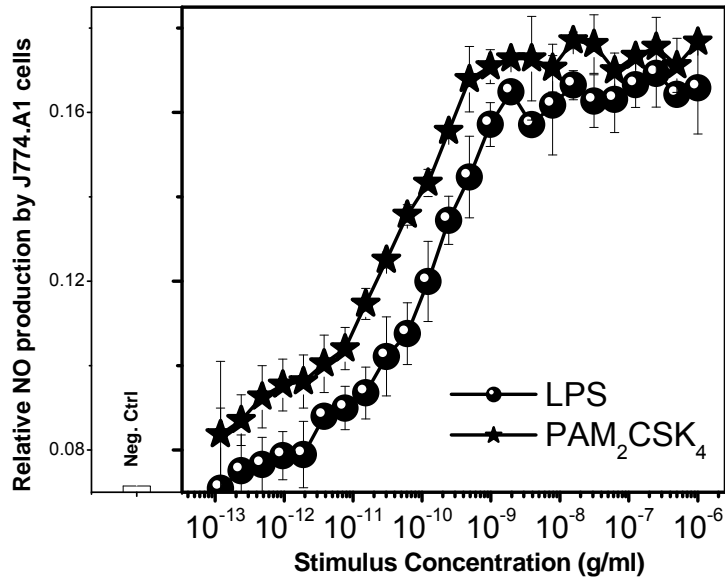


Figure 21. Induction of cytokine release by LPS and PAM₂CSK₄ in human blood.

NO Production in Murine M ϕ



p38MAPK Phosphorylation in Human Blood

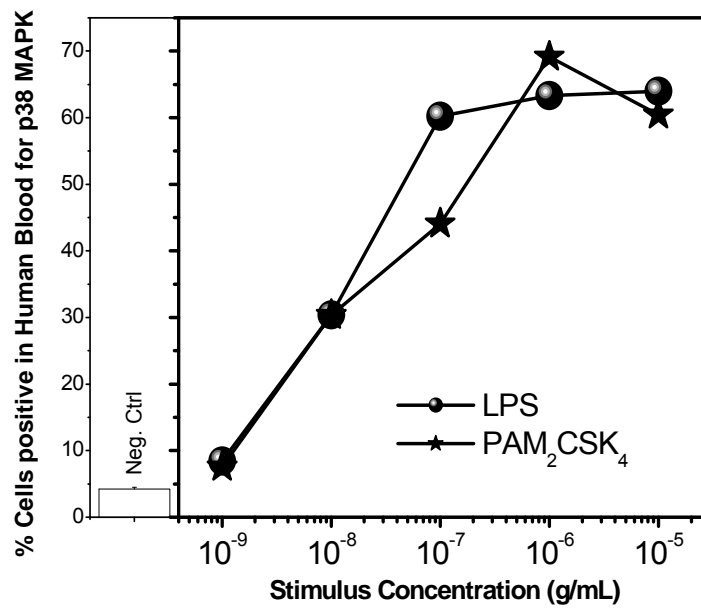


Figure 22. Induction of NO and phosphorylation of p38MAPK with LPS and PAM₂CSK₄.

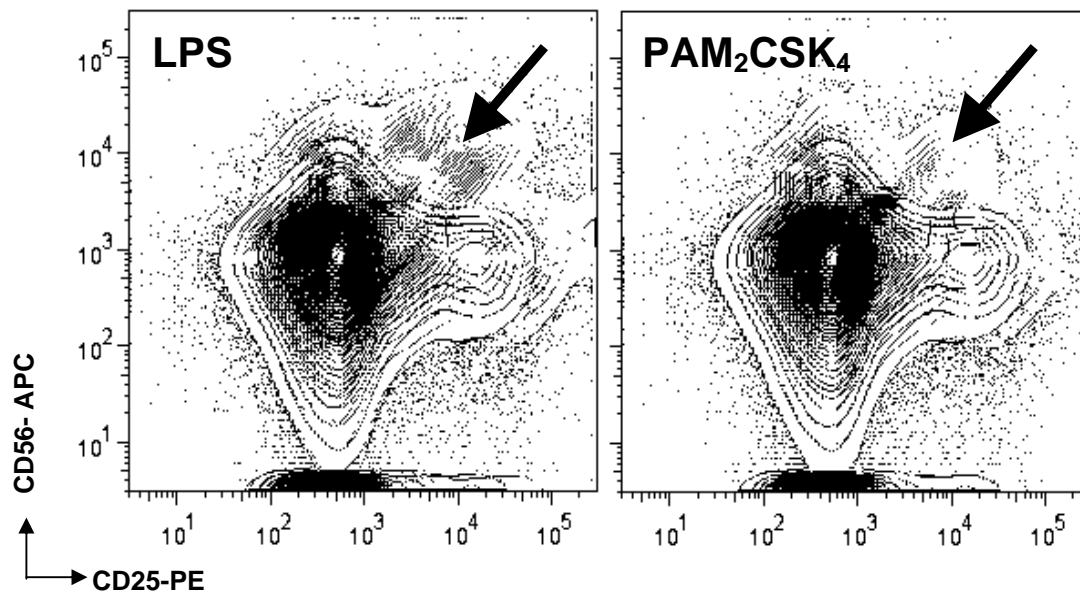


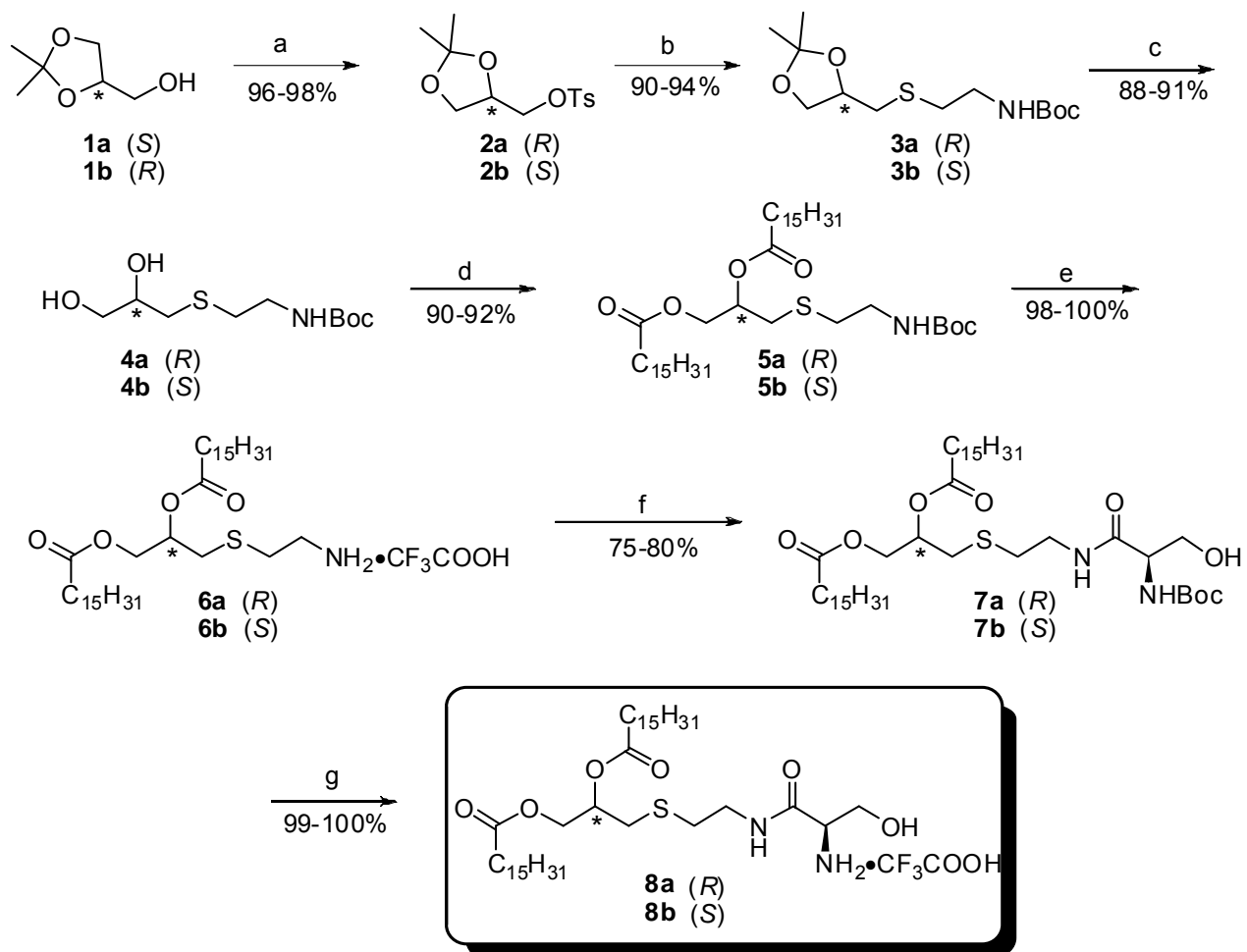
Figure 23. Expansion of CD25+/CD56+ double-positive natural killer (NK) cells population upon stimulation of human whole blood with 1 μ g/ml LPS or PAM₂CSK₄.

4.2 Syntheses and Evaluation of Cysteamine Analogs (6a-b) and Cysteamine-inverse serine analogs (8a-b)

Much of the previous work in the literature concerning the structure-activity relationships in lipopeptides have utilized murine TLR2, and in an effort to confirm the minimal part-structure of the lipopeptide that was TLR-agonistic on human TLR2, we first targeted the stereoselective syntheses of 1,2-dipalmitoyl (*R*)- and (*S*)-3-(2-aminoethylthio)propanediol (**6a** and **6b**, **Scheme 1**) starting from the corresponding enantiopure 1,2-isopropylidenglycerol. The (*R*)-cysteamine lipo-amino acid **6a** was weakly active (IC_{50} : 1 μ M, **Figure 24**) relative to the commercially available reference lipopeptide PAM₂CSK₄ (IC_{50} : 67 pM), while the (*S*)-analogue **6b** was

completely inactive. Coupling L-serine to the free amine of the cysteamine resulted in the lipodipeptides **8a** and **8b**; similar to the cysteamine analogues, only **8a** was active with an IC₅₀ of 1.2 μM; it is to be noted that in these latter compounds, the dipeptide unit is inverted since, unlike in the naturally occurring as well as in synthetic PAM₂CSK₄ (**Figure 19**), it is the carboxyl group of the serine that is coupled to the lipopeptide.

Scheme 1



Reagents and conditions: a: *p*-TsCl, pyr, DCM, 0 °C-r.t., 8 h;
 b: *N*-Boc-2-aminoethanethiol, NaH, DMF, 0 °C-r.t., 8 h;
 c: 70% AcOH, r.t., 12 h;
 d: C₁₅H₃₁COCl, pyr, DMAP, DCM, 0 °C-r.t., 10 h;
 e: TFA, r.t., 30 min; f: Boc-L-Serine-OH, EDCI, EDIPA, DMAP, DCM, 0 °C-r.t., 8 h;
 g: TFA, r.t., 30 min.

4.3 Syntheses and Evaluation of PAM₂C-OMe (11), PAM₂CS-OH (14a) and PAM₂CS-OMe (14b-d) analogs.

The L-cysteine-containing lipo-amino acid, compound **11** (**Scheme 2**) is also weakly TLR2-agonistic, which is in contradistinction to the virtually absent activity on murine cells described earlier.¹⁹⁹ The results emphasize differences in ligand specificity between murine and human TLR2. The difference in activity between the *R*- and *S*-isomers which was consistent with previous SAR results,^{152;203} served to focus our subsequent SAR in which we elected to examine only the *R*-diacylthioglycerol analogues.

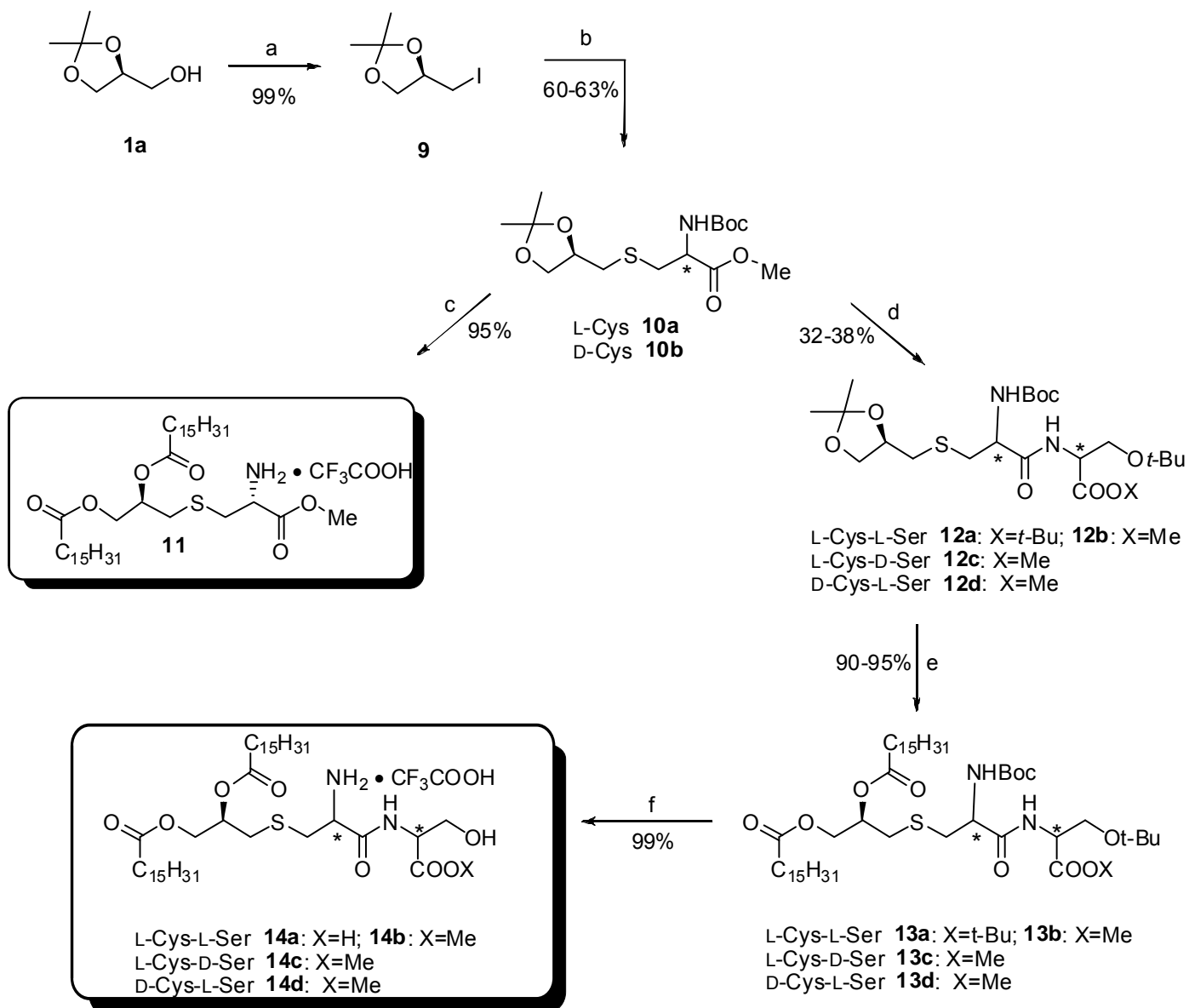
The PAM₂Cys-Ser compounds of the **14** series comprising of combination of L- or D-amino acids at either position, and with the carboxyl terminus as either the carboxylic acid or the methyl ester (**Scheme 2**) were all highly active with the IC₅₀ values in the mid-picomolar range (**Figure 24**), signifying that the stereochemistry of the dipeptide unit is non-critical as long as the orientation of the amide bond is in the correct configuration as discussed earlier. These results are constant with the crystal structure of PAM₂CSK₄ complexed with TLR2, in which the carbonyl Cys-Ser amide bond forms H-bonding with Pro315 and the NH of the amide interacts with Y326, but the side-chains of the dipeptide unit show no significant van der Waals interactions within the binding pocket.¹⁶⁷ The relative unimportance of the side-chains of the dipeptide core are also in agreement with observations that in naturally-occurring lipopeptides, the second amino acid is far less conserved, and can be replaced by other residues with non-bulky side-chains such as Gly,^{198;200-202} presumably as long as

steric interactions within the narrow neck region of the binding pocket¹⁶⁷ are not compromised. While the PAM₂CS methylester compounds are indeed highly active, they are about a fifth as potent as the reference PAM₂CSK₄ lipopeptide. We have found that, as with other amphipathic compounds that we have recently characterized,²⁰⁵ the apparent differences in potencies are related, at least in part, to the substantially higher binding of the more hydrophobic PAM₂CS analogues to albumin present in cell culture media, details of which will be published elsewhere.

4.4 Syntheses and Evaluation of *O*-bridged (21a-b) and Ether (28) Analogs.

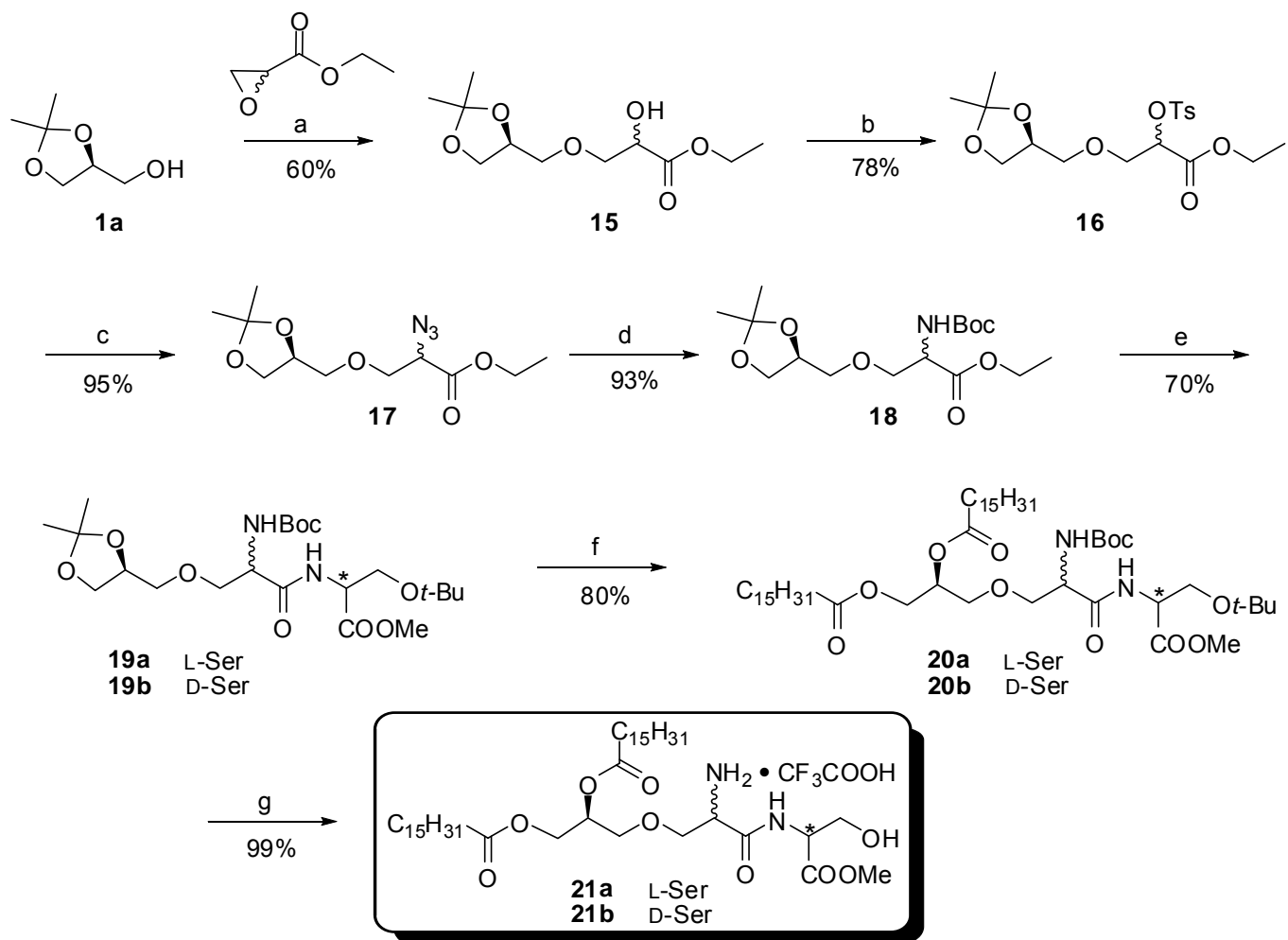
It was of particular interest to examine the role of the thioether bridge between the diacyl and dipeptide units. *O*-alkylation of *S*-1,2-isopropylidenglycerol with racemic ethyl 2,3-epoxypropanoate yielded the key intermediate **15**, from which the ether-bridged compounds were obtained (**21a** and **21b**, **Scheme 3**) in which two of the three stereocenters were held fixed. The activity of **21a** (lipopeptide terminating with L-Ser) was about eight orders of magnitude lower (IC₅₀: 1.2 mM) than that of PAM₂CSK₄ while **21b** (D-Ser) was inactive at the highest concentration tested (10 mM). While these results are indicative of the absolute requirement of the thioether linkage, we do not yet understand why the stereochemistry of the terminal Ser residue manifests in differential activity only in the ether-linked (**21a**, **21b**), but not in the thioether-linked analogues (**14a-d**).

Scheme 2



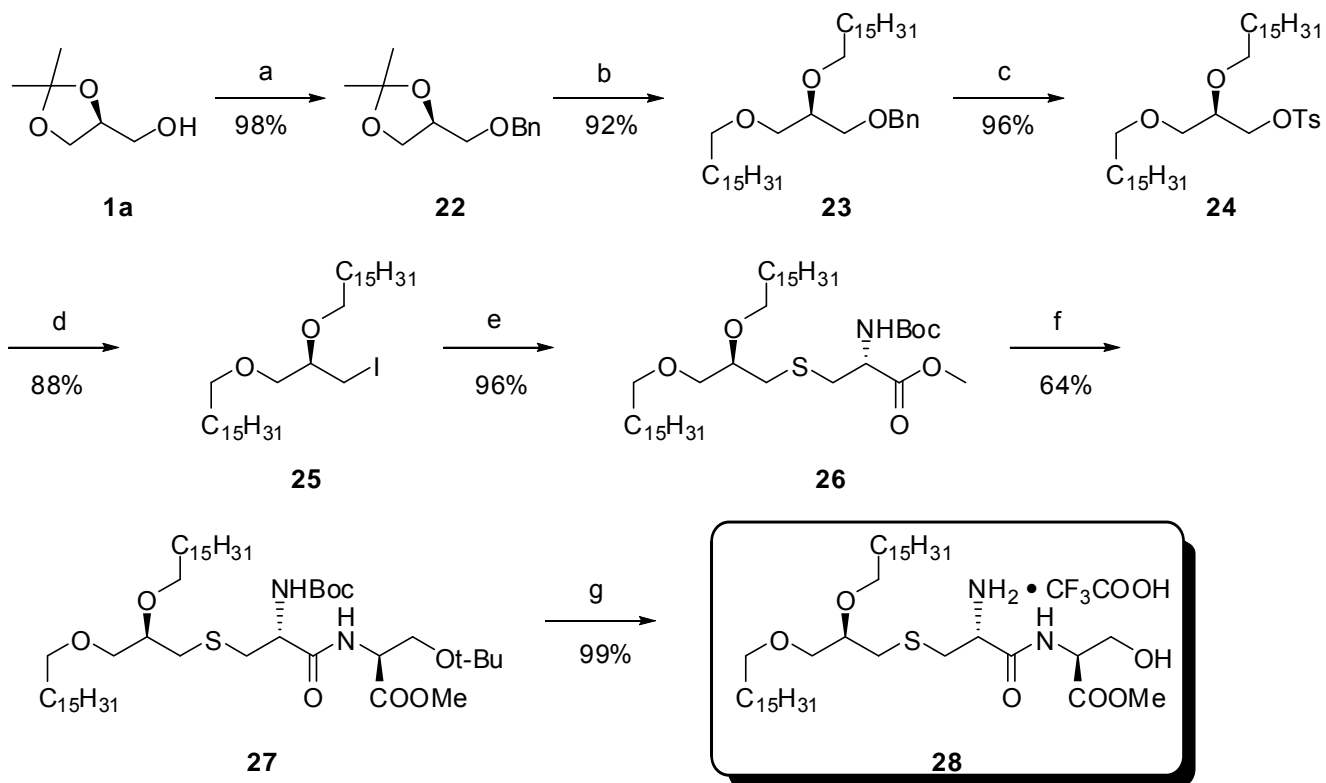
Reagents and conditions: a: PPh_3 , I_2 , imidazole, toluene, 90°C , 2 h;
 b: *N*-Boc-L- or -D-Cys-OMe, TEA, DMF, 85°C , 4 h;
 c: i) 70% AcOH, r.t., 24 h; ii) $\text{C}_{15}\text{H}_{31}\text{COCl}$, pyr, DMAP, DCM, 0°C -r.t., 12 h;
 iii) TFA, r.t., 30 min.
 d: i) LiOH, THF/ H_2O , r.t.; ii) H-L-Ser(OtBu)-OtBu•HCl or H-L-Ser(OtBu)-OMe•HCl
 or H-D-Ser(OtBu)-OMe•HCl, EDCI, EDIPA, DMAP, DCM, 0°C -r.t., 8 h;
 e: i) 70% AcOH, r.t., 12 h; ii) $\text{C}_{15}\text{H}_{31}\text{COCl}$, pyr, DMAP, DCM, 0°C -r.t., 10 h;
 f: TFA, r.t., 30 min.

Scheme 3



Reagents and conditions: a: Ethyl 2,3-epoxypropanoate, $\text{BF}_3 \cdot \text{OEt}_2$, DCM, r.t., 5 h;
 b: p-TsCl, TEA, DCM, 0°C -r.t., 3 h;
 c: NaN_3 , DMF, r.t., 12 h;
 d: i) PPh_3 , H_2O , THF, reflux, 6 h; ii) Boc_2O , TEA, DCM, r.t., 12 h;
 e: i) LiOH, THF/ H_2O , r.t., 12 h; ii) H-L-Ser(*t*Bu)-OMe•HCl or H-D-Ser(*t*Bu)-OMe•HCl, EDCI, EDIPA, DMAP, DCM, 0°C -r.t., 12 h;
 f: i) 70% AcOH, r.t., 12 h; ii) $\text{C}_{15}\text{H}_{31}\text{COCl}$, pyr, DMAP, DCM, 0°C -r.t., 12 h;
 g: TFA, r.t., 30 min.

Scheme 4



Reagents and conditions: a: BnBr, NaH, DMF, 0 °C- r.t., 8 h;
 b: i) 70% AcOH, r.t., 12 h; ii) C₁₆H₃₃I, NaH, DMF, 0 °C- r.t., 8 h;
 c: i) Pd/C, H₂; ii) TsCl, pyr, DMAP, DCM, 70 °C, 12 h;
 d: I₂, KI, DMF, 80 °C, 24 h;
 e: Boc-L-Cys-OMe, TEA, DMF, 80 °C, 2 h;
 f: i) LiOH, THF/H₂O, r.t., 4h; ii) H-L-Ser(*t*Bu)-OMe•HCl, EDCI, EDIPA, DMAP,
 DCM, 0 °C-r.t., 8 h;
 g: TFA, r.t., 30 min.

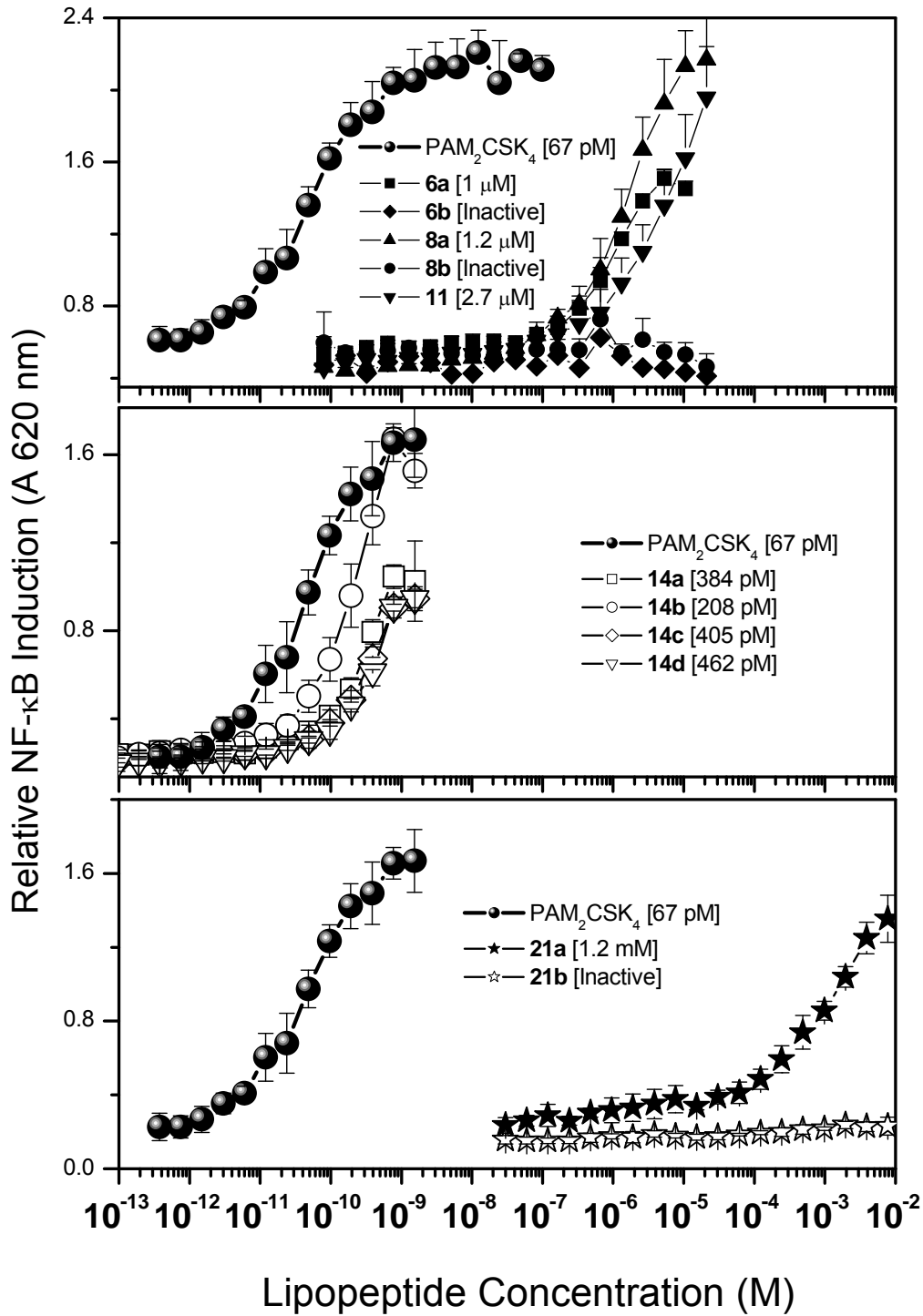


Figure 24 TLR2 agonistic activities of the lipopeptide analogues. HEK293 cells stably transfected with a TLR2-NF- κ B-SEAP reporter gene was used in a 384 well format. Data points represent means and sd determined on triplicate samples.

We next tested whether the ester-linked palmitoyl groups could be replaced with potentially hydrolytically more stable ether and amide linkages without compromising activity. Synthesis of analogue **28** with the ether-linked C₁₆ hydrocarbon appendages could not be obtained by direct *O*-alkylation of an advanced intermediate such as the deprotected species from series **12** under a variety of conditions. This necessitated the installation of the ether-linked C₁₆ groups on the glycerol backbone (**23**) first, followed by transformation of the free hydroxyl to the iodo intermediate (**25**), and subsequent *S*-alkylation with cysteine. We found that the ether analogue **28** was entirely inactive (**Figure 25**).

4.5 Syntheses and Evaluation of Monoamide (37) and Diamide (45) Analogs.

We next investigated the bioisoteric replacement of one (internal, secondary alcohol-derived; **Scheme 5**) ester as well as both the esters (**Scheme 6**) with amide-linked hydrocarbon chains. Synthesis of the monoamide analogue **37** proceeded smoothly starting from D-Ser-OMe (**29**). The diamide analogue, **45**, however, was more problematic to synthesize. Acetonide deprotection of the monoamide precursor **35**, followed by attempts at converting the free hydroxyl group to the amine via an azide intermediate was unsuccessful. The strategy of first *N*-acylating (*R*)-methyl 2,3-diaminopropanoate with palmitoyl chloride, and then converting the ester to the iodo via the alcohol as described in **Scheme 5** was also not fruitful because of unexpected difficulty in the conversion of the alcohol to the iodo group. This is probably due either to steric bulk of the long-chain amides or to an internal H-bond between the

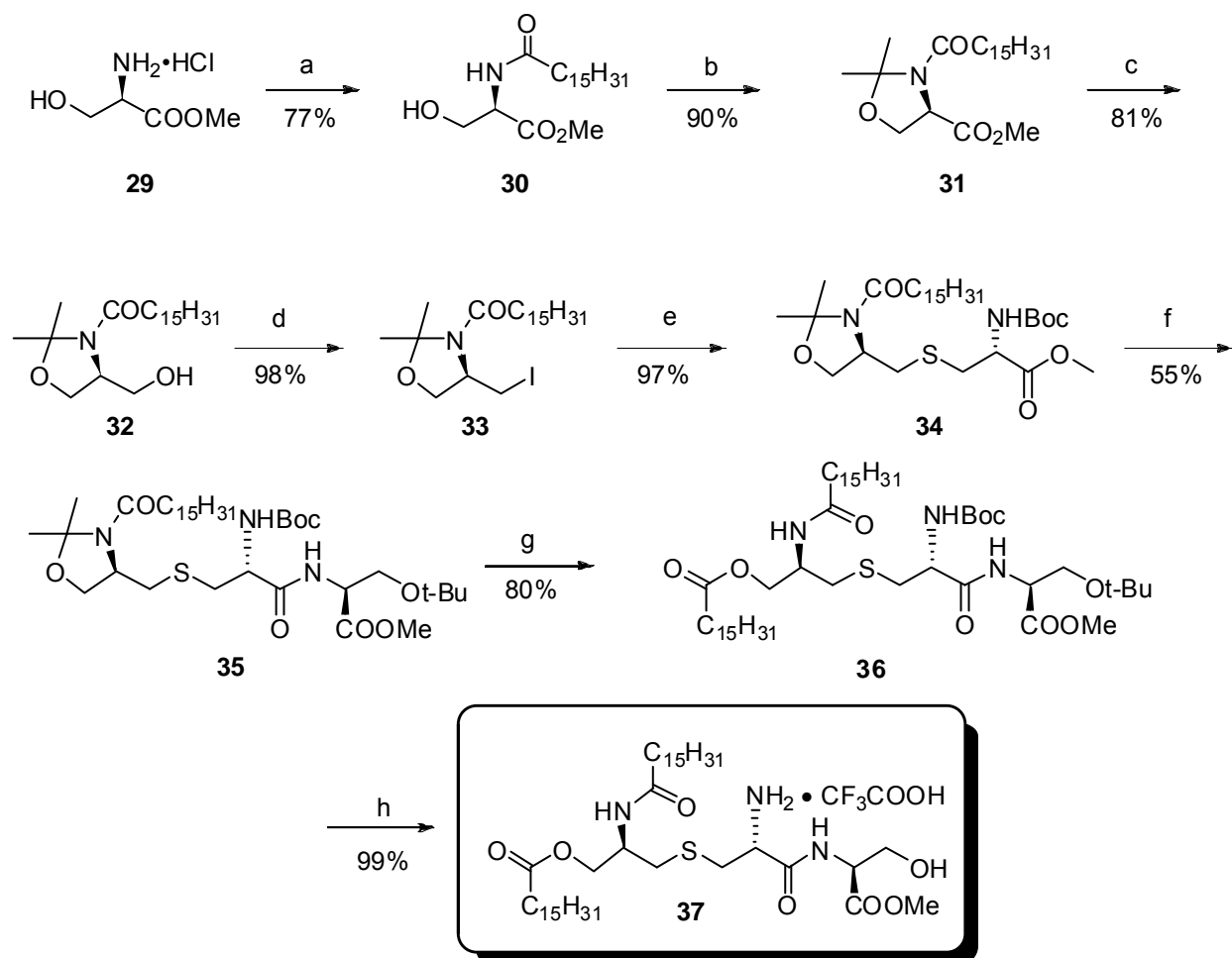
free alcohol and one of the amide groups. We therefore resorted to first installing the iodo on a N, N'-di-Boc-protected 2,3-diaminopropane-1-ol, followed by *S*-alkylation with *N*-Troc-L-Cys-OMe (**Scheme 6**), affording the required orthogonality of the protecting groups. The amines on the diaminopropane-thiol fragment of compound **41** were then acylated with hexadecanoic acid. Next, the base-labile *N*-Troc protecting group on the cysteine unit had to be converted to the *N*-Boc derivative in order to carry out subsequent base-catalyzed de-esterification step. Coupling of the terminal Ser residue proceeded smoothly.

The monoamide derivative **37** was found to be partially active (IC₅₀: 48 nM, **Figure 25**), although weaker by about three orders of magnitude compared to the reference lipopeptide PAM₂CSK₄. The diamide derivative **45** was completely inactive. The progressive loss of activity from the monoamide to the diamide analogue suggests that both ester groups are important for maximal TLR2-stimulatory activity, although this is yet to be formally tested by synthesizing the regioisomer of **37** with the amide group replacing the external (primary alcohol-derived) ester group.

We were also keen to test the possibility that some of the inactive compounds could perhaps behave as TLR2 antagonists, particularly with **8a** and **8b**, since we had designed these compounds with inverted cysteamine-serine amide bonds in the hope that this would be the case. It could be noted in this context that TLR2-mediated immunopathology has been implicated in a number of inflammatory bowel diseases,²⁰⁶⁻²⁰⁹ and the only reported TLR2 receptor antagonists are rather weak lipolanthionine derivatives.²¹⁰ Although we were disappointed that **6a-6b**, **21a-b**, **28**,

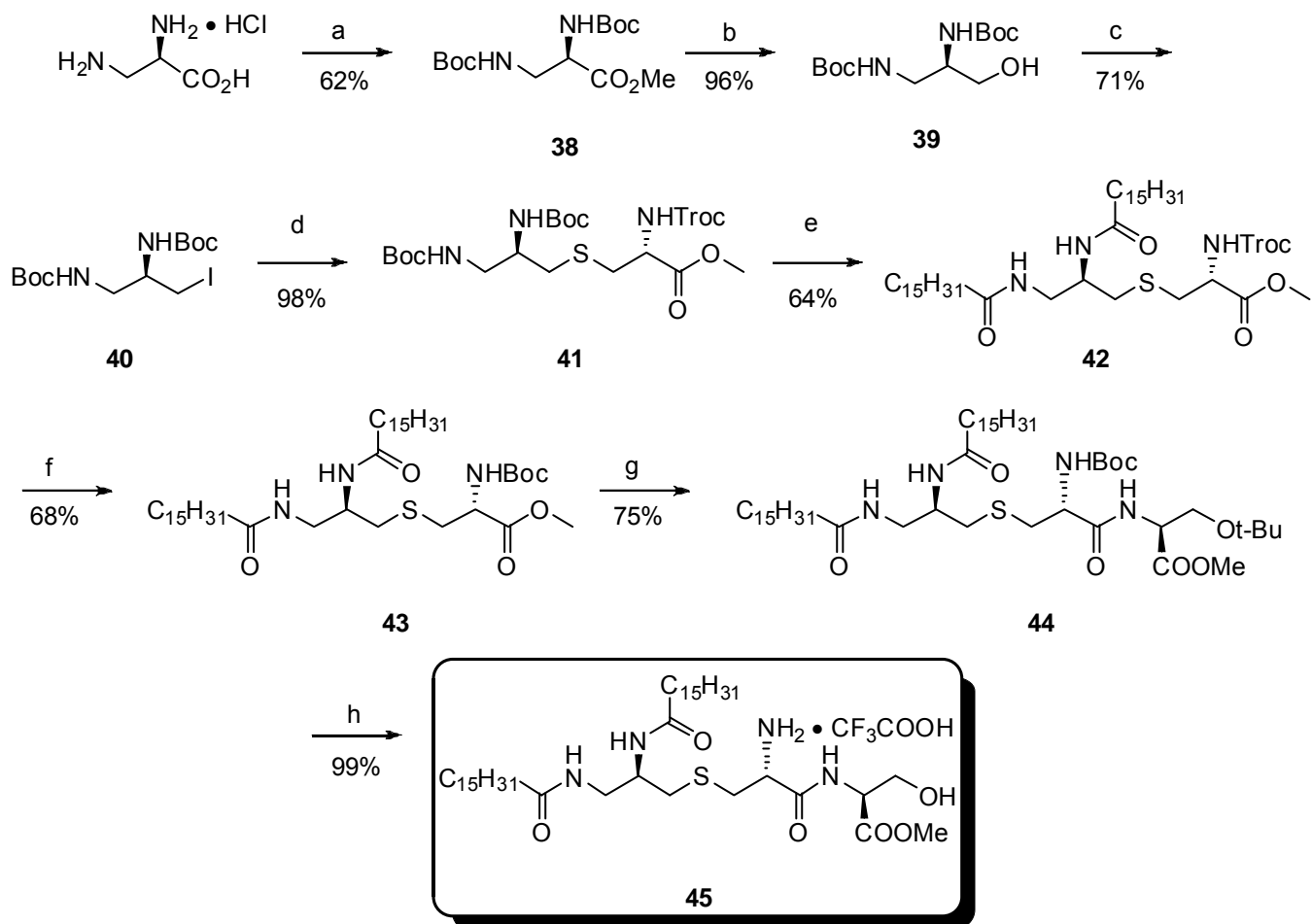
37 and **45** were all inactive as TLR2 receptor antagonists, the negative results add to the SAR data in that they demonstrate that these compounds do not bind to and engage TLR2.

Scheme 5



Reagents and conditions: a: $C_{15}H_{31}COCl$, aq. $NaHCO_3$, EtOAc, r.t., 1h; b: 2,2-DMP, PPTS, toluene, 90 °C, 22h; c: $LiBH_4$, THF, 0°C(3h) - r.t.(6h); d: PPh_3 , I_2 , toluene, 90°C, 2 h; e: Boc-L- or -D-Cys-OMe, TEA, DMF, 80°C, 2 h; f: i) $Ba(OH)_2$, CH_3CN/H_2O , 60 °C, 1h; ii) H-L-Ser(*t*Bu)-OMe · HCl, EDCI, EDIPA, DMAP, DCM, 0°C- r.t., 8h; g: i) 70% AcOH, r.t., 12h; ii) $C_{15}H_{31}COCl$, pyr, DMAP, DCM, 0°C-r.t., 10h; h: TFA, r.t., 30 min.

Scheme 6



Reagents and conditions: a: i) $(\text{Boc})_2\text{O}$, TEA, DCM, r.t., 2 h; ii) MeOH, EDCI, HOBT, TEA, DMAP, DCM, 10h;
 b: NaBH_4 , MeOH, THF, reflux, 4h;
 c: I_2 , PPh_3 , imidazole, DCM, 0 °C-rt, 2h;
 d: *N*-Troc-L-cysteine methyl ester, TEA, DMF, 85 °C, 2h;
 e: i) TFA, r.t., 30 min; ii) $\text{C}_{15}\text{H}_{31}\text{COOH}$, EDCI, HOBT, TEA, DMAP, DMF, 60 °C, 10h;
 f: i) Zn dust, AcOH, H_2O , THF, r.t., 1h; ii) $(\text{Boc})_2\text{O}$, TEA, DCM, r.t., 1h;
 g: i) $\text{Ba}(\text{OH})_2$, THF/ H_2O , 60 °C, 1h; ii) L-Ser(*t*-Bu)-OMe • HCl, EDCI, HOBT, EDIPA, DMAP, DMF, 60°C, 10h;
 h: TFA, r.t., 30 min.

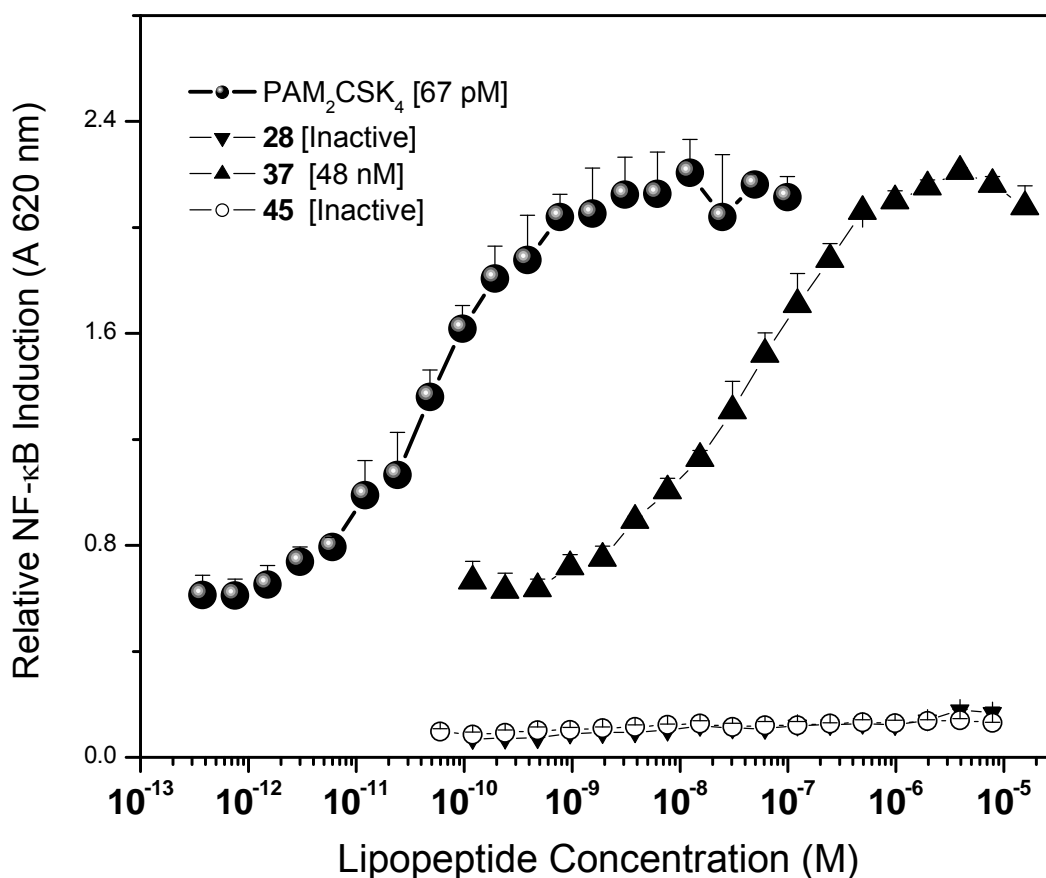


Figure 25 TLR2 agonistic activities of the lipopeptide analogues (continued).

In addition to the lipopeptides being potentially useful as immunotherapeutic agents for cancer, they also display potent adjuvant properties. Lipopeptides greatly enhance MHC Class I-restricted CTL proliferation to an immunodominant influenza peptide Mx₅₈₋₆₆ in a human autologous DC/CD8⁺ T cell co-culture model.¹⁷⁴ Lipopeptide-primed dendritic cells also stimulate the proliferation of allogeneic naïve CD8⁺ CTLs,¹⁷⁴ and immunization of mice with influenza-specific peptide results in greatly enhanced numbers of interferon- γ -secreting CD8⁺ CTLs when lipopeptides

were used as adjuvants.¹⁷⁵ Similarly, MALP-2 induces robust, long-lived CTL responses against HIV-1 Tat protein.^{176,177} The synthetic methods that we have developed are easily scalable, and the availability of a free amino group in PAM₂CS should allow the facile introduction of electrophilic labels such as isothiocyanate for covalent coupling to vaccine antigens. Differential protein binding should also allow considerable control of pharmacokinetic properties. These are currently being investigated.

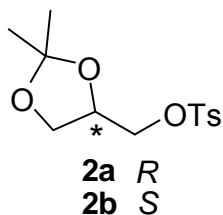
4.6 Conclusions.

The SAR exploration of the diacylthioglycerol lipopeptide compounds revealed the essential role of the dipeptide unit as well as the thio-linkage. The ester linkages on the diacyl hydrocarbon chains were also among the determinants for TLR2 agonistic activity, with replacement with ether or amide bonds leading to a dramatic loss in activity. The analog with one ester-linkage (internal) substituted by an amide linkage turned out to be merely partially active.

4.7 Experimental Data.

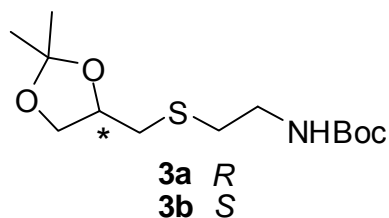
4.7.1 Experimental Procedures

4.7.1.1 Scheme 1:



Syntheses of Compounds 2a ((*R*)-(2,2-dimethyl-1,3-dioxolan-4-yl)methyl 4-methylbenzenesulfonate and 2b ((*S*)-(2,2-dimethyl-1,3-dioxolan-4-yl)methyl 4-methylbenzenesulfonate).

O-tosylation of (*S*)-(+)- **[1a]** and (*R*)-(-)-2,2-dimethyl-1,3-dioxolane-4-methanol **[1b]**. To enantiopure (*S*)-(+)- or (*R*)-(-)-2,2-dimethyl-1,3-dioxolane-4-methanol (compounds **1a** and **1b**, respectively, 1.0 g, 7.57 mmol, Sigma-Aldrich, Inc., St. Louis, MO) dissolved in anhydrous DCM (30 mL) and cooled to 0 °C was added pyridine (1.22 mL, 15.14 mmol), followed by *p*-toluenesulfonyl chloride (*p*-TsCl; 2.89 g, 22.70 mmol). The reaction solution was brought to r.t. and stirred for 8 h. After removal of solvent under vacuum, the residue was purified by flash column chromatography (hexane:EtOAc = 49:1) to afford the literature compounds **2a** (*R*) and **2b** (*S*) in 96-98% yields.^{211;212}

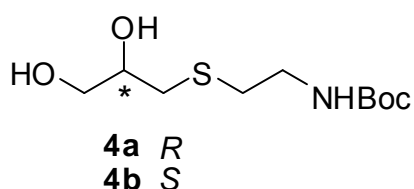


Syntheses of Compounds 3a ((*R*)-*tert*-butyl 2-((2,2-dimethyl-1,3-dioxolan-4-yl)methylthio) ethylcarbamate) and 3b ((*S*)-*tert*-butyl 2-((2,2-dimethyl-1,3-dioxolan-4-yl)methylthio) ethylcarbamate).

To a solution of **2a** or **2b** (800 mg, 2.80 mmol) in anhydrous DMF (15 mL) cooled to 0 °C was added sodium hydride (NaH; 101 mg, 4.19 mmol). After stirring for 30 min at 0 °C, *N*-Boc-cysteamine (*N*-Boc-2-aminoethanethiol; 595 mg, 3.36 mmol) was added dropwise. The reaction solution was then brought to r.t. and stirred for 8 h. After quenching unreacted NaH with 1 M HCl, the solvent was removed under reduced pressure, and the residue was dissolved in EtOAc and washed with water. The water layer was extracted thrice with EtOAc. The combined organic layers were washed with brine and dried over Na₂SO₄. After removal of solvent under reduced pressure, the residue was purified by flash column chromatography (hexane:EtOAc = 5:1) to afford the title compounds **3a** and **3b** as colorless oils (90-94%).

3a: ¹H NMR (400 MHz, CDCl₃) δ 4.98 (d, *J* = 27.4, 1H), 4.22 (p, *J* = 6.2, 1H), 4.07 (dd, *J* = 6.1, 8.3, 1H), 3.67 (dd, *J* = 6.4, 8.3, 1H), 3.35 (m, 2H), 2.78 – 2.58 (m, 4H), 1.41 (s, 9H), 1.40 (s, 3H), 1.32 (s, 3H). ¹³C NMR (126 MHz, CDCl₃) δ 155.78, 109.67, 79.48, 75.58, 68.82, 39.79, 33.01, 28.40, 26.90, 25.55. MS (ESI) calculated for C₁₃H₂₅NO₄S, *m/z* 291.15, found 292.16 (M+H)⁺ and 314.14 (M+Na)⁺.

3b: ^1H NMR (400 MHz, CDCl_3) δ 4.92 (s, 1H), 4.23 (p, $J = 6.2$, 1H), 4.12 – 4.04 (m, 1H), 3.68 (dd, $J = 6.4, 8.3$, 1H), 3.31 (m, 2H), 2.79 – 2.58 (m, 4H), 1.43 (s, 9H), 1.41 (d, $J = 0.4$, 3H), 1.34 (s, 3H). ^{13}C NMR (126 MHz, CDCl_3) δ 155.78, 109.65, 79.45, 75.57, 68.81, 39.80, 24.95, 32.98, 28.40, 26.89, 25.55. MS (ESI) calculated for $\text{C}_{13}\text{H}_{25}\text{NO}_4\text{S}$, m/z 291.15, found 292.15 ($\text{M}+\text{H}^+$) and 314.14 ($\text{M}+\text{Na}^+$).

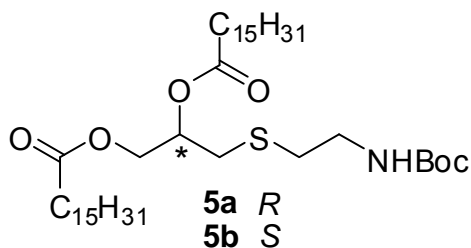


Syntheses of Compounds 4a ((*R*)-*tert*-butyl 2-(2,3-dihydroxypropylthio)-ethylcarbamate) and 4b ((*S*)-*tert*-butyl 2-(2,3-dihydroxypropylthio)-ethylcarbamate).

Acetonide deprotection of compounds **3a** and **3b** (900 mg, 3.09 mmol) was achieved by adding 70% acetic acid ($\text{AcOH}:\text{H}_2\text{O} = 7:3$) and stirring at r.t. for 12 h. After removal of solvent under vacuum, the reaction residue was dissolved in EtOAc, and washed with sat. NaHCO_3 solution. The aqueous layer was extracted thrice with EtOAc. The combined EtOAc layers were washed with brine and dried over Na_2SO_4 . After removal of solvent under vacuum, the residue was purified by flash column chromatography (hexane:EtOAc = 3:1) to afford the title compounds **4a** and **4b** (88-91%).

4a: ^1H NMR (400 MHz, CDCl_3) δ 7.78 (d, $J = 8.3$, 1H), 7.34 (d, $J = 8.0$, 1H), 4.93 (s, 1H), 3.85 – 3.75 (m, 1H), 3.70 (dt, $J = 5.2, 10.3$, 1H), 3.55 (dd, $J = 5.9, 11.3$, 1H), 3.31 (d, $J = 5.3$, 2H), 2.77 – 2.57 (m, 4H), 1.42 (s, 9H). ^{13}C NMR (126 MHz, CDCl_3) δ 156.20, 79.80, 70.40, 65.26, 39.85, 35.53, 32.96, 28.40. MS (ESI) calculated for $\text{C}_{10}\text{H}_{21}\text{NO}_4\text{S}$, m/z 251.12, found 252.13 ($\text{M}+\text{H}$) $^+$ and 274.11 ($\text{M}+\text{Na}$) $^+$.

4b: ^1H NMR (400 MHz, CDCl_3) δ 7.50 (s, 1H), 6.98 (s, 1H), 4.87 (s, 1H), 3.79 (ddd, $J = 4.2, 6.9, 12.0$, 1H), 3.75 – 3.68 (m, 1H), 3.55 (dt, $J = 5.6, 11.3$, 1H), 3.32 (d, $J = 3.9$, 2H), 2.78 – 2.55 (m, 4H), 1.43 (s, 9H). MS (ESI) calculated for $\text{C}_{10}\text{H}_{21}\text{NO}_4\text{S}$, m/z 251.34, found 252.13 ($\text{M}+\text{H}$) $^+$ and 274.12 ($\text{M}+\text{Na}$) $^+$.



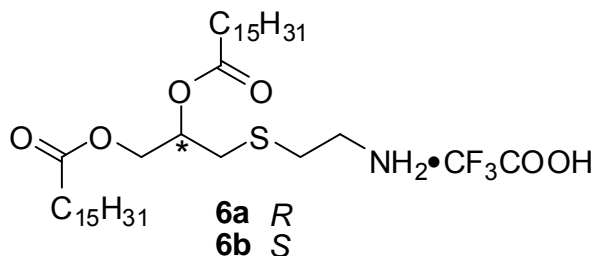
Syntheses of Compounds 5a ((*R*)-3-(2-(*tert*-butoxycarbonylamino)ethylthio)propane-1,2-diyl dipalmitate) and 5b ((*S*)-3-(2-(*tert*-butoxycarbonylamino)ethylthio)propane-1,2-diyl dipalmitate).

O-palmitoylation of compounds **5a** and **5b**. To a solution of compound **4a** and **4b** (200 mg, 0.80 mmol) in anhydrous DCM (8 mL) at 0 °C were added pyridine (385 μL , 4.78 mmol) and a catalytic amount of 4-(dimethylamino)pyridine (DMAP). Palmitoyl chloride (876 mg, 3.19 mmol) was then added dropwise and the reaction was brought to r.t., after which the reaction solution was stirred for 10 h. The reaction

mixture was sequentially washed with water, sat. NaHCO₃, brine, and then dried over Na₂SO₄. After removal of solvent under vacuum, the residue was purified by flash column chromatography (hexane:EtOAc = 8:1) to afford the title compounds **5a** and **5b** as white solids (90-92%).

5a: ¹H NMR (400 MHz, CDCl₃) δ 5.12 (m, 1H), 4.88 (s, 1H), 4.34 (dd, *J* = 3.5, 11.9, 1H), 4.15 (dd, *J* = 6.0, 11.9, 1H), 3.30 (d, *J* = 6.1, 2H), 2.68 (dd, *J* = 6.5, 11.5, 4H), 2.38 – 2.24 (m, 4H), 1.62 – 1.54 (m, 4H), 1.42 (s, 9H), 1.25 (d, *J* = 10.6, 48H), 0.86 (t, *J* = 6.9, 6H). ¹³C NMR (126 MHz, CDCl₃) δ 173.42, 173.16, 155.77, 79.50, 70.30, 63.56, 39.59, 34.31, 34.12, 43.14, 31.94, 29.72, 29.69, 29.66, 29.61, 29.52, 29.46, 29.38, 29.31, 29.26, 29.15, 29.13, 29.09, 28.39, 24.91, 24.74, 22.71, 14.15. MS (ESI) calculated for C₄₂H₈₁NO₆S, *m/z* 727.58, found 728.59 (M+H)⁺ and 750.57 (M+Na)⁺.

5b: ¹H NMR (400 MHz, CDCl₃) δ 5.12 (m, 1H), 4.88 (s, 1H), 4.34 (dd, *J* = 3.5, 11.9, 1H), 4.15 (dd, *J* = 6.0, 11.9, 1H), 3.30 (d, *J* = 6.1, 2H), 2.68 (dd, *J* = 6.4, 11.5, 4H), 2.34 – 2.25 (m, 4H), 1.64 – 1.56 (m, 4H), 1.42 (s, 9H), 1.23 (s, 48H), 0.86 (t, *J* = 6.8, 6H). MS (ESI) calculated for C₄₂H₈₁NO₆S, *m/z* 727.58, found 728.59 (M+H)⁺ and 750.57 (M+Na)⁺.

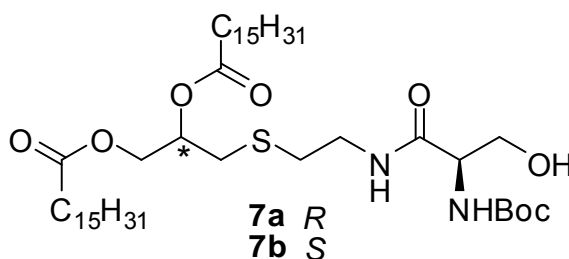


General procedure for *N*-Boc deprotection: Syntheses of Compounds 6a ((*R*)-3-(2-aminoethylthio)propane-1,2-diyl dipalmitate) and 6b ((*S*)-3-(2-aminoethylthio)propane-1,2-diyl dipalmitate).

To **5a** and **5b** was added excess dry trifluoroacetic acid (TFA) and stirred at r.t. for 30 min. TFA was removed by purging nitrogen and the residue was thoroughly washed with diethyl ether to obtain the title compounds as flaky white solids (98-100%).

6a: ^1H NMR (400 MHz, DMSO) δ 7.83 (s, 1H), 5.18 – 5.06 (m, 1H), 4.30 (dd, $J = 2.7, 11.9$, 1H), 4.10 (dd, $J = 7.2, 12.0$, 1H), 2.99 (t, $J = 7.2$, 2H), 2.90 – 2.65 (m, 4H), 2.32 – 2.14 (m, 4H), 1.58 – 1.42 (m, 4H), 1.23 (s, 48H), 0.84 (t, $J = 6.8$, 6H). ^{13}C NMR (126 MHz, DMSO) δ 172.47, 172.29, 69.64, 63.47, 33.62, 33.53, 33.37, 31.29, 30.87, 29.06, 29.03, 29.01, 28.93, 28.75, 28.71, 28.50, 28.42, 28.38, 24.47, 24.38, 22.08, 13.91. MS (ESI) calculated for $\text{C}_{37}\text{H}_{73}\text{NO}_4\text{S}$, m/z 627.53, found 628.51 ($\text{M}+\text{H}$) $^+$.

6b: ^1H NMR (400 MHz, DMSO) δ 7.80 (s, 1H), 5.16 – 5.05 (m, 1H), 4.30 (dd, $J = 2.8, 11.9$, 1H), 4.10 (dd, $J = 7.1, 12.0$, 1H), 2.99 (t, $J = 7.1$, 2H), 2.87 – 2.65 (m, 4H), 2.33 – 2.20 (m, 4H), 1.50 (d, $J = 6.2$, 4H), 1.23 (s, 48H), 0.84 (t, $J = 6.8$, 6H). MS (ESI) calculated for $\text{C}_{37}\text{H}_{73}\text{NO}_4\text{S}$, m/z 627.53, found 628.51 ($\text{M}+\text{H}$) $^+$.

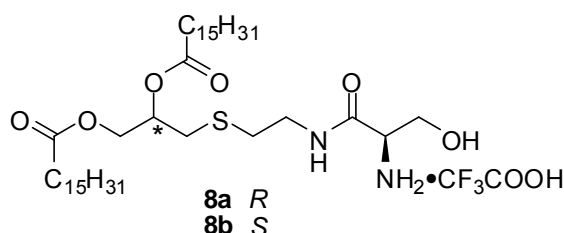


Syntheses of Compounds 7a ((6*R*,13*R*)-6-(hydroxymethyl)-2,2-dimethyl-4,7-dioxo-3-oxa-11-thia-5,8-diazatetradecane-13,14-diyl dipalmitate) and 7b ((6*S*,13*R*)-6-(hydroxymethyl)-2,2-dimethyl-4,7-dioxo-3-oxa-11-thia-5,8-diazatetradecane-13,14-diyl dipalmitate).

The terminal L-serine of the dipeptide unit was appended to **6a** and **6b** by conventional solution phase coupling procedures. To **6a** and **6b** (200 mg, 0.27 mmol) in anhydrous DCM (8 mL) at 0 °C were added Boc-L-Ser-OH (Bachem Americas, Inc., Torrance, CA, 83 mg, 0.40 mmol), (3-dimethylaminopropyl)-*N*'-ethylcarbodiimide hydrochloride (EDCI; 103 mg, 0.54 mmol), *N,N*-diisopropylethylamine (EDIPA; 53.4 μ L, 0.32 mmol), and a catalytic amount of DMAP. The reaction mixture was stirred at 0 °C for 30 min, and then brought to r.t., and stirred for an additional 8 h. After removal of solvent under vacuum, the residue was purified by flash column chromatography (hexane:EtOAc = 3:2) to afford the title compounds **7a** or **7b** as white solids (75-80%).

7a: ^1H NMR (400 MHz, CDCl_3) δ 6.92 (s, 1H), 5.54 (s, 1H), 5.11 (dt, $J = 5.0, 9.8$, 1H), 4.36 (dd, $J = 3.3, 11.9$, 1H), 4.16 – 4.04 (m, 3H), 3.64 (s, 1H), 3.56 – 3.37 (m, 2H), 2.90 (s, 1H), 2.77 – 2.61 (m, 4H), 2.29 (td, $J = 4.5, 7.5$, 4H), 1.58 (s, 4H), 1.44 (s, 9H), 1.23 (s, 48H), 0.86 (t, $J = 6.8$, 6H). ^{13}C NMR (126 MHz, CDCl_3) δ 172.30, 172.13, 170.33, 154.96, 79.32, 69.11, 62.38, 61.73, 53.57, 37.04, 33.11, 32.90, 31.01, 30.72, 28.50, 28.46, 28.44, 28.29, 28.16, 28.09, 27.92, 27.10, 23.68, 21.49, 12.92. MS (ESI) calculated for $\text{C}_{45}\text{H}_{86}\text{N}_2\text{O}_8\text{S}$, m/z 814.61, found 837.56 (M+Na) $^+$.

7b: ^1H NMR (400 MHz, CDCl_3) δ 6.91 (s, 1H), 5.53 (s, 1H), 5.12 (qd, $J = 3.4, 6.5$, 1H), 4.35 (dd, $J = 3.4, 11.9$, 1H), 4.16 – 4.03 (m, 3H), 3.64 (s, 1H), 3.57 – 3.34 (m, 2H), 2.91 (s, 1H), 2.78 – 2.61 (m, 4H), 2.29 (td, $J = 4.1, 7.6$, 4H), 1.60 (s, 4H), 1.44 (s, 9H), 1.23 (s, 48H), 0.86 (t, $J = 6.8$, 6H). MS (ESI) calculated for $\text{C}_{45}\text{H}_{86}\text{N}_2\text{O}_8\text{S}$, m/z 814.61, found 837.56 ($\text{M}+\text{Na}$) $^+$.



Syntheses of Compounds 8a ((*R*)-3-(2-((*R*)-2-amino-3-hydroxypropanamido)ethylthio)propane-1,2-diyl dipalmitate) and 8b ((*S*)-3-(2-((*R*)-2-amino-3-hydroxypropanamido)ethylthio)propane-1,2-diyl dipalmitate).

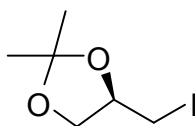
7a and **7b** were deprotected with TFA as described earlier in the general procedure for *N*-Boc deprotection (see syntheses of **6a**, **6b**). The title compounds were obtained as flaky white solids (99-100%).

8a: ^1H NMR (400 MHz, DMSO) δ 8.51 (t, $J = 5.7$, 1H), 8.08 (s, 1H), 5.47 (s, 1H), 5.08 (dd, $J = 4.5, 11.4$, 1H), 4.31 (dd, $J = 2.7, 11.9$, 1H), 4.10 (dd, $J = 7.1, 12.0$, 1H), 3.69 (dd, $J = 9.1, 33.4$, 3H), 3.28 (dd, $J = 6.5, 13.3$, 2H), 2.74 (ddd, $J = 6.6, 14.1, 21.4$, 2H), 2.62 (t, $J = 6.9$, 2H), 2.32 – 2.19 (m, 4H), 1.56 – 1.45 (m, 4H), 1.23 (s, 48H), 0.85 (t, $J = 6.8$, 6H). ^{13}C NMR (126 MHz, DMSO) δ 172.50, 172.27, 166.69, 69.88, 63.45, 60.27, 54.35, 38.52, 33.55, 33.37, 31.28, 31.04, 30.80, 29.05, 29.02,

29.00, 28.92, 28.91, 28.74, 28.71, 28.70, 28.41, 28.36, 24.47, 24.39, 22.08, 13.92. MS (ESI) calculated for C₄₀H₇₈N₂O₆S, *m/z* 714.56, found 715.54 (M+H)⁺.

8b: ¹H NMR (400 MHz, DMSO) δ 8.51 (t, *J* = 5.4, 1H), 8.08 (s, 1H), 5.48 (s, 1H), 5.09 (d, *J* = 5.8, 1H), 4.30 (dd, *J* = 2.6, 11.9, 1H), 4.10 (dd, *J* = 7.1, 11.9, 1H), 3.85 – 3.57 (m, 3H), 3.32 – 3.26 (m, 2H), 2.80 (dd, *J* = 5.8, 14.1, 1H), 2.65 (ddd, *J* = 7.0, 13.9, 20.3, 3H), 2.31 – 2.22 (m, 4H), 1.50 (d, *J* = 6.8, 4H), 1.23 (s, 48H), 0.84 (t, *J* = 6.7, 6H). ¹³C NMR (126 MHz, DMSO) δ 172.85, 172.63, 167.10, 70.25, 63.84, 60.65, 54.71, 38.92, 33.92, 33.75, 31.66, 31.42, 31.17, 29.44, 29.41, 29.39, 29.30, 29.13, 29.10, 29.09, 28.80, 28.75, 24.80, 22.46, 14.18. MS (ESI) calculated for C₄₀H₇₈N₂O₆S, *m/z* 714.56, found 715.54 (M+H)⁺.

4.7.1.2 Scheme 2:



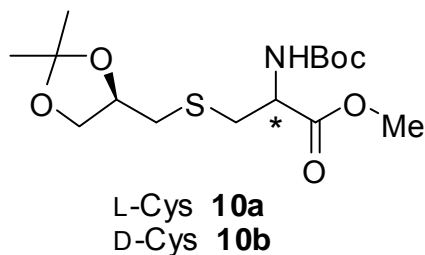
9

Synthesis of Compound 9 ((*R*)-4-(iodomethyl)-2,2-dimethyl-1,3-dioxolane).

To a solution of (*S*)-(+)-2,2-dimethyl-1,3-dioxolane-4-methanol (compound **1a**, 3.0 g, 22.70 mmol) in toluene (50 mL) was added triphenylphosphine (PPh₃; 37.15 g, 27.38 mmol), imidazole (4.64 g, 68.10 mmol) and iodine (7.0 g, 29.51 mmol).²¹³ The reaction mixture was stirred at 90 °C for 2 h. After removal of toluene under reduced

pressure, the residue was dissolved in DCM, washed with sat. Na₂S₂O₃ (to quench the unreacted iodine), brine, and dried over Na₂SO₄. The solvent was then removed under vacuum and the residue was purified by flash column chromatography (hexane:EtOAc = 49:1) to afford the literature compound **9**²¹⁴ as a colorless liquid (5.44 g, 99%).

9: ¹H NMR (400 MHz, CDCl₃) δ 4.30 – 4.21 (m, 1H), 4.12 (dd, *J* = 6.1, 8.6, 1H), 3.76 (dd, *J* = 5.4, 8.6, 1H), 3.23 (dd, *J* = 4.6, 9.8, 1H), 3.12 (dd, *J* = 8.5, 9.8, 1H), 1.43 (s, 1H), 1.32 (s, 3H). ¹³C NMR (126 MHz, CDCl₃) δ 109.47, 74.63, 68.57, 26.11, 24.57, 5.67.



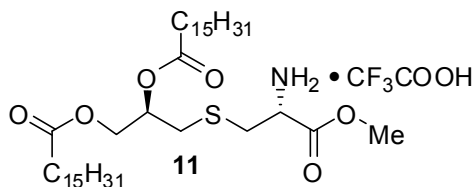
Syntheses of Compounds 10a ((*R*)-methyl 2-(*tert*-butoxycarbonylamino)-3-(((*R*)-2,2-dimethyl-1,3-dioxolan-4-yl)methylthio)propanoate) and 10b ((*S*)-methyl 2-(*tert*-butoxycarbonylamino)-3-(((*R*)-2,2-dimethyl-1,3-dioxolan-4-yl)methylthio)propanoate).

N-Boc protected L- and D- cysteine methyl esters were first obtained by treating H-L- and D-Cys-OMe·HCl (Sigma-Aldrich) with di-*tert*-butyl dicarbonate (Boc₂O; 2.0 eq.) in DCM, followed by slow addition of triethylamine (TEA; 1.0 eq.) at 0 °C. DCM was removed under vacuum after the reaction was stirred at 0 °C for 2 h and the

residue was then purified by flash column chromatography with 10% EtOAc/hexane.) S-alkylation of Boc-L-Cys-OMe and Boc-D-Cys-OMe with **9** were then carried out. Compound **10** was synthesized as follows: to a solution of **9** (900 mg, 3.72 mmol) in anhydrous DMF (8 mL) was added TEA (1.55 mL, 11.15 mmol), followed by Boc-L- or D-Cys-OMe (673 mg, 2.86 mmol). The reaction solution was stirred at 85 °C for 4 h. After removal of DMF under vacuum, the residue was purified by flash column chromatography (hexane:EtOAc = 9:1) to afford **10a** or **10b**, respectively as viscous oils (60-63%).

10a: ¹H NMR (400 MHz, CDCl₃) δ 5.39 (d, *J* = 7.1, 1H), 4.52 (d, *J* = 7.3, 1H), 4.21 (p, *J* = 6.2, 1H), 4.06 (dd, *J* = 6.1, 8.3, 1H), 3.74 (s, 3H), 3.66 (dd, *J* = 6.4, 8.3, 1H), 3.02 (d, *J* = 3.2, 2H), 2.73 (dd, *J* = 6.0, 13.4, 1H), 2.62 (dd, *J* = 6.5, 13.4, 1H), 1.43 (s, 9H), 1.40 (s, 3H), 1.33 (s, 3H). ¹³C NMR (126 MHz, CDCl₃) δ 171.49, 155.23, 109.73, 80.18, 75.64, 68.68, 53.45, 52.58, 38.78, 35.22, 28.31, 26.84, 25.55. MS (ESI) calculated for C₁₅H₂₇NO₆S, *m/z* 349.16, found 372.10 (M+Na)⁺.

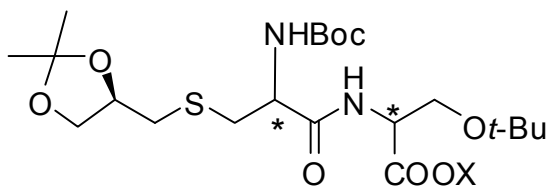
10b: ¹H NMR (400 MHz, CDCl₃) δ 5.43 (d, *J* = 7.0, 1H), 4.52 (s, 1H), 4.26 – 4.18 (m, 1H), 4.06 (dd, *J* = 6.1, 8.3, 1H), 3.76 (d, *J* = 11.0, 3H), 3.66 (dd, *J* = 6.5, 8.3, 1H), 3.02 (ddd, *J* = 5.2, 13.8, 19.4, 2H), 2.75 (dd, *J* = 5.9, 13.5, 1H), 2.63 (dd, *J* = 6.3, 13.5, 1H), 1.43 (s, 9H), 1.41 (s, 3H), 1.34 (s, 3H). ¹³C NMR (126 MHz, CDCl₃) δ 171.49, 155.23, 109.73, 80.18, 75.64, 68.68, 53.45, 52.58, 35.78, 35.22, 28.31, 26.84, 25.55. MS (ESI) calculated for C₁₅H₂₇NO₆S, *m/z* 349.16, found 372.10 (M+Na)⁺.



General procedure for acetonide deprotection and palmitoylation of the 1,2-isopropylidenglycerol unit: Synthesis of Compound 11 ((*R*)-3-((*R*)-2-amino-3-methoxy-3-oxopropylthio)propane-1,2-diyl dipalmitate).

To **10a** (200 mg, 0.57 mmol) was added 15 mL of 70% acetic acid (AcOH:H₂O = 7:3) and the reaction was stirred at r.t. for 24h. After complete removal of AcOH and water under reduced pressure, *O*-palmitoylation of the diol was carried out by sequential addition of pyridine (278 μL, 3.44 mmol), a catalytic amount of DMAP, followed by palmitoyl chloride (709 μL, 2.29 mmol) to the diol dissolved in anhydrous DCM (15 mL) and precooled to 0 °C. After stirring at 0 °C for 30 min, the reaction solution was brought to r.t. and stirred for 8 h. After removal of solvent under vacuum, the residue was purified by flash column chromatography (hexane:EtOAc = 19:1) to afford the *N*-Boc-protected intermediate as a colorless oil. Finally, *N*-Boc deprotection was carried out as described earlier (see syntheses of **6a**, **6b**) to obtain the title compound **11** as a white glassy solid (435 mg, 95%). ¹H NMR (400 MHz, CDCl₃) δ 8.01 (s, 2H), 5.13 (s, 1H), 4.41 – 4.06 (m, 3H), 3.81 (s, 3H), 3.20 (d, *J* = 41.1, 2H), 2.74 (s, 2H), 2.29 (dd, *J* = 7.9, 15.5, 4H), 1.58 (d, *J* = 4.7, 4H), 1.23 (s, 48H), 0.86 (t, *J* = 6.8, 6H). ¹³C NMR (126 MHz, CDCl₃) δ 173.66, 173.63, 168.19, 69.95, 63.47, 53.73, 52.50, 34.24, 34.02, 32.91, 32.46, 31.94, 29.72, 29.70,

29.68, 29.52, 29.38, 29.30, 29.13, 24.85, 22.70, 14.13. MS (ESI) calculated for $C_{39}H_{75}NO_6S$, m/z 685.53, found 686.59 (M+H)⁺.



L-Cys-L-Ser **12a**: X=*t*-Bu; **12b**: X=Me
L-Cys-D-Ser **12c**: X=Me
D-Cys-L-Ser **12d**: X=Me

General Procedure for de-esterification of 10a and 10b, and subsequent coupling of serine: Syntheses of Compounds 12a-d.

10a and **10b** were de-esterified with aqueous LiOH (165 mg, 6.87 mmol dissolved in 6mL water/15 mL THF) at r.t. for 10h. 1 M HCl solution was then added (to quench unreacted LiOH and to convert the lithium salt to the free-acid form) until a pH of 4 was reached. After removal of THF under vacuum, the residue was extracted thrice with DCM. The combined DCM layers were washed with brine and dried over Na_2SO_4 . After removal of DCM under vacuum, H-L-Ser(*t*Bu)-*Ot*Bu·HCl, or H-L-Ser(*t*Bu)-OMe·HCl, or H-D-Ser(*t*Bu)-OMe·HCl (all from Bachem Americas, Inc., Torrance, CA, 437 mg, 2.06 mmol) were coupled to the de-esterified intermediates as described earlier for the syntheses of **7a** and **7b**. After removal of solvent under vacuum, the residue was purified by flash column chromatography (hexane:EtOAc = 4:1) to afford the corresponding compounds **12a-d** as viscous oils (32-38%).

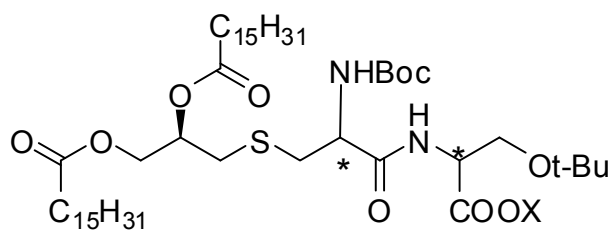
12a ((*S*)-*tert*-butyl 3-*tert*-butoxy-2-((*R*)-2-(*tert*-butoxycarbonylamino)-3-(((*R*)-2,2-dimethyl-1,3-dioxolan-4-yl)methylthio)propanamido)propanoate): ¹H NMR (400 MHz, CDCl₃) δ 7.31 (s, 1H), 5.48 (s, 1H), 4.70 – 4.47 (m, 2H), 4.38 – 4.22 (m, 2H), 4.07 (dd, *J* = 6.1, 8.2, 1H), 3.79 – 3.71 (m, 1H), 3.67 (dd, *J* = 6.6, 8.2, 1H), 3.59 – 3.45 (m, 1H), 3.10 (d, *J* = 6.5, 1H), 2.96 (ddd, *J* = 6.1, 13.9, 43.9, 1H), 2.74 (ddd, *J* = 6.1, 13.5, 44.1, 1H), 1.43 (s, 18H), 1.33 (s, 3H), 1.22 (s, 3H), 1.11 (d, *J* = 4.0, 9H). MS (ESI) calculated for C₂₅H₄₆N₂O₈S, *m/z* 534.30, found 557.29 (M+Na)⁺.

12b ((*S*)-methyl 3-*tert*-butoxy-2-((*R*)-2-(*tert*-butoxycarbonylamino)-3-(((*R*)-2,2-dimethyl-1,3-dioxolan-4-yl)methylthio)propanamido)propanoate): ¹H NMR (400 MHz, CDCl₃) δ 7.07 (d, *J* = 8.3, 1H), 5.48 (s, 1H), 4.71 – 4.59 (m, 1H), 4.41 – 4.22 (m, 2H), 4.15 – 4.02 (m, 1H), 3.80 (dd, *J* = 2.9, 9.1, 1H), 3.72 (s, 3H), 3.68 (dd, *J* = 6.5, 8.3, 1H), 3.55 (dd, *J* = 3.2, 9.1, 1H), 3.06 (ddd, *J* = 5.9, 12.2, 19.8, 1H), 2.98 – 2.87 (m, 1H), 2.85 – 2.76 (m, 1H), 2.71 (dt, *J* = 6.8, 13.5, 1H), 1.44 (s, 9H), 1.42 (s, 3H), 1.34 (s, 3H), 1.12 (s, 9H). ¹³C NMR (126 MHz, CDCl₃) δ 170.47, 170.41, 155.28, 109.70, 75.70, 74.81, 73.52, 68.73, 61.69, 54.10, 53.12, 52.43, 35.61, 35.22, 28.31, 27.30, 26.87, 25.56. MS (ESI) calculated for C₂₂H₄₀N₂O₈S, *m/z* 492.25, found 515.18 (M+Na)⁺.

12c ((*R*)-methyl 3-*tert*-butoxy-2-((*R*)-2-(*tert*-butoxycarbonylamino)-3-(((*R*)-2,2-dimethyl-1,3-dioxolan-4-yl)methylthio)propanamido)propanoate): ¹H NMR (400 MHz, CDCl₃) δ 7.19 (s, 1H), 5.55 (s, 1H), 4.71 (d, *J* = 8.2, 1H), 4.39 (s, 1H), 4.35 – 4.25 (m, 1H), 4.16 – 4.08 (m, 1H), 3.85 (d, *J* = 9.0, 1H), 3.76 (s, 3H), 3.70 (t, *J* = 7.3, 1H), 3.57 (d, *J* = 9.0, 1H), 3.13 (d, *J* = 15.0, 1H), 2.93 (dd, *J* = 6.1, 13.9, 1H), 2.86 –

2.71 (m, 2H), 1.48 (s, 9H), 1.45 (s, 3H), 1.38 (s, 3H), 1.15 (s, 9H). ^{13}C NMR (126 MHz, CDCl_3) δ 170.60, 170.34, 155.39, 109.70, 75.52, 74.79, 73.50, 68.68, 61.75, 53.99, 52.86, 52.41, 35.51, 30.95, 28.31, 27.30, 26.88, 25.52. MS (ESI) calculated for $\text{C}_{22}\text{H}_{40}\text{N}_2\text{O}_8\text{S}$ m/z 492.25, found 515.18 ($\text{M}+\text{Na}$) $^+$.

12d ((*S*)-methyl 3-*tert*-butoxy-2-((*S*)-2-(*tert*-butoxycarbonylamino)-3-(((*R*)-2,2-dimethyl-1,3-dioxolan-4-yl)methylthio)propanamido)propanoate): ^1H NMR (400 MHz, CDCl_3) δ 7.07 (d, $J = 8.3$, 1H), 5.48 (s, 1H), 4.71 – 4.59 (m, 1H), 4.41 – 4.22 (m, 2H), 4.15 – 4.02 (m, 1H), 3.80 (dd, $J = 2.9, 9.1$, 1H), 3.72 (s, 3H), 3.68 (dd, $J = 6.5, 8.3$, 1H), 3.55 (dd, $J = 3.2, 9.1$, 1H), 3.06 (ddd, $J = 5.9, 12.2, 19.8$, 1H), 2.98 – 2.87 (m, 1H), 2.85 – 2.76 (m, 1H), 2.71 (dt, $J = 6.8, 13.5$, 1H), 1.44 (s, 9H), 1.42 (s, 3H), 1.34 (s, 3H), 1.12 (s, 9H). MS (ESI) calculated for $\text{C}_{22}\text{H}_{40}\text{N}_2\text{O}_8\text{S}$, m/z 492.25, found 515.18 ($\text{M}+\text{Na}$) $^+$.



L-Cys-L-Ser **13a**: X=t-Bu; **13b**: X=Me
 L-Cys-D-Ser **13c**: X=Me
 D-Cys-L-Ser **13d**: X=Me

Syntheses of Compounds 13a-d.

Acetonide deprotection followed by *O*-palmitoylation of **12a-d** were performed as per the general procedure outlined earlier (synthesis of compound **11**) to afford the corresponding compounds **13a-d** in 90-95% yields.

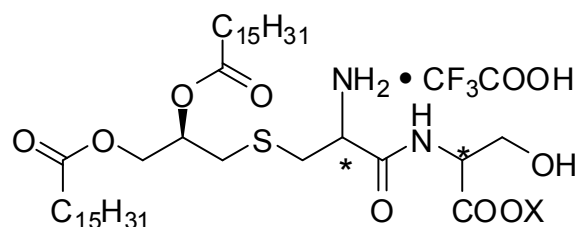
13a ((*R*)-3-((*R*)-2-(*tert*-butoxycarbonylamino)-3-((*S*)-1,3-di-*tert*-butoxy-1-oxopropan-2-ylamino)-3-oxopropylthio)propane-1,2-diyl dipalmitate): ^1H NMR (400 MHz, CDCl_3) δ 7.02 (d, $J = 7.9$, 1H), 5.37 (s, 1H), 5.19 – 5.09 (m, 1H), 4.51 (dt, $J = 2.9$, 8.0, 1H), 4.31 (dd, $J = 3.5$, 11.9, 2H), 4.14 (dd, $J = 5.9$, 11.9, 1H), 3.76 (dd, $J = 2.9$, 8.8, 1H), 3.51 (dd, $J = 3.0$, 8.8, 1H), 2.93 (d, $J = 6.2$, 2H), 2.79 (d, $J = 6.1$, 2H), 2.30 (ddd, $J = 5.8$, 10.8, 12.0, 4H), 1.59 (dd, $J = 6.6$, 12.8, 5H), 1.43 (d, $J = 2.6$, 17H), 1.23 (s, 48H), 1.12 (d, $J = 2.6$, 9H), 0.86 (t, $J = 6.8$, 6H). ^{13}C NMR (126 MHz, CDCl_3) δ 173.40, 173.13, 170.13, 168.92, 81.97, 73.17, 70.32, 63.52, 61.97, 53.51, 35.61, 34.31, 34.11, 33.71, 33.13, 31.94, 29.72, 29.68, 29.66, 29.53, 29.38, 29.33, 29.32, 29.16, 29.15, 28.30, 28.02, 27.34, 24.90, 24.74, 22.71, 14.14. MS (ESI) calculated for $\text{C}_{54}\text{H}_{102}\text{N}_2\text{O}_{10}\text{S}$, m/z 970.73, found 993.82 ($\text{M}+\text{Na}$) $^+$.

13b ((*R*)-3-((*R*)-3-((*S*)-3-*tert*-butoxy-1-methoxy-1-oxopropan-2-ylamino)-2-(*tert*-butoxycarbonylamino)-3-oxopropylthio)propane-1,2-diyl dipalmitate): ^1H NMR (400 MHz, CDCl_3) δ 7.06 (d, $J = 8.1$, 1H), 5.17 (s, 1H), 4.69 – 4.58 (m, 1H), 4.31 (dd, $J = 3.5$, 11.9, 2H), 4.15 (dd, $J = 5.9$, 11.9, 1H), 3.80 (dd, $J = 3.0$, 9.1, 1H), 3.72 (s, 3H), 3.55 (dd, $J = 3.2$, 9.1, 1H), 2.94 (d, $J = 6.1$, 2H), 2.79 (d, $J = 5.9$, 2H), 2.29 (td, $J = 4.9$, 7.5, 4H), 1.59 (s, 4H), 1.43 (s, 9H), 1.23 (s, 48H), 1.12 (s, 9H), 0.86 (t, $J = 6.8$, 6H). ^{13}C NMR (126 MHz, CDCl_3) δ 173.37, 173.14, 170.44, 170.30, 155.22,

73.51, 70.29, 63.49, 61.67, 53.14, 52.41, 35.52, 34.30, 34.09, 33.20, 31.93, 29.71, 29.51, 29.37, 29.32, 29.31, 29.15, 29.14, 28.29, 27.29, 24.90, 24.88, 22.70, 14.13. MS (ESI) calculated for $C_{51}H_{96}N_2O_{10}S$, m/z 928.68, found 951.57 (M+Na)⁺.

13c ((R)-3-((R)-3-((R)-3-*tert*-butoxy-1-methoxy-1-oxopropan-2-ylamino)-2-(*tert*-butoxycarbonylamino)-3-oxopropylthio)propane-1,2-diyl dipalmitate): ¹H NMR (400 MHz, CDCl₃) δ 7.15 – 7.06 (m, 1H), 5.19 – 5.11 (m, 1H), 4.65 (d, $J = 8.4$, 1H), 4.31 (dd, $J = 3.6, 11.9$, 2H), 4.14 (dd, $J = 5.9, 11.9$, 1H), 3.81 (dd, $J = 2.9, 9.0$, 1H), 3.72 (s, 3H), 3.53 (dd, $J = 3.3, 9.0$, 1H), 2.94 (dd, $J = 14.0, 20.2$, 2H), 2.78 (s, 2H), 2.29 (dd, $J = 7.5, 13.4$, 4H), 1.59 (d, $J = 6.7$, 4H), 1.44 (s, 9H), 1.23 (s, 47H), 1.12 (d, $J = 1.9$, 9H), 0.86 (t, $J = 6.9$, 6H). ¹³C NMR (126 MHz, CDCl₃) δ 173.76, 172.63, 171.22, 170.29, 73.10, 70.42, 63.59, 55.56, 52.96, 34.36, 34.05, 31.93, 30.96, 29.73, 29.68, 29.61, 29.55, 29.38, 29.32, 29.15, 19.12, 24.84, 22.70, 14.13. MS (ESI) calculated for $C_{51}H_{96}N_2O_{10}S$, m/z 928.68, found 951.57 (M+Na)⁺.

13d ((R)-3-((S)-3-((S)-3-*tert*-butoxy-1-methoxy-1-oxopropan-2-ylamino)-2-(*tert*-butoxycarbonylamino)-3-oxopropylthio)propane-1,2-diyl dipalmitate): ¹H NMR (400 MHz, CDCl₃) δ 7.06 (d, $J = 8.1$, 1H), 5.17 (s, 1H), 4.69 – 4.58 (m, 1H), 4.31 (dd, $J = 3.5, 11.9$, 2H), 4.15 (dd, $J = 5.9, 11.9$, 1H), 3.80 (dd, $J = 3.0, 9.1$, 1H), 3.72 (s, 3H), 3.55 (dd, $J = 3.2, 9.1$, 1H), 2.94 (d, $J = 6.1$, 2H), 2.79 (d, $J = 5.9$, 2H), 2.29 (td, $J = 4.9, 7.5$, 4H), 1.59 (s, 4H), 1.43 (s, 9H), 1.23 (s, 48H), 1.12 (s, 9H), 0.86 (t, $J = 6.8$, 6H). MS (ESI) calculated for $C_{51}H_{96}N_2O_{10}S$, m/z 928.68, found 951.57 (M+Na)⁺.



L-Cys-L-Ser **14a**: X=H; **14b**: X=Me

L-Cys-D-Ser **14c**: X=Me

D-Cys-L-Ser **14d**: X=Me

General Procedure for one-step deprotection of *N*-Boc and *O*-*t*Bu: Syntheses of Compounds **14a-d**.

13a-d were deprotected with dry TFA as described earlier (general procedure for *N*-Boc deprotection) which allowed for the simultaneous deprotection of the *N*-Boc and *O*-*t*Bu groups. Consequently, **14a** was obtained as the –Ser-OH (free acid), while **14b-d** were the –Ser-OMe esters. All title compounds (**14a-d**) were obtained as white glassy solids in near-quantitative yields.

14a ((*S*)-2-((*R*)-2-amino-3-((*R*)-2,3-bis(palmitoyloxy)propylthio)propanamido)-3-hydroxypropanoic acid): ^1H NMR (400 MHz, DMSO) δ 9.10 (d, $J = 7.4$, 1H), 8.82 (d, $J = 7.9$, 1H), 8.23 (s, 1H), 5.16 (d, $J = 7.5$, 1H), 4.81 – 4.58 (m, 1H), 4.42 – 4.23 (m, 2H), 4.18 – 4.07 (m, 1H), 3.79 (dd, $J = 4.8, 11.0$, 1H), 3.70 – 3.58 (m, 1H), 3.07 (dt, $J = 6.7, 13.0$, 1H), 2.94 – 2.65 (m, 3H), 2.31 – 2.13 (m, 4H), 1.55 – 1.44 (m, 4H), 1.22 (s, 48H), 0.84 (t, $J = 6.7$, 6H). ^{13}C NMR (126 MHz, DMSO) δ 179.71, 177.74, 177.51, 176.39, 74.88, 68.75, 66.29, 60.04, 56.60, 38.87, 38.78, 38.61, 38.23, 36.53, 34.30, 34.25, 34.20, 34.17, 34.13, 34.03, 33.98, 33.95, 33.76, 33.68, 33.63, 29.71,

29.62, 27.32, 19.16. MS (ESI) calculated for C₄₁H₇₈N₂O₈S, *m/z* 758.55, found 759.66 (M+H)⁺.

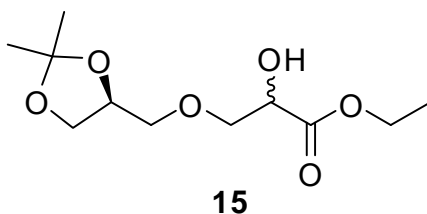
14b ((*R*)-3-((*R*)-2-amino-3-((*S*)-3-hydroxy-1-methoxy-1-oxopropan-2-ylamino)-3-oxopropylthio)propane-1,2-diyl dipalmitate): ¹H NMR (500 MHz, CDCl₃) δ 8.21 (s, 1H), 5.28 (s, 1H), 5.20 – 5.07 (m, 1H), 4.79 – 4.60 (m, 2H), 4.47 – 4.26 (m, 2H), 4.14 – 4.04 (m, 1H), 3.99 – 3.90 (m, 1H), 3.74 (s, 3H), 3.24 – 2.97 (m, 2H), 2.75 (s, 2H), 2.36 – 2.23 (m, 4H), 1.57 (s, 4H), 1.23 (s, 48H), 0.86 (t, *J* = 7.0, 6H). ¹³C NMR (126 MHz, CDCl₃) δ 174.39, 173.97, 169.90, 70.27, 70.08, 63.65, 63.52, 61.90, 52.92, 34.32, 34.05, 31.93, 29.73, 29.68, 29.55, 59.53, 29.38, 29.0, 29.14, 29.11, 24.89, 24.86, 24.82, 22.70, 14.12. MS (ESI) calculated for C₄₂H₈₀N₂O₈S, *m/z* 772.56, found 773.53 (M+H)⁺.

14c ((*R*)-3-((*R*)-2-amino-3-((*R*)-3-hydroxy-1-methoxy-1-oxopropan-2-ylamino)-3-oxopropylthio)propane-1,2-diyl dipalmitate): ¹H NMR (400 MHz, CDCl₃) δ 8.86 – 8.37 (m, 1H), 5.40 – 5.22 (m, 1H), 5.21 – 5.01 (m, 1H), 4.72 – 4.42 (m, 2H), 4.42 – 4.16 (m, 2H), 4.08 (s, 1H), 4.01 – 3.88 (m, 1H), 3.73 (s, 3H), 3.39 – 2.98 (m, 2H), 2.73 (s, 2H), 2.29 (s, 4H), 1.56 (s, 4H), 1.23 (s, 48H), 0.85 (t, *J* = 6.8, 6H). ¹³C NMR (126 MHz, CDCl₃) δ 174.22, 173.92, 70.02, 69.83, 63.66, 63.60, 53.02, 34.30, 34.05, 31.94, 29.73, 29.69, 29.56, 29.55, 29.39, 29.32, 29.16, 29.13, 24.88, 24.83, 22.70, 14.13. MS (ESI) calculated for C₄₂H₈₀N₂O₈S, *m/z* 772.56, found 773.53 (M+H)⁺.

14d ((*R*)-3-((*S*)-2-amino-3-((*S*)-3-hydroxy-1-methoxy-1-oxopropan-2-ylamino)-3-oxopropylthio)propane-1,2-diyl dipalmitate): ¹H NMR (400 MHz, CDCl₃) δ 8.74 (s, 1H), 7.87 (s, 1H), 5.32 (s, 1H), 5.13 (s, 1H), 4.46 (d, *J* = 80.5, 3H), 4.13 (s, 1H),

3.99 (s, 2H), 3.78 (s, 3H), 3.23 (s, 2H), 2.78 (s, 2H), 2.33 (s, 4H), 1.61 (s, 4H), 1.61 (s, 3H), 1.27 (s, 48H), 0.89 (t, $J = 6.7$, 6H). ^{13}C NMR (126 MHz, CDCl_3) δ 174.49, 173.76, 70.42, 63.59, 55.56, 53.70, 52.96, 48.56, 34.36, 34.05, 31.93, 29.73, 29.68, 29.55, 29.38, 29.32, 29.15, 29.12, 24.84, 22.70, 14.13. MS (ESI) calculated for $\text{C}_{42}\text{H}_{80}\text{N}_2\text{O}_8\text{S}$, m/z 772.56, found 773.53 ($\text{M}+\text{H}$) $^+$.

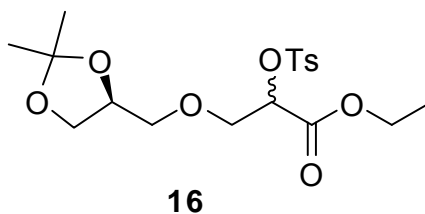
4.7.1.3 Scheme 3:



Synthesis of compound 15 (ethyl 3-(((*S*)-2,2-dimethyl-1,3-dioxolan-4-yl)methoxy)-2-hydroxypropanoate).

To a solution of ethyl-2,3-epoxypropanoate (Sigma-Aldrich, Inc., 375 mg, 2.91 mmol) in anhydrous DCM (10 mL) was added boron trifluoride diethyl etherate ($\text{BF}_3 \cdot \text{OEt}_2$; 83 mg, 0.58 mmol), followed by (*S*)-(+)- 2,2-dimethyl-1,3-dioxolane-4-methanol (**1a**, 1.20 g, 8.72 mmol).²¹⁵ The reaction mixture was stirred at r.t. for 5 h. After removal of solvent under reduced pressure, a mixture of ethyl 3-((2,2-dimethyl-1,3-dioxolan-4-yl)methoxy)-2-hydroxypropanoate (compound **15**) and (*S*)-(+)- 2,2-dimethyl-1,3-dioxolane-4-methanol (unreacted starting material, **1a**) were obtained. The R_f values of both the required product as well as the starting material were identical which

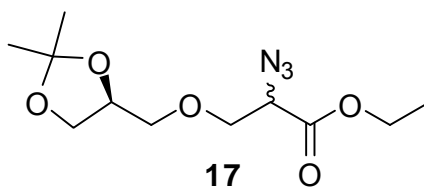
presented difficulty in chromatographic isolation. The mixture was therefore subjected to selective protection of the primary hydroxyl group of the acetonide-protected glycerol **1a** with TBDMSCl (*tert*-butyldimethylsilyl chloride), which allowed the facile isolation of compound **15** by flash column chromatography using 20% EtOAc/hexane (433 mg, 60%). ¹H NMR (400 MHz, CDCl₃) δ 4.34 – 4.22 (m, 4H), 4.05 (dd, *J* = 6.4, 8.3, 1H), 3.88 – 3.80 (m, 2H), 3.75 (ddd, *J* = 6.3, 7.5, 8.2, 1H), 3.66 – 3.52 (m, 2H), 3.15 (dd, *J* = 6.6, 15.6, 1H), 1.44 – 1.27 (m, 9H). ¹³C NMR (126 MHz, CDCl₃) δ 171.49, 171.44, 108.42, 73.59, 73.55, 72.11, 72.04, 71.56, 69.95, 69.85, 65.57, 65.54, 60.85, 28.68, 25.68, 25.67, 24.37, 24.33, 13.17. MS (ESI) calculated for C₁₁H₁₀O₆, *m/z* 248.13, found 271.12 (M+Na⁺) and 519.245 (M+M+Na)⁺.



Synthesis of compound 16 (ethyl 3-(((*S*)-2,2-dimethyl-1,3-dioxolan-4-yl)methoxy)-2-tosyloxypropanoate).

O-tosylation was performed by sequentially adding TEA (590 μL, 4.23 mmol) and *p*-TsCl (806 mg, 4.23 mmol) to a solution of **15** (350 mg, 1.41 mmol) in anhydrous DCM (10 mL) cooled to 0 °C. The reaction mixture was brought to r.t. and stirred for 8 h. After removal of solvent under vacuum, the residue was purified by flash column chromatography (hexane:EtOAc = 9:1) to afford the title compound **16** (443 mg,

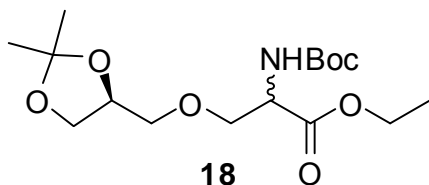
78%). ^1H NMR (400 MHz, CDCl_3) δ 7.80 (d, $J = 8.4$, 2H), 7.31 (d, $J = 8.0$, 2H), 5.02 – 4.96 (m, 1H), 4.18 – 4.06 (m, 3H), 3.96 – 3.77 (m, 3H), 3.62 (ddd, $J = 3.4$, 6.3, 8.4, 1H), 3.54–3.38 (m, 2H), 2.42 (s, 3H), 1.35 (s, 3H), 1.31 (s, 3H), 1.19 (t, $J = 7.1$, 3H). ^{13}C NMR (126 MHz, CDCl_3) δ 165.34, 143.94, 132.12, 132.09, 128.55, 126.92, 108.23, 108.20, 75.73, 73.22, 71.20, 69.59, 65.31, 60.90, 25.48, 24.18, 20.49, 12.77. MS (ESI) calculated for $\text{C}_{18}\text{H}_{26}\text{O}_8$, m/z 402.13, found 425.13 ($\text{M}+\text{Na}$) $^+$.



Synthesis of compound 17 (ethyl 2-azido-3-(((S)-2,2-dimethyl-1,3-dioxolan-4-yl)methoxy)propanoate).

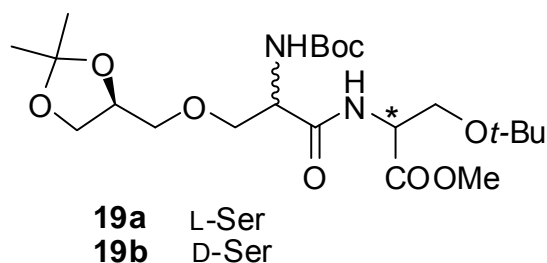
To a solution of compound **16** (380 mg, 0.94 mmol) in anhydrous DMF (10 mL) was added sodium azide (184 mg, 2.83 mmol). The reaction mixture was stirred at r.t. for 12 h. After removal of DMF under vacuum, the reaction residue was dissolved in DCM, washed with water, brine, and dried over Na_2SO_4 . After removal of solvent under reduced pressure, the residue was purified by flash column chromatography (hexane:EtOAc = 9:1) to afford the title compound **17** (245 mg, 95%). ^1H NMR (400 MHz, CDCl_3) δ 4.29 – 4.18 (m, 3H), 3.74 (ddd, $J = 6.2$, 8.4, 11.2, 1H), 3.61 – 3.48 (m, 2H), 1.39 (d, $J = 0.9$, 3H), 1.32 (d, $J = 5.0$, 3H), 1.29 (t, $J = 7.1$, 3H). ^{13}C NMR (126 MHz, CDCl_3) δ 166.54, 107.70, 107.67, 72.67, 70.55, 69.89, 64.82, 60.53, 59.86,

24.94, 23.58, 12.37. MS (ESI) calculated for C₁₁H₁₉N₃O₅, *m/z* 273.13, found 296.14 (M+Na)⁺.



Synthesis of compound 18 (ethyl 2-((*tert*-butoxycarbonylamino)-3-(((*S*)-2,2-dimethyl-1,3-dioxolan-4-yl)methoxy)propanoate).

Reduction of the azide to the amine under Staudinger conditions.²¹⁶ To **17** (230 mg, 0.84 mmol) dissolved in THF (8 mL) and H₂O (30.3 mg, 1.68 mmol) was added PPh₃ (265 mg, 1.01 mmol). The reaction mixture was refluxed for 6 h. After removal of solvent, the reaction residue was dissolved in anhydrous DCM (5 mL) and di-*tert*-butyl dicarbonate (Boc₂O; 551 mg, 2.52 mmol) and TEA (351 μL, 2.52 mmol) was added and stirred at r.t. for 8h. The solvent was removed under vacuum and the residue was purified by flash column chromatography (hexane:EtOAc = 17:3) to afford the title compound **18** (272 mg, 93%). ¹H NMR (400 MHz, CDCl₃) δ 5.37 (t, *J* = 8.2, 1H), 4.42 – 4.32 (m, 1H), 4.26 – 4.13 (m, 3H), 3.99 (dd, *J* = 6.4, 8.3, 1H), 3.94 – 3.86 (m, 1H), 3.75 – 3.63 (m, 2H), 3.55 – 3.40 (m, 2H), 1.43 (s, 9H), 1.38 (d, *J* = 1.9, 3H), 1.33 (d, *J* = 0.6, 3H), 1.25 (t, *J* = 7.1, 3H). ¹³C NMR (126 MHz, CDCl₃) δ 168.21, 153.15, 107.09, 77.59, 70.07, 69.60, 69.36, 64.18, 59.17, 51.70, 25.95, 24.32, 23.02, 11.81. MS (ESI) calculated for C₁₆H₂₉NO₇, *m/z* 347.19, found 370.28 (M+Na)⁺.



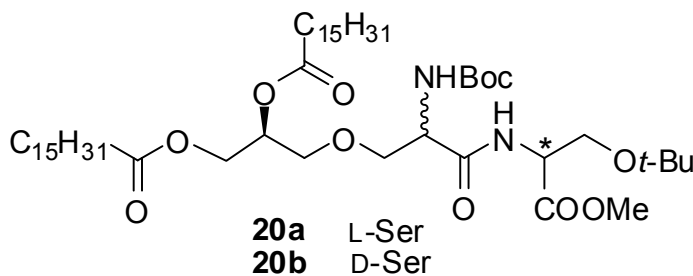
Syntheses of compounds 19a ((*S*)-methyl 3-*tert*-butoxy-2-(2-(*tert*-butoxycarbonylamino)-3-(((*S*)-2,2-dimethyl-1,3-dioxolan-4-yl)methoxy)propanamido)propanoate) and 19b ((*R*)-methyl 3-*tert*-butoxy-2-(2-(*tert*-butoxycarbonylamino)-3-(((*S*)-2,2-dimethyl-1,3-dioxolan-4-yl)methoxy)propanamido)propanoate).

De-esterification of the ethyl ester of **18** and subsequent coupling to H-L- and -D-Ser(*t*Bu)-OMe.HCl were performed as described for the syntheses of compounds **12a-d** to yield **19a** and **19b**, respectively (70-75%).

19a: ^1H NMR (400 MHz, CDCl_3) δ 7.21 (s, 1H), 5.48 (s, 1H), 4.71 – 4.62 (m, 1H), 4.25 (dt, $J = 5.9, 11.7$, 2H), 4.06 – 3.98 (m, 1H), 3.89 (ddd, $J = 2.4, 4.0, 9.5$, 1H), 3.82 – 3.68 (m, 5H), 3.66 – 3.50 (m, 4H), 1.44 (s, 9H), 1.40 (d, $J = 2.4$, 3H), 1.33 (d, $J = 2.2$, 3H), 1.15-1.08 (m, 9H). ^{13}C NMR (126 MHz, CDCl_3) δ 168.88, 168.87, 168.81, 108.18, 73.14, 62.15, 71.24, 71.00, 69.90, 65.30, 65.06, 60.56, 51.78, 51.03, 28.38, 26.98, 25.97, 25.43, 24.10. MS (ESI) calculated for $\text{C}_{22}\text{H}_{40}\text{N}_2\text{O}_9$, m/z 476.27, found 499.19 ($\text{M}+\text{Na}$) $^+$.

19b: ^1H NMR (400 MHz, CDCl_3) δ 7.21 (s, 1H), 5.49 (s, 1H), 4.66 (ddd, $J = 3.2, 7.2, 11.3$, 1H), 4.25 (ddd, $J = 5.7, 11.6, 17.0$, 2H), 4.06 – 3.98 (m, 1H), 3.89 (ddd, $J = 2.4, 4.0, 9.5$, 1H), 3.84 – 3.76 (m, 1H), 3.75 – 3.67 (m, 4H), 3.64 – 3.50 (m, 4H), 1.44 (s,

9H), 1.42 – 1.38 (m, 3H), 1.36 – 1.31 (m, 3H), 1.13-1.08 (m, 9H). ¹³C NMR (126 MHz, CDCl₃) δ 167.90, 167.83, 107.19, 72.16, 71.16, 70.27, 70.03, 68.94, 64.32, 64.09, 59.58, 50.80, 50.05, 27.40, 26.00, 24.99, 24.46, 23.12. MS (ESI) calculated for C₂₂H₄₀N₂O₉, *m/z* 476.27, found 499.19 (M+Na)⁺.



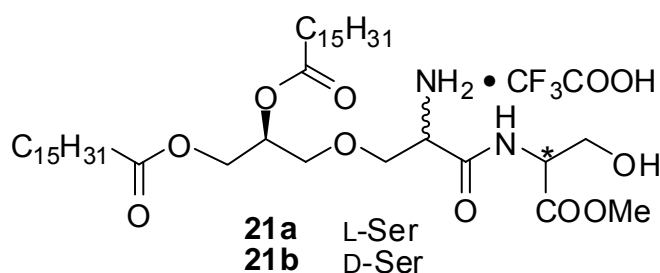
Syntheses of compounds 20a ((S)-3-(3-((S)-3-*tert*-butoxy-1-methoxy-1-oxopropan-2-ylamino)-2-(*tert*-butoxycarbonylamino)-3-oxopropoxy)propane-1,2-diyl dipalmitate), and 20b ((S)-3-(3-((R)-3-*tert*-butoxy-1-methoxy-1-oxopropan-2-ylamino)-2-(*tert*-butoxycarbonylamino)-3-oxopropoxy)propane-1,2-diyl dipalmitate).

Acetonide deprotection and *O*-palmitoylation were performed as described earlier (see syntheses of **13a-d**). **20a** or **20b** were obtained in 80-83% yield.

20a: ¹H NMR (400 MHz, CDCl₃) δ 7.11 (t, *J* = 8.3, 1H), 5.40 (s, 1H), 5.16 (dd, *J* = 3.3, 5.5, 1H), 4.66 (tt, *J* = 3.0, 8.8, 1H), 4.38 – 4.22 (m, 2H), 4.18 – 4.06 (m, 1H), 3.96 – 3.76 (m, 2H), 3.71 (d, *J* = 1.5, 3H), 3.66 – 3.49 (m, 4H), 2.28 (dd, *J* = 7.7, 15.5, 4H), 1.58 (d, *J* = 5.7, 4H), 1.44 (s, 9H), 1.23 (s, 48H), 1.13 – 1.08 (m, 9H), 0.85 (t, *J* = 6.8, 6H). ¹³C NMR (126 MHz, CDCl₃) δ 172.18, 171.88, 169.40, 168.79,

154.25, 79.11, 72.29, 69.96, 69.69, 68.70, 68.63, 68.58, 68.55, 68.48, 68.44, 68.41, 61.19, 60.94, 51.90, 51.66, 51.17, 33.06, 32.91, 30.74, 28.52, 28.48, 28.32, 28.18, 18.12, 27.94, 27.11, 26.09, 23.70, 21.51, 12.94. MS (ESI) calculated for $C_{51}H_{96}N_2O_{11}$, m/z 912.70, found 935.54 (M+Na)⁺.

20b: ¹H NMR (400 MHz, CDCl₃) δ 7.11 (t, J = 9.0, 1H), 5.40 (s, 1H), 5.23 – 5.11 (m, 1H), 4.66 (tt, J = 3.0, 8.6, 1H), 4.30 (ddd, J = 4.3, 10.2, 15.3, 2H), 4.11 (ddt, J = 5.0, 6.0, 10.3, 1H), 3.91 – 3.76 (m, 2H), 3.71 (d, J = 1.3, 3H), 3.68 – 3.49 (m, 4H), 2.28 (dd, J = 7.8, 15.5, 4H), 1.58 (dd, J = 6.9, 12.8, 4H), 1.44 (s, 9H), 1.23 (s, 48H), 1.14 – 1.07 (m, 9H), 0.85 (t, J = 6.8, 6H). ¹³C NMR (126 MHz, CDCl₃) δ 171.84, 171.56, 168.96, 168.46, 153.92, 78.72, 71.96, 69.62, 69.40, 68.37, 68.30, 68.25, 68.22, 68.15, 68.08, 60.86, 60.31, 51.57, 51.32, 50.84, 32.74, 32.58, 30.41, 28.19, 28.15, 27.99, 27.85, 27.79, 27.62, 26.78, 25.72, 23.38, 21.18, 12.61. MS (ESI) calculated for $C_{51}H_{96}N_2O_{11}$, m/z 912.70, found 935.54 (M+Na)⁺.



Syntheses of compound 21a ((S)-3-(2-amino-3-((S)-3-hydroxy-1-methoxy-1-oxopropan-2-ylamino)-3-oxopropoxy)propane-1,2-diyl dipalmitate; trifluoroacetate) and 21b ((S)-3-(2-amino-3-((R)-3-hydroxy-1-methoxy-1-oxopropan-2-ylamino)-3-oxopropoxy)propane-1,2-diyl dipalmitate; trifluoroacetate).

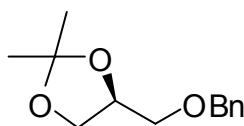
One-step deprotection of the *N*-Boc and *O*-*t*Bu groups utilizing TFA was carried out as described earlier (syntheses of **14a-d**). Title compounds were obtained as white glassy solids **21a** or **21b** (99-100%).

21a: ^1H NMR (400 MHz, CDCl_3) δ 8.38 (s, 1H), 8.03 (d, $J = 28.1$, 1H), 5.28 (s, 1H), 5.15 (s, 1H), 4.71 (dd, $J = 69.3, 103.2$, 2H), 4.17 (ddd, $J = 7.3, 17.4, 18.6$, 2H), 4.06 – 3.81 (m, 3H), 3.76 (d, $J = 14.3$, 3H), 3.58 (dd, $J = 10.2, 15.7$, 2H), 2.28 (dd, $J = 7.3, 11.9$, 4H), 1.56 (s, 4H), 1.23 (s, 48H), 0.86 (t, $J = 6.8$, 6H). ^{13}C NMR (126 MHz, CDCl_3) δ 172.76, 172.47, 172.41, 172.34, 168.73, 68.50, 68.31, 68.22, 67.59, 61.22, 61.10, 60.49, 54.08, 53.97, 51.92, 51.63, 51.47, 32.90, 32.78, 30.63, 28.42, 28.37, 28.24, 28.08, 28.02, 27.85, 27.80, 23.55, 21.40, 12.82. MS (ESI) calculated for $\text{C}_{42}\text{H}_{80}\text{N}_2\text{O}_9$, m/z 756.59, found 757.45 ($\text{M}+\text{H}$) $^+$.

21b: ^1H NMR (400 MHz, CDCl_3) δ 8.33 (s, 1H), 8.04 (s, 1H), 5.28 (s, 1H), 5.15 (s, 1H), 4.58 (d, $J = 51.7$, 2H), 4.18 (d, $J = 42.7$, 2H), 3.90 (s, 3H), 3.76 (d, $J = 14.5$, 3H), 3.59 (s, 2H), 2.28 (dd, $J = 7.4, 11.7$, 4H), 1.56 (s, 4H), 1.23 (s, 48H), 0.86 (t, $J = 6.8$, 6H). ^{13}C NMR (126 MHz, CDCl_3) δ 172.11, 171.82, 171.76, 171.69, 168.06, 67.84, 67.64, 67.55, 66.89, 60.55, 60.41, 59.84, 53.42, 53.32, 51.27, 50.98, 50.82,

32.24, 32.14, 29.97, 27.76, 27.72, 27.58, 27.42, 27.35, 27.19, 27.14, 22.89, 20.74, 12.16. MS (ESI) calculated for C₂₂H₃₀N₂O₉, *m/z* 756.59, found 757.45 (M+H)⁺.

4.7.1.4 Scheme 4:

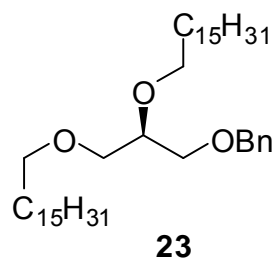


22

Synthesis of compound **22** ((*S*)-4-(benzyloxymethyl)-2,2-dimethyl-1,3-dioxolane).

O-benzylation of **1a** was performed by first adding sodium hydride (NaH; 60% in mineral oil, 363 mg) to a solution of (*S*)-(+)-2,2-dimethyl-1,3-dioxolane-4-methanol (**1a**, 200 mg, 1.51 mmol) in anhydrous DMF (5 mL) on ice. After stirring for 10 min, benzyl bromide (BnBr; 360 μ L, 3.03 mmol) was added slowly to the reaction mixture. The reaction was brought to r.t. after 30 min and stirred for an additional 8 h. NaH was quenched by slowly adding methanol to the reaction vessel at 0 °C. After removal of solvent, the residue was dissolved in DCM and washed with water (1X) and the resulting water layer was extracted with DCM (3X). The combined DCM layers were washed with brine and dried over Na₂SO₄. After removal of solvent, the residue was purified by flash column chromatography (hexane:EtOAc = 19:1) to yield the title compound **22** (330 mg, 98%). ¹H NMR (400 MHz, CDCl₃) δ 7.36 – 7.30 (m, 4H), 7.29 – 7.24 (m, 1H), 4.62 – 4.51 (m, 2H), 4.33 – 4.25 (m, 1H), 4.04 (dd,

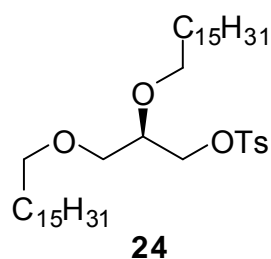
$J = 6.4, 8.3, 1\text{H}$), 3.73 (dd, $J = 6.3, 8.3, 1\text{H}$), 3.54 (dd, $J = 5.7, 9.8, 1\text{H}$), 3.46 (dd, $J = 5.5, 9.8, 1\text{H}$), 1.40 (s, 3H), 1.35 (s, 3H). ^{13}C NMR (126 MHz, CDCl_3) δ 136.87, 127.39, 126.73, 126.71, 108.39, 73.68, 72.47, 70.00, 65.81, 25.74, 24.35. MS (ESI) calculated for $\text{C}_{13}\text{H}_{18}\text{O}_3$, m/z 222.13, found 245.13 ($\text{M}+\text{Na}$) $^+$.



Synthesis of compound 23 ((*R*)-((2,3-bis(hexadecyloxy)propoxy)methyl)benzene).

Deprotection of the acetonide protecting group of **22** was achieved by stirring the compound (180 mg, 0.81 mmol) in 70% acetic acid ($\text{AcOH}:\text{H}_2\text{O} = 7:3$) as described for the syntheses of **4a** and **4b**. After complete removal of acetic acid and water under reduced pressure, the residue was dissolved in DMF (5 mL) and cooled to 0 °C. The resulting diol was *O*-alkylated with 1-iodohexadecane (1.14g, 3.24 mmol) in the presence of NaH (60 % in mineral oil, 770 mg) in anhydrous DMF (8 mL) at 0 °C. The reaction mixture was stirred for 30 min at 0 °C and the temperature was then raised to r.t. for 8 h. The excess NaH was quenched by slowly adding methanol to the reaction at 0 °C. After removal of solvent, the residue was dissolved in DCM and washed with water (1X). And the resulting water layer was extracted with DCM (3X). The combined DCM layers were washed with brine and dried over Na_2SO_4 . After removal of solvent under vacuum, the residue was purified by flash column

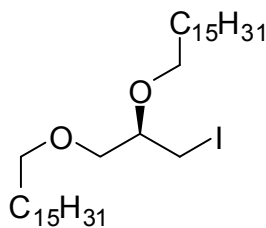
chromatography (hexane:EtOAc = 49:1) to afford a white solid (470 mg, 92%). ^1H NMR (400 MHz, CDCl_3) δ 7.31 (d, $J = 4.3$, 4H), 7.28 – 7.24 (m, 1H), 4.54 (s, 2H), 3.62 – 3.44 (m, 7H), 3.41 (t, $J = 6.7$, 2H), 1.60 – 1.47 (m, 4H), 1.26 (d, 52H), 0.86 (t, $J = 6.8$, 6H). ^{13}C NMR (126 MHz, CDCl_3) δ 138.42, 128.31, 127.58, 77.88, 73.34, 71.66, 70.79, 70.62, 70.24, 31.93, 30.09, 29.72, 29.66, 29.52, 29.38, 26.10, 22.70, 14.14. MS (ESI) calculated for $\text{C}_{42}\text{H}_{78}\text{O}_3$, m/z 630.60, found 653.61 ($\text{M}+\text{Na}$) $^+$.



Synthesis of compound 24 ((*R*)-2,3-bis(hexadecyloxy)propyl 4-methylbenzenesulfonate).

O-debenzylation followed by *O*-tosylation of **23** en route to the iodo intermediate **25** was obtained as follows: Hydrogenolysis of **23** (500 mg, 0.79 mmol) dissolved in a mixture of 20 mL MeOH/DCM (1:1) was carried out using $\text{Pd}(\text{OH})_2/\text{C}$ (500 mg) and H_2 at 55 psi in a Parr apparatus for 8 h. The catalyst was removed by filtration over celite, and the solvent was removed to afford the *O*-debenzylated intermediate as a white solid (425 mg, ~100%). After drying completely, the solid was dissolved in anhydrous CH_3CN (15 mL), followed by addition of pyridine (320 μL , 3.96 mmol) and a catalytic amount of DMAP. Then *p*-TsCl (755 mg, 3.96 mmol) was added and the reaction mixture was heated at 70 $^\circ\text{C}$ for 12 h. After removal of solvent under

vacuum, the residue was purified by flash column chromatography (hexane:EtOAc = 17:1) to afford the title compound **24** (527 mg, 96%). ^1H NMR (400 MHz, CDCl_3) δ 7.77 (d, $J = 8.2$, 2H), 7.31 (d, $J = 8.5$, 2H), 4.13 (dd, $J = 4.1$, 10.3, 1H), 4.00 (dd, $J = 5.8$, 10.3, 1H), 3.62 – 3.54 (m, 1H), 3.47 – 3.41 (m, 2H), 3.38 (t, 2H), 3.33 (t, $J = 6.7$, 2H), 2.42 (s, 3H), 1.45 (s, 4H), 1.23 (s, 52H), 0.86 (t, $J = 6.8$, 6H). ^{13}C NMR (126 MHz, CDCl_3) δ 143.66, 131.93, 128.75, 126.98, 75.16, 70.75, 69.80, 68.64, 68.30, 30.91, 28.85, 28.69, 28.65, 28.63, 28.60, 28.50, 28.46, 28.44, 28.35, 25.01, 24.94, 21.68, 20.62, 13.11. MS (ESI) calculated for $\text{C}_{42}\text{H}_{78}\text{O}_5\text{S}$, m/z 694.56, found 717.52 ($\text{M}+\text{Na}$) $^+$.

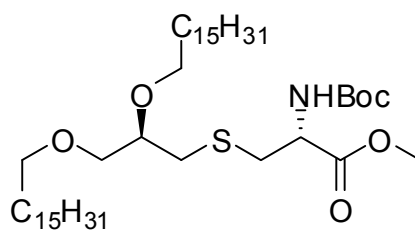


25

Synthesis of compound 25 ((*R*)-1-(1-(hexadecyloxy)-3-iodopropan-2-yl)hexadecane).

The *O*-tosyl derivative **24** was converted to the iodo derivative **25**. Iodine (310 mg, 12.23 mmol) and potassium iodide (KI; 2.03 g, 12.23 mmol) were added to a solution of **25** (850 mg, 1.22 mmol) in anhydrous DMF (15 mL) and the reaction was stirred at 80 °C for 24 h. After removal of DMF under vacuum, the residue was diluted with DCM and washed with water (1X), brine (1X) and dried over Na_2SO_4 . The solvent

was removed and the residue was purified by flash column chromatography (hexane:EtOAc = 49:1) to yield the title compound **25** (700 mg, 88%). ¹H NMR (400 MHz, CDCl₃) δ 3.51 (m, 3H), 3.45 – 3.39 (m, 3H), 3.37 – 3.24 (m, 3H), 1.60 – 1.50 (m, 4H), 1.23 (s, 52H), 0.86 (t, *J* = 6.9, 6H). ¹³C NMR (126 MHz, CDCl₃) δ 76.40, 70.86, 70.73, 69.25, 30.91, 28.91, 28.69, 28.66, 28.65, 28.61, 28.45, 28.43, 28.35, 25.09, 25.07, 21.68, 13.11, 6.39. MS (ESI) calculated for C₃₅H₇₁IO₂, *m/z* 650.45, found 673.42 (M+Na)⁺.

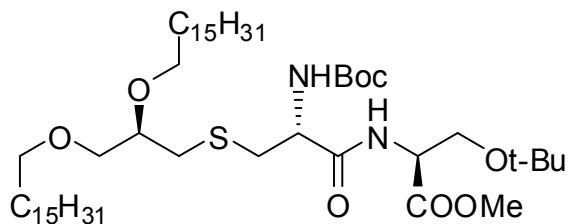


26

Synthesis of compound 26 ((6*R*,10*R*)-methyl 10-(hexadecyloxy)-2,2-dimethyl-4-oxo-3,12-dioxo-8-thia-5-azaoctacosane-6-carboxylate).

S-alkylation of Boc-L-Cys-OMe with **25** was carried out as follows: Boc-L-Cys-OMe (752 mg, 3.20 mmol) and TEA (445 μL, 3.20 mmol) were added to the solution of **25** (260 mg, 0.40 mmol) in anhydrous DMF (8 mL). The reaction was stirred at 85 °C for 2h. After removal of DMF under vacuum, the residue was purified by flash column chromatography (hexane:EtOAc = 19:1) to afford the title compound **26** (291 mg, 96%). ¹H NMR (500 MHz, CDCl₃) δ 5.53 (d, *J* = 8.0, 1H), 4.51 (s, 1H), 3.73 (s, 3H), 3.48 (m, 5H), 3.40 (m, 6.7, 2H), 3.07 – 2.93 (m, 2H), 2.75 (dd, *J* = 4.9, 13.7, 1H),

2.63 (dd, $J = 6.0, 13.7$, 1H), 1.57 – 1.49 (m, 4H), 1.42 (s, 9H), 1.31 – 1.20 (m, 52H), 0.85 (t, $J = 7.0$, 6H). ^{13}C NMR (126 MHz, CDCl_3) δ 170.63, 154.23, 28.97, 77.55, 70.68, 70.28, 69.55, 52.47, 51.47, 34.44, 33.51, 30.90, 28.97, 28.69, 28.64, 28.35, 27.28, 25.08, 25.05, 21.68, 13.13. MS (ESI) calculated for $\text{C}_{44}\text{H}_{87}\text{O}_6\text{S}$, m/z 757.63, found 780.61 ($\text{M}+\text{Na}$) $^+$.

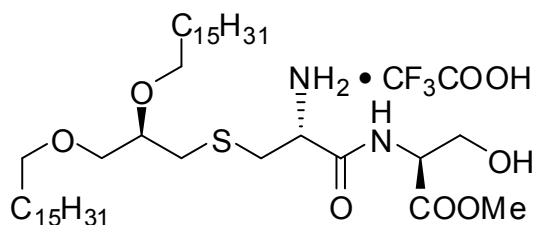


27

Synthesis of compound 27 ((5*S*,8*R*,12*R*)-methyl 8-(tert-butoxycarbonylamino)-12-(hexadecyloxy)-2,2-dimethyl-7-oxo-3,14-dioxo-10-thia-6-azatriacontane-5-carboxylate).

Compound **26** was obtained as a viscous oil (228 mg, 64%) via procedures similar to those described for the syntheses of compounds **12a-d**. ^1H NMR (500 MHz, CDCl_3) δ 5.60 (s, 1H), 4.64 (d, $J = 8.1$, 1H), 4.30 (s, 1H), 3.79 (dd, $J = 3.0, 9.1$, 1H), 3.71 (s, 3H), 3.60 – 3.47 (m, 7H), 3.45 – 3.35 (m, 2H), 2.95 (dd, $J = 5.8, 13.9$, 1H), 2.87 (dd, $J = 6.9, 13.8$, 1H), 2.78 (s, 2H), 1.58 – 1.49 (m, 4H), 1.43 (s, 6H), 1.30 – 1.20 (m, 52H), 1.11 (s, 8H), 0.85 (t, $J = 7.0$, 6H). ^{13}C NMR (126 MHz, CDCl_3) δ 169.58, 169.46, 154.24, 77.23, 72.40, 70.68, 70.27, 69.54, 60.72, 52.13, 51.33, 34.57, 33.34,

30.90, 28.95, 28.69, 28.64, 28.62, 28.50, 28.35, 27.28, 26.26, 25.08, 25.03, 21.68, 13.13. MS (ESI) calculated for $C_{51}H_{100}N_2O_8S$, m/z 900.72 found 923.69 (M+Na)⁺.



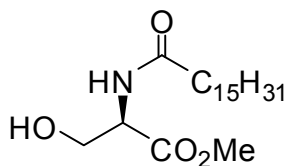
28

Synthesis of compound 28 ((S)-methyl 2-((R)-2-amino-3-((R)-2,3-bis(hexadecyloxy)propylthio)propanamido)-3-hydroxypropanoate; trifluoroacetate).

N-Boc deprotection with neat TFA was performed as described for the synthesis of **6a** and **6b**.

¹H NMR (400 MHz, CDCl₃) δ 8.30 (s, 1H), 4.64 (s, 1H), 4.32 (s, 1H), 4.00 – 3.82 (m, 1H), 3.74 (s, 3H), 3.61 – 3.48 (m, 3H), 3.47 – 3.37 (m, 3H), 3.18 – 3.07 (m, 1H), 3.01 – 2.89 (m, 1H), 2.86 – 2.66 (m, 1H), 1.59 – 1.47 (m, 4H), 1.23 (s, 48H), 0.86 (t, *J* = 6.8, 6H). ¹³C NMR (126 MHz, CDCl₃) δ 170.05, 77.85, 71.80, 71.12, 70.91, 61.75, 55.32, 53.06, 52.74, 34.98, 34.32, 31.93, 29.73, 29.68, 29.55, 29.51, 29.42, 29.38, 26.06, 25.87, 22.69, 14.12. MS (ESI) calculated for $C_{42}H_{84}N_2O_6S$, m/z 744.61 found 645.61 (M+H)⁺.

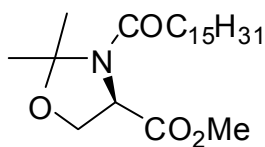
4.7.1.5 Scheme 5:



30

Synthesis of compound 30 ((*R*)-methyl 3-hydroxy-2-palmitamidopropanoate).

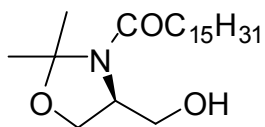
N-palmitoylation of **29** was carried out as follows: H-D-Ser-OMe·HCl (**29**) was *N*-acylated by first generating the free-base by the addition of 10 mL of sat. aqueous NaHCO₃ solution to a solution of **29** (200 mg, 1.04 mmol, Bachem) in EtOAc (10 mL), and then adding palmitoyl chloride (377 μL, 1.24 mmol) dropwise to the reaction. The reaction mixture, after stirring for 1 h, was extracted with EtOAc (3X). The combined EtOAc layers were washed with brine and dried over Na₂SO₄. After removal of solvent under vacuum, the residue was purified by flash column chromatography (hexane:EtOAc = 7:3) to afford the title compound as a white solid (286 mg, 77%). ¹H NMR (500 MHz, CDCl₃) δ 6.61 (s, 1H), 4.65 – 4.58 (m, 1H), 3.92 (dd, *J* = 3.6, 11.1, 1H), 3.83 (d, *J* = 11.1, 1H), 3.73 (s, 3H), 2.25 – 2.18 (m, 3H), 1.64 – 1.54 (m, 2H), 1.27 – 1.18 (m, 24H), 0.83 (t, *J* = 6.9, 3H). ¹³C NMR (126 MHz, CDCl₃) δ 173.98, 171.65, 63.23, 54.59, 52.68, 36.48, 31.82, 29.70, 29.67, 29.66, 29.64, 29.52, 29.37, 29.36, 29.26, 25.59, 22.69, 14.12. MS (ESI) calculated for C₂₀H₃₉NO₄, *m/z* 357.29, found 358.30 (M+H)⁺ and 380.28 (M+Na)⁺.



31

Synthesis of compound 31 ((*R*)-methyl 2,2-dimethyl-3-palmitoyloxazolidine-4-carboxylate).

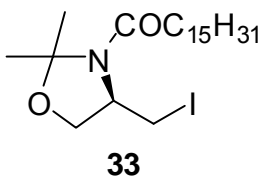
Compound **30** was acetonide protected with 2,2-dimethoxypropane (2,2-DMP; 24 mL, 195.8 mmol) and pyridinium *p*-toluenesulfonate (PPTS; 281 mg, 1.12 mmol) by adding the above reagents to compound **30** (2.0 g, 5.59 mmol) in toluene (25 mL), and the reaction refluxed at 90 °C for 22 h. After concentrating under reduced pressure, the residue was purified by flash column chromatography (hexane:EtOAc = 9:1) to afford the title compound as a white solid (2.0 g, 90%). ¹H NMR (500 MHz, CDCl₃) δ 4.42 (dd, *J* = 1.3, 6.3, 1H), 4.20 (dd, *J* = 1.4, 9.3, 1H), 4.14 (dd, *J* = 6.3, 9.3, 1H), 3.78 (s, 3H), 2.18 – 2.03 (m, 2H), 1.67 (s, 2H), 1.63 – 1.57 (m, 2H), 1.54 (s, 3H), 1.28 – 1.20 (m, 24H), 0.85 (t, *J* = 7.0, 3H). ¹³C NMR (126 MHz, CDCl₃) δ 171.15, 170.17, 96.62, 66.99, 59.49, 52.89, 35.64, 31.93, 29.70, 29.66, 29.64, 29.56, 29.48, 29.37, 29.25, 25.15, 24.57, 23.57, 22.70, 14.13. MS (ESI) calculated for C₂₃H₄₃NO₄, *m/z* 397.59, found 398.33 (M+H)⁺ and 420.31 (M+Na)⁺.



32

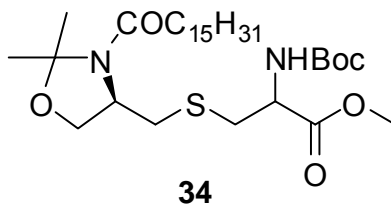
Synthesis of compound 32 ((S)-1-(4-(hydroxymethyl)-2,2-dimethyloxazolidin-3-yl)hexadecan-1-one).

The ester functional group of **31** was reduced to the primary alcohol by first diluting lithium borohydride (LiBH₄; 2.0 M in THF, 1.89 mL, 3.77 mmol) in 5 mL of THF (5 mL) cooled to 0°C for 30 min. Compound **31** (500 mg, 1.26 mmol), dissolved in THF (5 mL) was then added dropwise, after which the reaction was stirred at 0 °C for 3 h and then maintained at r.t. for an additional 6 h. After quenching the unreacted LiBH₄ with water, the reaction mixture was extracted with EtOAc (3X) and the combined EtOAc layers were washed by brine and dried over Na₂SO₄. The solvent was removed under vacuum and the resulting residue was purified by flash column chromatography (hexane:EtOAc = 4:1) to yield a white solid (489 mg, 81%). ¹H NMR (500 MHz, CDCl₃) δ 4.40 (s, 1H), 4.04 (d, *J* = 9.0, 1H), 4.01 – 3.88 (m, 2H), 3.64 (d, *J* = 10.5, 2H), 2.39 – 2.26 (m, 2H), 1.62 (s, 2H), 1.59 (d, *J* = 17.8, 4H), 1.52 (s, 2H), 1.25 (d, *J* = 22.7, 24H), 0.86 (t, *J* = 6.9, 3H). ¹³C NMR (126 MHz, CDCl₃) δ 170.41, 95.27, 65.43, 62.93, 58.55, 35.49, 31.94, 29.71, 29.68, 29.65, 29.54, 29.38, 26.83, 25.20, 22.93, 22.71, 14.15. MS (ESI) calculated for C₂₃H₄₃NO₄, *m/z* 369.58, found 370.33 (M+H)⁺, 392.31 (M+Na)⁺.



Synthesis of compound 33 ((*R*)-1-(4-(iodomethyl)-2,2-dimethyloxazolidin-3-yl)hexadecan-1-one).

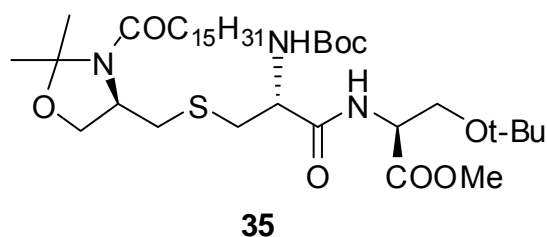
Compound **33** (151 mg, 97%) was obtained following the procedure described for the synthesis of **9**. ¹H NMR (400 MHz, CDCl₃) δ 4.17 – 4.10 (m, 2H), 4.03 – 3.96 (m, 1H), 3.26 (dd, *J* = 9.9, 11.4, 1H), 3.16 (dt, *J* = 2.5, 9.9, 1H), 2.34 – 2.16 (m, 2H), 1.67-1.62 (m, 3H), 1.53 – 1.46 (m, 3H), 1.39 – 1.16 (m, 26H), 0.86 (t, *J* = 6.9, 3H). MS (ESI) calculated for C₂₂H₄₂INO₂ *m/z* 479.23, found 502.21 (M+Na)⁺.



General procedure for *S*-alkylation: Synthesis of compound 34 (methyl 2-(tert-butoxycarbonylamino)-3-(((*R*)-2,2-dimethyl-3-palmitoyloxazolidin-4-yl)methylthio)propanoate).

To a solution of **33** (300 mg, 0.63 mmol) in anhydrous DMF (8 mL) was added TEA (872 μL, 6.26 mmol), followed by Boc-L-Cys-OMe (1.03 g, 4.38 mmol). The reaction solution was stirred at 85°C for 2 h. After removal of DMF under vacuum, the residue was purified by flash column chromatography (hexane:EtOAc = 9:1) to afford **34** as a viscous oil (356 mg, 97%). ¹H NMR (400 MHz, CDCl₃) δ 5.32 – 5.24 (m, 1H), 4.61-4.48 (m, 1H), 4.03 (d, *J* = 9.2, 1H), 3.95 – 3.89 (m, 1H), 3.87 – 3.81 (m, 1H), 3.76 (s, 3H), 3.07 – 2.92 (m, 2H), 2.79 – 2.63 (m, 2H), 2.36 – 2.17 (m, 2H), 1.70

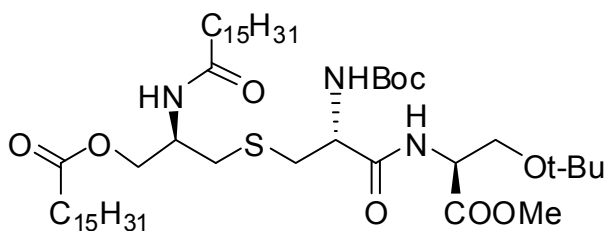
– 1.58 (m, 6H), 1.43 (s, 9H), 1.36 – 1.17 (m, 27H), 0.86 (t, $J = 6.9$, 3H). ^{13}C NMR (126 MHz, CDCl_3) δ 171.10, 169.73, 155.02, 95.54, 80.37, 66.36, 57.42, 53.39, 52.79, 35.86, 35.49, 35.46, 31.92, 29.70, 29.69, 29.68, 29.66, 29.59, 29.37, 28.27, 26.96, 25.08, 22.90, 22.70, 14.15. MS (ESI) calculated for $\text{C}_{31}\text{H}_{158}\text{N}_2\text{O}_6\text{S}$, m/z 586.40, found 609.39 ($\text{M}+\text{Na}$) $^+$.



Synthesis of compound 35 ((S)-methyl 3-tert-butoxy-2-((R)-2-(tert-butoxycarbonylamino)-3-(((R)-2,2-dimethyl-3-palmitoyloxazolidin-4-yl)methylthio)propanamido)propanoate).

Compound **34** (400 mg, 0.68 mmol) in 15 mL THF was de-esterified using procedures as described for the syntheses of **12a-d** with the exception that barium hydroxide octahydrate (645 mg, 2.04 mmol, in 6 mL H_2O at $60\text{ }^\circ\text{C}$, 1h), and not LiOH was used; we elected to use the much milder $\text{Ba}(\text{OH})_2$ conditions in view of potential lability of the amide bond in **34**. Subsequent coupling to H-L-Ser(*t*Bu)-OMe·HCl was carried out as described earlier for **12a-d**. Compound **35** was obtained as a viscous oil (274 mg, 55%). ^1H NMR (400 MHz, CDCl_3) δ 7.03 (d, $J = 8.2$, 1H), 5.40 (s, 1H), 4.63 (d, $J = 8.2$, 1H), 4.35 – 4.24 (m, 1H), 4.11– 4.02 (m, 1H), 3.96 – 3.87 (m, 2H),

3.81 (dd, $J = 2.8, 9.1, 1\text{H}$), 3.74 – 3.69 (m, 3H), 3.54 (dd, $J = 3.2, 9.1, 1\text{H}$), 3.05 – 2.94 (m, 1H), 2.93 – 2.79 (m, 2H), 2.77 – 2.67 (m, 1H), 2.38 – 2.23 (m, 2H), 1.61 (s, 5H), 1.53 – 1.48 (m, 3H), 1.31 – 1.20 (m, 24H), 1.12 (s, 9H), 0.85 (t, $J = 6.8, 3\text{H}$). ^{13}C NMR (126 MHz, CDCl_3) δ 173.80, 170.63, 170.51, 170.02, 95.57, 80.38, 73.69, 73.58, 66.43, 63.58, 61.68, 61.61, 57.45, 53.15, 52.50, 52.48, 51.49, 36.71, 35.40, 35.13, 34.94, 32.92, 31.93, 30.95, 29.69, 29.66, 29.65, 29.54, 29.52, 29.38, 29.37, 29.31, 28.32, 28.28, 27.30, 27.28, 26.96, 25.71, 25.16, 22.96, 22.70. MS (ESI) calculated for $\text{C}_{38}\text{H}_{71}\text{N}_3\text{O}_8\text{S}$, m/z 729.50, found 752.48 ($\text{M}+\text{Na}$) $^+$.

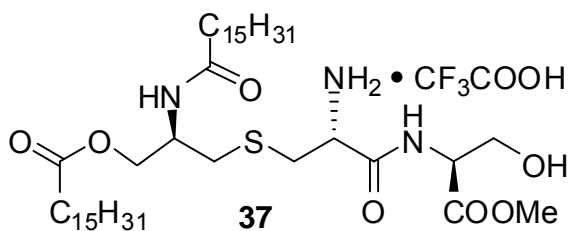


36

Synthesis of compound 36 ((5*S*,8*R*,12*R*)-methyl 8-(tert-butoxycarbonylamino)-2,2-dimethyl-7,14-dioxo-12-(palmitoyloxymethyl)-3-oxa-10-thia-6,13-diazanonacosane-5-carboxylate).

The general procedure of acetonide deprotection and subsequent *O*-palmitoylation described earlier for the synthesis of **11** was utilized. The reaction residue was purified by flash column chromatography (hexane:EtOAc = 3:1) to afford the intermediate as a colorless oil. (203 mg, 80%). ^1H NMR (500 MHz, CDCl_3) δ 6.21 (d, $J = 7.9, 1\text{H}$), 5.56 (d, $J = 6.7, 1\text{H}$), 4.68 – 4.58 (m, 1H), 4.43 – 4.31 (m, 2H), 4.21 (dd,

$J = 5.0, 11.3, 1\text{H}$), 4.08 (dd, $J = 4.9, 11.3, 1\text{H}$), 3.81 (dd, $J = 3.0, 9.1, 1\text{H}$), 3.72 (s, 3H), 3.55 (dd, $J = 3.3, 9.1, 1\text{H}$), 3.01 (dd, $J = 5.5, 13.9, 1\text{H}$), $2.91 - 2.79$ (m, 2H), $2.75 - 2.64$ (m, $J = 5.4, 14.0, 1\text{H}$), $2.35 - 2.26$ (m, 2H), $2.23 - 2.10$ (m, 2H), $1.63 - 1.55$ (br s, 4H), 1.43 (s, 6H), $1.30 - 1.19$ (m, 52H), $1.14 - 1.10$ (m, 8H), 0.85 (t, $J = 7.0, 6\text{H}$). ^{13}C NMR (126 MHz, CDCl_3) δ 173.90, 173.29, 170.59, 170.47, 155.40, 80.21, 73.57, 64.46, 61.65, 53.72, 53.14, 52.47, 48.83, 36.70, 34.12, 31.93, 29.71, 29.67, 29.55, 29.50, 29.46, 29.42, 29.37, 29.30, 29.27, 29.18, 28.31, 27.27, 25.65, 24.88, 22.70, 14.15. MS (ESI) calculated for $\text{C}_{51}\text{H}_{97}\text{N}_3\text{O}_9\text{S}$, m/z 927.69, found 950.68 ($\text{M}+\text{Na}$) $^+$.

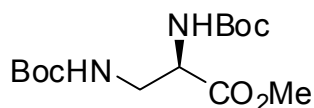


Synthesis of compound 37 ((*R*)-3-((*R*)-2-amino-3-((*S*)-3-hydroxy-1-methoxy-1-oxopropan-2-ylamino)-3-oxopropylthio)-2-palmitamidopropyl palmitate; trifluoroacetate).

The previously described *N*-Boc/*O*-*t*Bu deprotection procedure (see syntheses of **14a-d**) was used. The title compound was obtained as a flaky yellow solid (99%). ^1H NMR (500 MHz, CDCl_3) δ 8.46 (s, 1H), 6.57 (s, 1H), 4.73 – 4.59 (m, 1H), 4.53 – 4.34 (m, 1H), 4.34 – 4.23 (m, 1H), 4.23 – 4.15 (m, 1H), 4.15 – 4.06 (br s, 1H), 4.03 – 3.84 (m, 2H), 3.79 – 3.67 (m, 3H), 3.21 – 2.93 (m, 2H), 2.90 – 2.63 (m, 2H), 2.37 – 2.10 (m, 4H), 1.64 – 1.49 (m, 4H), 1.32 – 1.16 (m, 48H), 0.85 (t, $J = 6.9, 6\text{H}$). ^{13}C

NMR (126 MHz, CDCl₃) δ 174.32, 170.36, 170.21, 64.40, 53.13, 52.76, 52.64, 50.29, 49.20, 36.61, 34.02, 31.94, 29.75, 29.73, 29.72, 29.70, 29.68, 29.60, 29.55, 29.38, 29.34, 29.28, 29.23, 29.20, 29.12, 25.70, 24.85, 24.78, 22.70, 14.13. MS (ESI) calculated for C₄₂H₈₁N₃O₇S, m/z 771.58, found 772.59 (M+H)⁺ and 794.57 (M+Na)⁺.

4.7.1.6 Scheme 6:

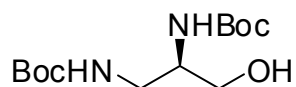


38

Synthesis of compound 38 ((*R*)-methyl 2,2,11,11-tetramethyl-4,9-dioxo-3,10-dioxa-5,8-diazadodecane-6-carboxylate).

D-2,3-diaminopropionic acid monohydrochloride (Sigma-Aldrich, 500 mg, 3.56 mmol) was *N*-boc protected by Boc₂O (2.33 g, 10.67 mmol) in the presence of TEA (1.49 mL, 10.67 mmol) in DCM (10 mL). After stirring at r.t. for 2 h, the solvent was removed under vacuum and the residue was purified by silica flash chromatography (DCM:MeOH = 17:3). The free carboxyl group of the intermediate was converted to methyl ester by dissolving it in anhydrous DCM (10 mL), followed by sequential addition of EDCI (1.11 g, 5.81 mmol), 1-hydroxybenzotriazole hydrate (HOBt; 785 mg, 5.81 mmol), TEA (810 μ L, 5.81 mmol), anhydrous MeOH (353 μ L, 8.71 mmol) and a catalytic amount of DMAP. After stirring at r.t. for 10 h, solvent was removed from the reaction under vacuum and the reaction residue was dissolved in DCM,

washed with water (1X), brine (1X) and dried over Na₂SO₄. The residue was purified by silica flash chromatography (hexane:EtOAc = 22: 3) to afford the title compound **38** (702 mg, 62%). ¹H NMR (400 MHz, CDCl₃) δ 5.40 (s, 1H), 4.82 (s, 1H), 4.32 (s, 1H), 3.73 (s, 3H), 3.56 – 3.40 (m, 2H), 1.44 – 1.39 (m, 18H). ¹³C NMR (126 MHz, CDCl₃) δ 171.30, 156.13, 155.41, 80.14, 79.85, 54.17, 52.65, 42.40, 30.95, 28.29, 28.28. MS (ESI) calculated for C₁₄H₂₆N₂O₆, *m/z* 318.18, found 341.17 (M+Na)⁺ and 659.35 (M+M+Na)⁺.

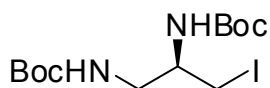


39

Synthesis of compound 39 ((*R*)-tert-butyl 3-hydroxypropane-1,2-diyldicarbamate).

Sodium borohydride (NaBH₄; 285 mg, 7.54 mmol) was added to a solution of **39** (600mg, 2.20mmol) for reducing the ester to the corresponding primary alcohol. We used NaBH₄ as an alternative to LiBH₄ described in the synthesis of **32** with significantly better yields. The reaction mixture was refluxed at 75 °C and then anhydrous methanol (3 mL) was added dropwise over a period of 1 h. After refluxing for an additional 3 h, the reaction was acidified to pH 2.0 with 1 M HCl and THF was removed under vacuum. The residue was extracted with DCM (3X) and the combined DCM layers were washed with brine and dried over Na₂SO₄. The residue was purified by silica flash chromatography (hexane:EtOAc = 3:1) to yield **39** as a colorless oil (525 mg, 96%). ¹H NMR (400 MHz, CDCl₃) δ 5.10 (s, 1H), 4.97 (s, 1H), 3.76 – 3.45

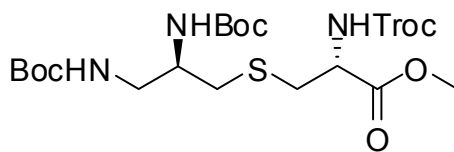
(m, 4H), 3.41 – 3.16 (m, 2H), 1.58 – 1.36 (m, 18H). ^{13}C NMR (126 MHz, CDCl_3) δ 157.75, 155.74, 80.41, 79.62, 61.56, 52.27, 40.12, 30.95, 28.36, 28.29. MS (ESI) calculated for $\text{C}_{13}\text{H}_{16}\text{N}_2\text{O}_5$, m/z 290.18, found 313.18 ($\text{M}+\text{Na}$) $^+$ and 603.37 ($\text{M}+\text{M}+\text{Na}$) $^+$.



40

Synthesis of compound 40 ((*R*)-tert-butyl 3-iodopropane-1,2-diyl dicarbamate).

A procedure essentially identical to that described for the synthesis of **9** was followed; however the reaction was carried out at 0 °C and then warming to r.t. instead of at 90 °C in an effort to minimize side-reactions and improve yield. No significant improvements in yield, unfortunately, were obtained. Compound **40** was obtained as a white solid (489 mg, 71%). ^1H NMR (400 MHz, CDCl_3) δ 5.30 (s, 1H), 4.83 (s, 1H), 3.62 (s, 1H), 3.44 – 3.21 (m, 4H), 1.46 (s, 18H). ^{13}C NMR (126 MHz, CDCl_3) δ 155.76, 154.44, 79.00, 50.54, 43.16 29.92, 27.31, 27.19, 7.69. MS (ESI) calculated for $\text{C}_{13}\text{H}_{25}\text{N}_2\text{O}_4$, m/z 400.09, found 423.09 ($\text{M}+\text{Na}$) $^+$ and 823.18 ($\text{M}+\text{M}+\text{Na}$) $^+$.

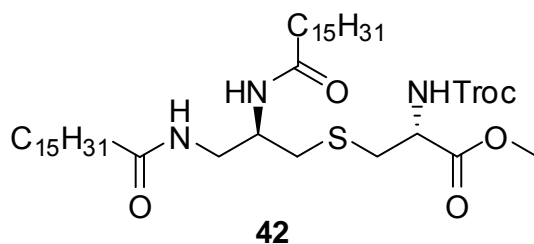


41

Synthesis of compound 41 ((6*R*,10*R*)-methyl 10-(tert-butoxycarbonylamino)-1,1,1-trichloro-15,15-dimethyl-4,13-dioxo-3,14-dioxo-8-thia-5,12-diazahexadecane-6-carboxylate).

Orthogonal protection of the amines of the 2,3-diaminopropionic acid fragment, and of the amine of the cysteine unit was necessary. We elected to utilize Troc-L-Cys-OMe, which was obtained from L-cystine dimethylester (Sigma-Aldrich) as follows. 2,2,2-trichloroethyl chloroformate (805 μ L, 5.86 mmol) was slowly added to a stirring solution of L-cystine dimethylester dihydrochloride (500 mg, 1.47 mmol) in anhydrous DCM (10 mL) and pyridine (10 mL) cooled to 0 $^{\circ}$ C. The reaction was brought to r.t. and stirred for 8 h. After removal of solvent under vacuum, the residue was purified by flash chromatography (hexane:EtOAc = 4:1) to afford *N*-Troc cystine dimethylester as a white solid. The disulfide bond of the *N*-Troc-protected cystine ester was reduced by dissolving the solid in THF (10 mL), and adding tributylphosphine (Bu₃P; 542 μ L, 2.20 mmol) and H₂O (132 μ L, 7.33 mmol).²¹⁷ The reaction was stirred at r.t. for 2 h. After removal of solvent, the residue was purified by flash column chromatography (hexane:EtOAc = 9:1) to afford the title compound as a oil (410 mg, 90%). The characterization data for Troc-L-Cys-OMe (Scheme 6, step d) is provided in the Supplemental Data. *S*-alkylation of Troc-L-Cys-OMe with **40** was performed as described earlier for **26**. Compound **41** was obtained as a mixture with the oxidized *N*-Troc cystine dimethylester as ascertained by LC-MS and ¹H NMR. The R_fs of both components were virtually identical, rendering the isolation of **41** very difficult by flash chromatography. Reverse-phase HPLC employing

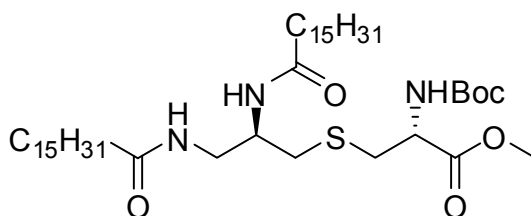
several solvent combinations also did not yield good separations. We reasoned, however, that *N*-Troc cystine dimethylester would be inert to both *N*-Boc deprotection and *N*-acylation conditions that were to follow (see synthesis of **42** below). We therefore proceeded without further purification.



Synthesis of compound 42 ((6*R*,10*R*)-methyl 1,1,1-trichloro-4,13-dioxo-10-palmitamido-3-oxa-8-thia-5,12-diazaoctacosane-6-carboxylate).

A crude sample of **41** (200 mg, 0.34 mmol) was dissolved in excess dry TFA and stirred at r.t. for 30 min to effect *N*-Boc deprotection on the 2,3-diaminopropionic acid fragment. Excess TFA was removed by purging nitrogen. The resulting diamino intermediate was coupled with palmitic acid (264 mg, 1.03 mmol) using EDCI (197 mg, 1.03 mmol), HOBt (139 mg, 1.03 mmol) and TEA (287 mL, 2.06 mmol), and a catalytic amount of DMAP in anhydrous DMF (8 mL). The reaction was stirred at 60 °C for 10 h. After DMF was removed under reduced pressure, the residue was dissolved with DCM and washed with water (1X), brine (1X) and dried over Na₂SO₄. The residue was purified by silica flash chromatography (hexane:EtOAc = 39:11) to afford the title compound **42** (185 mg, 64%). ¹H NMR (500 MHz, CDCl₃) δ 6.90 (d, *J* = 6.5, 1H), 6.24 – 6.14 (m, 1H), 4.82 – 4.73 (m, 1H), 4.73 – 4.63 (m, 1H), 4.62 – 4.54

(m, 1H), 3.98 (br s, 1H), 3.76 (d, $J = 4.3$, 3H), 3.53 – 3.43 (m, 1H), 3.41 – 3.30 (m, 1H), 3.12 – 2.97 (m, 2H), 2.92 – 2.78 (m, 2H), 2.57 – 2.43 (m, 1H), 2.23 – 2.09 (m, 4H), 1.63 – 1.50 (m, 4H), 1.22 (s, 48H), 0.85 (t, $J = 6.9$, 6H). ^{13}C NMR (126 MHz, CDCl_3) δ 173.07, 171.90, 168.27, 151.86, 92.87 72.24, 52.01, 50.44, 48.60, 34.42, 34.16, 32.08, 31.71, 29.48, 27.27, 27.24, 27.22, 27.10, 27.07, 26.92, 26.85, 23.17, 20.25, 11.69. MS (ESI) calculated for $\text{C}_{42}\text{H}_{78}\text{Cl}_3\text{N}_3\text{O}_6\text{S}$, m/z 857.47, found 880.45, 881.45, 882.45 ($\text{M}+\text{Na}^+$ with expected chlorine isotopic mass-spectral envelope).

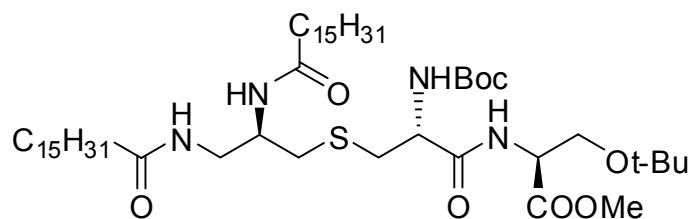


43

Synthesis of compound 43 ((6*R*,10*R*)-methyl 2,2-dimethyl-4,13-dioxo-10-palmitamido-3-oxa-8-thia-5,12-diazaoctacosane-6-carboxylate).

The base-labile *N*-Troc protecting group on the cysteine unit had to be converted to the *N*-Boc derivative in order to carry out subsequent base-catalyzed de-esterification step (see synthesis of **44** below). Accordingly, **42** (350mg, 0.41 mmol) was dissolved in THF (3 mL) and zinc dust (266 mg, 4.07 mmol), AcOH (15 mL) and H₂O (1 mL) was added to the reaction. After stirring at r.t. for 1 h, zinc was filtered on celite and the filtrate was concentrated under reduced pressure. Reprotection with Boc₂O was achieved by dissolving the completely dried intermediate in DCM and the addition of Boc₂O (444 mg, 2.04 mmol) in the presence of TEA (284 μL , 2.04 mmol), and

stirring the reaction mixture at r.t. for 1h. After the solvent was removed, the residue was purified by silica flash chromatography (hexane:EtOAc = 7:3) to yield the desired product **43** as a white solid (217 mg, 68%). ¹H NMR (400 MHz, CDCl₃) δ 6.81 (s, 1H), 5.43 (s, 1H), 4.55 (s, 1H), 4.03 (s, 1H), 3.82 – 3.77 (m, 3H), 3.53 (s, 1H), 3.42 (s, 1H), 3.11 – 2.86 (m, 3H), 2.30 – 2.13 (m, 4H), 1.69 – 1.56 (m, 4H), 1.54 – 1.44 (m, 7H), 1.27 (s, 48H). ¹³C NMR (126 MHz, CDCl₃) δ 173.14, 141.89, 169.32, 169.22, 78.11, 72.52, 51.39, 50.52, 48.69, 48.31, 40.02, 39.64, 34.60, 34.46, 33.77, 33.19, 32.16, 29.76, 27.55, 27.52, 27.50, 27.38, 27.36, 27.21, 27.17, 27.14, 27.12, 26.13, 23.57, 23.50, 23.48, 23.37, 20.53. MS (ESI) calculated for C₄₄H₈₅N₃O₆S, *m/z* 783.62, found 806.61 (M+Na)⁺.



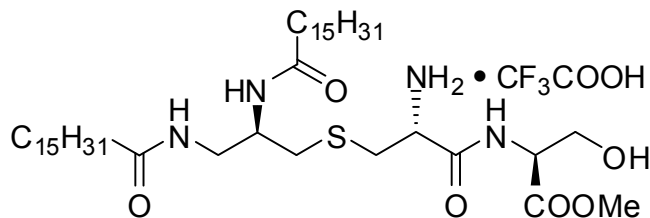
44

Synthesis of compound 44 ((5*S*,8*R*,12*R*)-methyl 8-(tert-butoxycarbonylamino)-2,2-dimethyl-7,15-dioxo-12-palmitamido-3-oxa-10-thia-6,14-diazatriacontane-5-carboxylate).

De-esterification followed by serine coupling was carried out as described for the synthesis of **35**. (75%)

¹H NMR (400 MHz, CDCl₃) δ 6.91 (s, 1H), 6.52 (s, 1H), 5.52 (s, 1H), 4.68 – 4.61 (m, 1H), 3.83 – 3.77 (m, 1H), 3.74 – 3.69 (m, 3H), 3.59 – 3.51 (m, 1H), 3.50 – 3.32 (m,

2H), 2.98 – 2.83 (m, 2H), 2.23 – 2.09 (m, 4H), 1.65 – 1.51 (m, 4H), 1.46 – 1.40 (m, 8H), 1.22 (s, 48H), 1.14 – 1.09 (m, 9H), 0.85 (t, $J = 6.8$, 6H). ^{13}C NMR (126 MHz, CDCl_3) δ 174.15, 173.17, 169.65, 169.56, 154.54, 79.12, 72.61, 60.69, 52.18, 51.40, 50.55, 41.27, 35.75, 35.61, 30.91, 29.92, 28.69, 28.66, 28.65, 28.54, 28.52, 28.39, 28.38, 28.35, 28.32, 28.30, 27.32, 27.29, 26.26, 24.76, 24.67, 21.67, 13.11. MS (ESI) calculated for $\text{C}_{51}\text{H}_{98}\text{N}_4\text{O}_8\text{S}$, m/z 926.71, found 949.70 ($\text{M}+\text{Na}$) $^+$.



45

Synthesis of compound 45 ((*S*)-methyl 2-((*R*)-2-amino-3-((*R*)-2,3-dipalmitamidopropylthio)-propanamido)-3-hydroxypropanoate; trifluoroacetate).

Compound **45** was deprotected with TFA as described earlier. The title compounds were obtained as a flaky yellow solid (99%). ^1H NMR (500 MHz, CDCl_3) δ 7.21 – 7.11 (m, 1H), 7.20 – 7.11 (m, 1H), 4.70 – 4.54 (m, 1H), 4.51 – 4.37 (m, 1H), 3.90 (s, 2H), 3.71 (s, 3H), 3.49 – 3.35 (m, 1H), 3.33 – 3.22 (m, 1H), 3.21 – 3.01 (m, 1H), 2.80 – 2.53 (m, 1H), 2.15 (s, 3H), 1.53 (s, 3H), 1.25 (d, $J = 21.5$, 49H), 0.85 (t, $J = 6.9$, 6H). ^{13}C NMR (126 MHz, CDCl_3) δ 132.65, 131.11, 129.02, 68.37, 52.91, 38.92, 36.93, 36.56, 36.55, 32.15, 30.56, 30.37, 29.97, 29.88, 29.83, 29.76, 29.68, 29.60,

29.56, 29.54, 29.51, 29.47, 29.46, 29.13, 25.98, 25.86, 25.77, 23.94, 23.20, 22.92, 14.41, 14.34, 14.28, 11.17. MS (ESI) calculated for C₄₂H₈₂N₄O₆S, *m/z* 770.60, found 771.60 (M+H)⁺.

4.7.2 Materials and Methods

4.7.2.1 Chemistry: See 2.6.1.1

4.7.2.2 Assays

NF-κB induction: The induction of NF-κB was performed in HEK cells stably transfected with human TLR2 using procedures described in section **2.6.1.2**.

Nitric Oxide Assay: See **2.6.1.2**

Phosflow™ flow cytometric assay for p38MAPK: One ml aliquots of fresh whole blood, anticoagulated with heparin (obtained by venipuncture from healthy human volunteers with informed consent and as per guidelines approved by the Human Subjects Experimentation Committee) were incubated with 25 μl of a mix of 8 μg/ml of *E. coli* 0111:B4 LPS and graded concentrations of test compounds diluted in saline (typically serially diluted from 80 μM) for 15 minutes at 37°C. This resulted in final concentrations of 100 ng/ml of LPS and 1 nM of compound (at the lowest dilution). Positive (LPS alone) and negative (saline) controls were included in each experiment. Erythrocytes were lysed and leukocytes were fixed in one step by mixing 200 μl of the samples in 4 ml pre-warmed whole blood lyse/fix Buffer (Becton-Dickinson

Biosciences, San Jose, CA). After washing the cells at 500 x g for 8 minutes in CBA buffer, the cells were permeabilized in ice-cold methanol for 30 min, washed twice in CBA buffer and transferred to a Millipore MultiScreen BV 1.2 μ filter plate and stained with either phycoerythrin (PE)-conjugated mouse anti-p38MAPK (pT180/pY182; BD Biosciences) mAb, or a matched PE-labeled mouse IgG₁ κ isotype control mAb for 60 minutes. The cells were washed twice in the plate by aspiration as per protocols supplied by the vendor. Cytometry was performed using a BD FACSAArray instrument in the single-color mode for PE acquisition on 20,000 gated events. Post-acquisition analyses were performed using FlowJo v 7.0 software (Treestar, Ashland, OR).

Multiplexed cytokine assay *ex vivo* in human blood: See 2.6.1.2

Pyrogenicity response assay: Adult New Zealand White rabbits were administered intravenously saline (negative control), LPS (200 ng/kg), or varying doses of PAM₂CSK₄ (10, 50, or 200 μ g/kg) and their core temperatures were monitored for 3 hours using an indwelling rectal thermometer connected to an electronic temperature recorder. All experiments were performed in accordance with animal care protocols approved by the University of Kansas IACUC Committee.

Flow-cytometric immunostimulation experiments: Heparin-anticoagulated whole blood samples were obtained by venipuncture from healthy human volunteers with

informed consent and as per guidelines approved by the University of Kansas Human Subjects Experimentation Committee. A minimum of six blood samples obtained from individuals of both sexes and diverse ancestry were analyzed for each experiment. Two mL aliquots of whole human blood samples were stimulated with a final concentration of 1 µg/mL of one of the various stimuli under study in a 6-well polystyrene plate and incubated at 37°C in a rotary (100 rpm) incubator for 16.5 h. Negative (endotoxin free water) controls were included in each experiment. Following incubation, 200 µL aliquots of anticoagulant whole blood were stained with 40 µL of fluorochrome-conjugated antibodies at 37°C in the dark for 30 min. For triple color flow cytometry experiments, CD3-PE, CD56-APC, CD69-PE-Cy7 were used to analyze CD69 activation of each of the main peripheral blood lymphocyte populations: natural killer lymphocytes (NK cells: CD3⁻CD56⁺), cytokine-induced killer phenotype (CIK cells: CD3⁺CD56⁺), nominal B lymphocytes (CD3⁻CD56⁻), and nominal T lymphocytes (CD3⁺CD56⁻). These experiments were complemented with separate experiments using PE-CD3, APC-CD4 (CD4⁺ T lymphocytes)/ APC-CD8 (CD8⁺ T lymphocytes)/APC-CD19 (B lymphocytes), in combination with PE-Cy7-conjugated CD69 antibodies. Following staining, erythrocytes were lysed and leukocytes fixed in one step by mixing 200 µL of the samples in 4 mL pre-warmed Whole Blood Lyse/Fix Buffer (Becton-Dickinson Biosciences, San Jose, CA). After washing the cells twice at 200 g for 8 minutes in saline, the cells were transferred to a 96-well plate. Flow cytometry was performed using a BD FACSAArray instrument in the tri-color mode (tri-color flow experiment) and two-color mode (two-color flow

experiment) for acquisition on 100,000 gated events. Post-acquisition analyses were performed using FlowJo v 7.0 software (Treestar, Ashland, OR). Compensation for spillover was computed for each experiment on singly-stained samples. Statistical significance of data were analyzed using both two-way ANOVA with Bonferroni correction,²¹⁸ and the Friedman nonparametric test.²¹⁹

References

1. Felty, A. R. and Keefer, C. S. *Bacillus coli* sepsis: A clinical study of twenty-eight cases of bloodstream infection by the colon bacillus. *JAMA* **1924**, 82, 1430-1433.
2. Gelfand, J. A. and Shapiro, L. Cytokines and sepsis: pathophysiology and therapy. *New Horizons* **1993**, 1, 13-22.
3. Gasche, Y.; Pittet, D.; and Sutter, P. Outcome and prognostic factors in bacteremic sepsis. In *Clinical trials for treatment of sepsis*. Sibbald, W. J. and Vincent, J. L. Eds.; Springer-Verlag: Berlin, 1995; pp 35-51.
4. Centers for Diseases Control. Increases in national hospital discharge survey rates for septicemia - United States, 1979-1987. *MMWR* **1990**, 39, 31-34.
5. Martin, G. S.; Mannino, D. M.; Eaton, S.; and Moss, M. The epidemiology of sepsis in the United States from 1979 through 2000. *N. Engl. J. Med.* **2003**, 348, 1546-1554.
6. Danai, P. and Martin, G. S. Epidemiology of sepsis: recent advances. *Curr. Infect. Dis. Rep.* **2005**, 7, 329-334.
7. Cross, A. and Opal, S. M. Therapeutic intervention in sepsis with antibody to endotoxin: is there a future? *J. Endotoxin Res.* **1994**, 1, 57-59.
8. Rietschel, E. T.; Kirikae, T.; Schade, U. F.; Ulmer, A. J.; Holst, O.; Brade, H.; Schmidt, G.; Mamat, U.; Grimmecke, H.-D.; Kusumoto, S.; and Zähringer, U.

The chemical structure of bacterial endotoxin in relation to bioactivity.

Immunobiol. **1993**, *187*, 169-190.

9. Takahashi, I.; Kotani, S.; Takada, H.; Tsujimoto, M.; Ogawa, T.; Shiba, T.; Kusumoto, S.; Yamamoto, M.; Hasegawa, A.; Kiso, M.; Nishijima, M.; Amano, F.; Akamatsu, Y.; Harada, K.; Tanaka, S.; Okamura, H.; and Tamura, T. Requirement of a properly acylated $\beta(1\text{-}\rightarrow\text{6})\text{-D-glucosamine}$ disaccharide bisphosphate structure for efficient manifestation of full endotoxic and associated bioactivities of lipid A. *Infect. Immun.* **1987**, *65*, 57-68.
10. Rietschel, E. Th, Brade, H., Brade, L., Brandenburg, K., Schade, U. F., Seydel, U., Zähringer, U., Galanos, C., Lüderitz, O., Westphal, O., Labischinski, H., Kusumoto, S., and Shiba, T. Lipid A, the endotoxic center of bacterial lipopolysaccharides: Relation of chemical structure to biological activity. Progress in clinical and biological research (New York NY) 231, 25-53. **1987**.
11. Brade, H.; Brade, L.; and Rietschel, E. T. Structure-activity relationships of bacterial lipopolysaccharides (Endotoxins). Current and Future Aspects. *Zbl. Bakt. Hyg. ,I Abt. Orig.* **1988**, *A 268/2*, 151-179.
12. Galanos, C.; Lüderitz, O.; Rietschel, E. T.; Westphal, O.; Brade, H.; Brade, L.; Freudenberg, M. A.; Schade, U. F.; Imoto, M.; Yoshimura, S.; Kusumoto, S.; and Shiba, T. Synthetic and natural *Escherichia coli* free lipid A express identical endotoxic activities. *Eur. J. Biochem.* **1985**, *148*, 1-5.

13. Rietschel, E. T.; Brade, L.; Lindner, B.; and Zähringer, U. Biochemistry of lipopolysaccharides. In *Bacterial endotoxic lipopolysaccharides, vol. I. Molecular biochemistry and cellular biology*. Morrison, D. C. and Ryan, J. L. Eds.; CRC Press: Boca Raton, 1992; pp 1-41.
14. Bone, R. C. Gram-negative sepsis: a dilemma of modern medicine. *Clin. Microbiol. Rev.* **1993**, *6*, 57-68.
15. Dinarello, C. A. Cytokines as mediators in the pathogenesis of septic shock. *Curr. Top. Microbiol. Immunol.* **1996**, *216*, 133-165.
16. Saadia, R.; Schein, M.; MacFarlane, C.; and Boffard, K. Gut barrier function and the surgeon. *Br. J. Surg.* **1990**, *77*, 487-492.
17. Jones II, W.; Minei, J.; Barber, A.; Fahey, T.; and Shires III, G. T. Splanchnic vasoconstriction and bacterial translocation after thermal injury. *Am. J. Physiol.* **1991**, *261*, H1190-H1196.
18. Rocke, D.; Gaffin, S.; Wells, M.; Koen, Y.; and Brocke-Utine, J. Endotoxemia associated with cardiopulmonary bypass. *J. Thorac. Cardiovasc. Surg.* **1987**, *93*, 832-837.
19. van Deventer, S.; ten Cate, J.; and Tygat, G. Intestinal endotoxemia- Clinical significance. *Gastroenterology* **1998**, *94*, 825-831.
20. Ingalls, R. R.; Heine, H.; Lien, E.; Yoshimura, A.; and Golenbock, D. Lipopolysaccharide recognition, CD14, and lipopolysaccharide receptors. *Infect. Dis. Clin. North Am.* **1999**, *13*, 341-53, vii.

21. Pugin, J.; Ulevitch, R. J.; and Tobias, P. S. A critical role for monocytes and CD14 in endotoxin-induced endothelial cell activation. *The Journal of Experimental Medicine* **1993**, *178*, 2193-2200.
22. Ulevitch, R. and Tobias, P. Receptor-dependent mechanisms of cell stimulation by bacterial endotoxin. *Annu. Rev. Immunol.* **1995**, *13*, 437-457.
23. Din, Z. Z.; Mukerjee, P.; Kastowsky, M.; and Takayama, K. Effect of pH on solubility and ionic state of lipopolysaccharide obtained from the deep rough mutant of *Escherichia coli*. *Biochemistry* **1993**, *32*, 4579-4586.
24. Pugin, J.; Schürer-Maly, C.-C.; Leturcq, D.; Moriarty, A.; Ulevitch, R. J.; and Tobias, P. S. Lipopolysaccharide activation of human endothelial and epithelial cells is mediated by lipopolysaccharide-binding protein and soluble CD14. *Proc. Natl. Acad. Sci. USA* **1993**, *90*, 2744-2748.
25. Ingalls, R. R. and Golenbock, D. T. CD11c/CD18, a transmembrane signaling receptor for lipopolysaccharide. *J. Exp. Med.* **1995**, *181*, 1473-1479.
26. Fenton, M. J. and Golenbock, D. T. LPS-binding proteins and receptors. *J. Leukoc. Biol.* **1998**, *64*, 25-32.
27. Mathison, J. C.; Tobias, P. S.; Wolfson, E.; and Ulevitch, R. J. Plasma lipopolysaccharide (LPS)-binding protein. A key component in macrophage recognition of gram-negative LPS. *J. Immunol.* **1992**, *149*, 200-206.
28. Tobias, P. S.; Mathison, J.; Mintz, D.; Lee, J.-D.; Kravchenko, V.; Kato, K.; Pugin, J.; and Ulevitch, R. J. Participation of lipopolysaccharide-binding

- protein in lipopolysaccharide-dependent macrophage activation. *Am. J. Respir. Cell Mol. Biol.* **1992**, *7*, 239-245.
29. Schumann, R. R.; Leong, S. R.; Flaggs, G. W.; Gray, P. W.; Wright, S. D.; Mathison, J. C.; Tobias, P. S.; and Ulevitch, R. J. Structure and function of lipopolysaccharide-binding protein. *Science* **1990**, *249*, 1429-1431.
 30. Lien, E.; Means, T. K.; Heine, H.; Yoshimura, A.; Kusumoto, S.; Fukase, K.; Fenton, M. J.; Oikawa, M.; Qureshi, N.; Monks, B.; Finberg, R. W.; Ingalls, R. R.; and Golenbock, D. T. Toll-like receptor 4 imparts ligand-specific recognition of bacterial lipopolysaccharide. *J. Clin. Invest.* **2000**, *105*, 497-504.
 31. Poltorak, A.; He, X.; Smirnova, I.; Liu, M. Y.; Huffel, C. V.; Du, X.; Birdwell, D.; Alejos, E.; Silva, M.; Galanos, C.; Freudenberg, M.; Ricciardi, C. P.; Layton, B.; and Beutler, B. Defective LPS signaling in C3H/HeJ and C57BL/10ScCr mice: mutations in Tlr4 gene. *Science* **1998**, *282*, 2085-2088.
 32. Geppert, T. D.; Whitehurst, C. E.; Thompson, P.; and Beutler, B. Lipopolysaccharide signals activation of tumor necrosis factor biosynthesis through the ras/raf-1/MEK/MAPK pathway. *Mol. Med.* **1994**, *1*, 93-103.
 33. Han, J.; Lee, J. D.; Bibbs, L.; and Ulevitch, R. J. A MAP kinase targeted by endotoxin and hyperosmolarity in mammalian cells. *Science* **1994**, *265*, 808-811.
 34. Bohuslav, J.; Kravchenko, V. V.; Parry, G. C.; Erlich, J. H.; Gerondakis, S.; Mackman, N.; and Ulevitch, R. J. Regulation of an essential innate immune

- response by the p50 subunit of NF-kappaB. *J. Clin. Invest.* **1998**, *102*, 1645-1652.
35. Ulevitch, R. J. and Tobias, P. Recognition of gram-negative bacteria and endotoxin by the innate immune system. *Curr.Opin.Immunol.* **1999**, *11*, 19-23.
36. Zeni, F.; Freeman, B.; and Natanson, C. Anti-inflammatory therapies to treat sepsis and septic shock: A reassessment. *Crit. Care Med.* **1997**, *25*, 1097-1100.
37. Siegel, J. P. Antiendotoxin antibodies. *Ann. Intern. Med.* **1995**, *122*, 315.
38. Ziegler, E. J.; Fisher, C. J., Jr.; Sprung, C. L.; Straube, R. C.; Sadoff, J. C.; Foulke, G. E.; Wortel, C. H.; Fink, M. P.; Dellinger, R. P.; Teng, N. N. H.; Allen, I. E.; Berger, H. J.; Knatterud, G. L.; LoBuglio, A. F.; Smith, C. R.; and HA-1A Sepsis Study Group Treatment of gram-negative bacteremia and septic shock with HA- 1A human monoclonal antibody against endotoxin--A randomized, double-blind, placebo-controlled trial. *N. Engl. J. Med.* **1991**, *324*, 429-436.
39. Bone, R. C.; Balk, R. A.; Fein, A. M.; Perl, T. M.; Wenzel, R. P.; Reines, H. D.; Quenzer, R. W.; Iberti, T. J.; Macintyre, N.; and Schein, R. M. A second large controlled clinical study of E5, a monoclonal antibody to endotoxin: results of a prospective, multicenter, randomized, controlled trial. The E5 Sepsis Study Group [see comments]. *Crit. Care Med.* **1995**, *23*, 994-1006.
40. Warren, H. S.; Amato, S. F.; Fitting, C.; Black, K. M.; Loiselle, P. M.; Pasternack, M. S.; and Cavillon, J.-M. Assessment of ability of murine and

- human anti-lipid A monoclonal antibodies to bind and neutralize lipopolysaccharide. *J. Exp. Med.* **1993**, *177*, 89-97.
41. Helmerhorst, E. J.; Maaskant, J. J.; and Appelmelk, B. J. Anti-lipid A monoclonal antibody centoxin (HA-1A) binds to a wide variety of hydrophobic ligands. *Infect. Immun.* **1998**, *66*, 870-873.
 42. Di Padova, F. E.; Mikol, V.; Barclay, G. R.; Poxton, I. R.; Brade, H.; and Rietschel, E. T. Anti-lipopolysaccharide core antibodies. *Prog. Clin. Biol. Res.* **1994**, *388*, 85-94.
 43. Di Padova, F.; Brade, H.; Barclay, G. R.; Poxton, I. R.; Liehl, E.; Schuetze, E.; Kocher, H. P.; Ramsay, G.; Schreier, M. H.; McClelland, D. B. L.; and Rietschel, E. T. A broadly cross-protective monoclonal antibody binding to *Escherichia coli* and *Salmonella* lipopolysaccharide. *Infect. Immun.* **1993**, *61*, 3863-3872.
 44. Vaarala, O.; Vaara, M.; and Palosuo, T. Effective inhibition of cardiolipin-binding antibodies in gram-negative infections by bacterial lipopolysaccharide. *Scand. J. Immunol.* **1988**, *28*, 607-612.
 45. Leturcq, D. J.; Moriarty, A. M.; Talbott, G.; Winn, R. K.; Martin, T. R.; and Ulevitch, R. J. Antibodies against CD14 protect primates from endotoxin-induced shock. *J. Clin. Invest.* **1996**, *98*, 1533-1538.
 46. Schimke, J.; Mathison, J.; Morgiewicz, J.; and Ulevitch, R. J. Anti-CD14 mAb treatment provides therapeutic benefit after in vivo exposure to endotoxin. *Proc. Natl. Acad. Sci. U. S. A.* **1998**, *95*, 13875-13880.

47. Le Roy, D., Di Padova, F., Tees, R., Lengacher, S., Landmann, R., Glauser, M. P., Calandra, T., and Heumann, D. Monoclonal antibodies to murine lipopolysaccharide (LPS)-binding protein (LBP) protects mice from lethal endotoxemia by blocking either the binding of LPS to LBP or the presentation of LPS/LBP complexes to CD14. *Journal of Immunology (Baltimore MD)* **1999**, *162*, 7454-7461.
48. Leturcq, D. J.; Moriarty, A. M.; Talbott, G.; Winn, R. K.; Martin, T. R.; and Ulevitch, R. J. Therapeutic strategies to block LPS interactions with its receptor. *Prog. Clin. Biol. Res.* **1995**, *392*, 473-477.
49. Evans, T. J.; Carpenter, A.; Moyes, D.; Martin, R.; and Cohen, J. Protective effects of a recombinant amino-terminal fragment of human Bactericidal/Permeability-increasing protein in an animal model of gram-negative sepsis. *J. Infect. Dis.* **1995**, *171*, 153-160.
50. Gazzano-Santoro, H.; Parent, J. B.; Conlon, P. J.; Kasler, H. G.; Tsai, C.-M.; Lill-Elghanian, D. A.; and Hollingsworth, R. I. Characterization of the structural elements in lipid A required for binding of a recombinant fragment of bactericidal/permeability-increasing protein. *Infect. Immun.* **1995**, *63*, 2201-2205.
51. Elsbach, P.; Weiss, J.; Doerfler, M.; Shu, C.; Kohn, F.; Ammons, W. S.; Kung, A. H.; Meszaros, K. K.; and Parent, J. B. The bactericidal/permeability increasing protein of neutrophils is a potent antibacterial and anti-endotoxin agent in vitro and in vivo. *Prog. Clin. Biol. Res.* **1994**, *388*, 41-51.

52. Peterson, A.; Hancock, R. E. W.; and McGroarty, E. J. Binding of polycationic antibiotics and polyamines to lipopolysaccharides of *Pseudomonas aeruginosa*. *Journal of Bacteriology* **1985**, *164*, 1256-1261.
53. Storm, D. R. and Rosenthal, K. Polymyxin and related peptide antibiotics. *Annual Reviews of Biochemistry* **1977**, *46*, 723-763.
54. Morrison, D. C. and Jacobs, D. M. Binding of polymyxin B to the lipid A portion of bacterial lipopolysaccharides. *Immunochemistry* **1976**, *13*, 813-818.
55. Yao, Y. M.; Tian, H. M.; Sheng, Z. Y.; Wang, Y. P.; Yu, Y.; Sun, S. R.; and Xu, S. H. Inhibitory effects of low-dose polymyxin B on hemorrhage-induced endotoxin/bacterial translocation and cytokine formation in rats. *J. Trauma*. **1995**, *38*, 924-930.
56. Durando, M. M.; MacKay, R. J.; Linda, S.; and Skelley, L. A. Effects of polymyxin B and Salmonella typhimurium antiserum on horses given endotoxin intravenously. *Am. J. Vet. Res.* **1994**, *55*, 921-927.
57. Stokes, D. C.; Shenep, J. L.; Fishman, M.; Hilder, W. K.; Bysani, G. K.; and Rufus, K. Polymyxin B prevents lipopolysaccharide-induced release of TNF. *J. Infect. Dis.* **1989**, *160*, 52-57.
58. Rustici, A.; Velucchi, M.; Faggioni, R.; Sironi, M.; Ghezzi, P.; Quataert, S.; Green, B.; and Porro, M. Molecular mapping and detoxification of the lipid A binding site by synthetic peptides. *Science* **1993**, *259*, 361-365.
59. Vaara, M. and Vaara, T. Sensitization of Gram-negative bacteria to antibiotics and complement by a nontoxic oligopeptide. *Nature* **1983**, *303*, 526-528.

60. Kimura, Y.; Matsunaga, H.; and Vaara, M. Polymyxin B octapeptide and polymyxin B heptapeptide are potent outer membrane permeability-increasing agents. *J. Antibiot. Tokyo.* **1992**, *45*, 742-749.
61. Iwagaki, A.; Porro, M.; and Pollack, M. Influence of synthetic antiendotoxin peptides on lipopolysaccharide (LPS) recognition and LPS-induced proinflammatory cytokine responses by cells expressing membrane-bound CD14. *Infect. Immun.* **2000**, *68*, 1655-1663.
62. Scott, M. G.; Vreugdenhil, A. C.; Buurman, W. A.; Hancock, R. E.; and Gold, M. R. Cationic antimicrobial peptides block the binding of lipopolysaccharide (LPS) to LPS binding protein. *J. Immunol.* **2000**, *164*, 549-553.
63. Aoki, H.; Kodama, M.; Tani, T.; and Hanasawa, K. Treatment of sepsis by extracorporeal elimination of endotoxin using polymyxin B-immobilized fiber. *Am. J. Surg.* **1994**, *167*, 412-417.
64. Medzhitov, R. Toll-like receptors and innate immunity. *Nature Rev. Immunol.* **2001**, *1*, 135-145.
65. Nathan, C. and Ding, A. TREM-1: a new regulator of innate immunity in sepsis syndrome. *Nat. Med* **2001**, *7*, 530-532.
66. Read, T. E.; Grunfeld, C.; Kumwenda, Z. L.; Calhoun, M. C.; Kane, J. P.; Feingold, K. R.; and Rapp, J. H. Triglyceride-rich lipoproteins prevent septic death in rats. *J. Exp. Med.* **1995**, *182*, 267-272.
67. Bhattacharjya, S.; David, S. A.; Mathan, V. I.; and Balaram, P. Polymyxin B nonapeptide: Conformations in water and in the lipopolysaccharide-bound

state determined by two-dimensional NMR and molecular dynamics.

Biopolymers **1997**, *41*, 251-265.

68. Martin, G. S.; Mannino, D. M.; Eaton, S.; and Moss, M. The epidemiology of sepsis in the United States from 1979 through 2000. *N. Engl. J. Med.* **2003**, *348*, 1546-1554.
69. David, S. A.; Bechtel, B.; Annaiah, C.; Mathan, V. I.; and Balaram, P. Interaction of cationic amphiphilic drugs with lipid A: Implications for development of endotoxin antagonists. *Biochim. Biophys. Acta Lipids Lipid Metab.* **1994**, *1212*, 167-175.
70. David, S. A.; Mathan, V. I.; and Balaram, P. Interactions of linear dicationic molecules with lipid A: Structural requisites for optimal binding affinity. *J. Endotoxin. Res.* **1995**, *2*, 325-336.
71. Edwards, K. J., Jenkins, T. C., and Neidle, S. Crystal structure of a pentamidine-oligonucleotide complex: implications for DNA-binding properties. *Biochemistry (Washington DC)*. **1992**, *31*, 7104-7109.
72. Heine, H.; Brade, H.; Kusumoto, S.; Kusama, T.; Rietschel, E. T.; Flad, H.-D.; and Ulmer, A. J. Inhibition of LPS binding on human monocytes by phosphonoxyethyl analogs of lipid A. *J. Endotoxin. Res.* **1994**, *1*, 14-20.
73. Geller, D. A.; Kispert, P. H.; Su, G. L.; Wang, S. C.; Di Silvio, M.; Twardy, D. J.; Billiar, T. R.; and Simmons, R. L. Induction of hepatocyte lipopolysaccharide binding protein in models of sepsis and the acute-phase response. *Arch. Surg.* **1993**, *128*, 22-28.

74. Tobias, P. S.; Mathison, J. C.; and Ulevitch, R. J. A family of lipopolysaccharide binding proteins involved in responses to gram-negative sepsis. *J. Biol. Chem.* **1988**, *263*, 13479-13481.
75. Beamer, L. J.; Carroll, S. F.; and Eisenberg, D. The BPI/LBP family of proteins: a structural analysis of conserved regions. *Protein Sci* **1998**, *7*, 906-914.
76. Gazzano-Santoro, H.; Mészáros, K.; Birr, C.; Carroll, S. F.; Theofan, G.; Horwitz, A. H.; Lim, E.; Aberle, S.; Kasler, H.; and Parent, J. B. Competition between rBPI₂₃, a Recombinant Fragment of Bactericidal/Permeability-Increasing Protein, and Lipopolysaccharide (LPS)-Binding Protein for Binding to LPS and Gram-Negative Bacteria. *Infection and Immunity* **1994**, *62*, 1185-1191.
77. Hailman, E.; Lichenstein, H. S.; Wurfel, M. M.; Miller, D. S.; Johnson, D. A.; Kelley, M.; Busse, L. A.; Zukowski, M. M.; and Wright, S. D. Lipopolysaccharide (LPS)-binding protein accelerates the binding of LPS to CD14. *J. Exp. Med.* **1994**, *179*, 269-277.
78. Yu, B. and Wright, S. D. Catalytic properties of lipopolysaccharide (LPS) binding protein. Transfer of LPS to soluble CD14. *J. Biol. Chem.* **1996**, *271*, 4100-4105.
79. Schumann, R. R.; Rietschel, E. T.; and Loppnow, H. The role of CD14 and lipopolysaccharide-binding protein (LBP) in the activation of different cell types by endotoxin. *Med. Microbiol. Immunol.* **1994**, *183*, 279-297.

80. Gallay, P.; Barras, C.; Tobias, P. S.; Calandra, T.; Glauser, M. P.; and Heumann, D. Lipopolysaccharide (LPS)-binding protein in human serum determines the tumor necrosis factor response of monocytes to LPS. *J. Infect. Dis.* **1994**, *170*, 1319-1322.
81. Wilde, C. G.; Seilhamer, J. J.; McGrogan, M.; Ashton, N.; Snable, J. L.; Lane, J. C.; Leong, S. R.; Thornton, M. B.; Miller, K. L.; Scott, R. W.; and Marra, M. N. Bactericidal/permeability-increasing protein and lipopolysaccharide (LPS)-binding protein. LPS binding properties and effects on LPS-mediated cell activation. *J. Biol. Chem.* **1994**, *269*, 17411-17416.
82. von der Möhlen, M. A. M.; Kimmings, N.; Wedel, N. I.; Mevissen, M. L. C. M.; Jansen, J.; Friedmann, N.; Lorenz, T. J.; Nelson, B. J.; White, M. L.; Bauer, R.; Hack, C. E.; Eerenberg, A. J. M.; and Van Deventer, S. J. H. Inhibition of endotoxin-induced cytokine release and neutrophil activation in humans by use of recombinant bactericidal/permeability-increasing protein. *J. Infect. Dis.* **1995**, *171*, 144-151.
83. Beamer, L. J.; Carroll, S. F.; and Eisenberg, D. Crystal structure of human BPI and two bound phospholipids at 2.4 angstrom resolution. *Science* **1997**, *276*, 1861-1864.
84. Garcia, C.; Saladino, R.; Thompson, C.; Hammer, B.; Parsonnet, J.; Wainwright, N.; Novitsky, T.; Fleisher, G. R.; and Siber, G. Effect of a recombinant endotoxin-neutralizing protein on endotoxin shock in rabbits. *Crit. Care Med.* **1994**, *22*, 1211-1218.

85. Kuppermann, N.; Nelson, D. S.; Saladino, R. A.; Thompson, C. M.; Sattler, F.; Novitsky, T. J.; Fleisher, G. R.; and Siber, G. R. Comparison of a recombinant endotoxin-neutralizing protein with a human monoclonal antibody to endotoxin for the treatment of Escherichia coli sepsis in rats. *J. Infect. Dis.* **1994**, *170*, 630-635.
86. Hoess, A.; Watson, S.; Siber, G. R.; and Liddington, R. Crystal structure of an endotoxin-neutralizing protein from the horseshoe crab, Limulus anti-LPS factor, at 1.5 Å resolution. *EMBO J.* **1993**, *12*, 3351-3356.
87. Danner, R. L.; Joiner, K. A.; Rubin, M.; Patterson, W. H.; Johnson, N.; Ayers, K. M.; and Parillo, J. E. Purification, toxicity, and anti-endotoxic activity of polymyxin B nonapeptide. *Antimicrobial Agents and Chemotherapy* **1989**, *33*, 1428-1434.
88. David, S. A.; Awasthi, S. K.; Wiese, A.; Ulmer, A. J.; Lindner, B.; Brandenburg, K.; Seydel, U.; Rietschel, E. T.; Sonesson, A.; and Balaram, P. Characterization of the interactions of a polycationic, amphiphilic, terminally branched oligopeptide with lipid A and lipopolysaccharide from the deep rough mutant of *Salmonella minnesota*. *J. Endotoxin Res.* **1996**, *3*, 369-379.
89. Thomas, C. J.; Surolia, N.; and Surolia, A. Surface plasmon resonance studies resolve the enigmatic endotoxin neutralizing activity of polymyxin B. *J. Biol. Chem.* **1999**, *274*, 29624-29627.
90. Srimal, S., Surolia, N., Balasubramanian, S., and Surolia, A. Titration calorimetric studies to elucidate the specificity of the interactions of

polymyxin B with lipopolysaccharides and lipid A. *Biochemical Journal* (London). **1996**, *315*, 679-686.

91. Thomas, C. J.; Surolia, N.; and Surolia, A. Surface plasmon resonance studies resolve the enigmatic endotoxin neutralizing activity of polymyxin B. *J. Biol. Chem.* **1999**, *274*, 29624-29627.
92. Geall, A. J. and Blagbrough, I. S. Homologation of polyamines in the synthesis of lipospermine conjugates and related lipoplexes. *Tetrahedron Letters.* **1998**, *39*, 443-446.
93. Behr, J.-P. Gene transfer with synthetic cationic amphiphiles: Prospects for gene therapy. *Bioconjug. Chem.* **1994**, *5*, 382-389.
94. Lee, E. R., Marshall, J., Siegel, C. S., Jiang, C., Yew, N. S., Nichols, M. R., Nietupski, J. B., Ziegler, R. J., Lane, M. B., Wang, K. X., Wan, N. C., Scheule, R. K., Harris, D. J., Smith, A. E., and Seng, S. H. Detailed analysis of structures and formulations of cationic lipids for efficient gene transfer to the lung. *Hum. Gene Ther.* **1996**, *7*, 1701-1717.
95. Gao, X and Huang, L. Cationic liposome-mediated gene transfer. *Gene Therapy.* **1995**, *2*, 710-722.
96. Nabel, G. J.; Nabel, E. G.; Yang, Z. Y.; Fox, B. A.; Plautz, G. E.; Gao, X.; Huang, L.; Shu, S.; Gordon, D.; and Chang, A. E. Direct gene transfer with DNA-liposome complexes in melanoma: expression, biologic activity, and lack of toxicity in humans. *Proc. Natl. Acad. Sci U. S. A.* **1993**, *90*, 11307-11311.

97. Nabel, G. J.; Yang, Z. Y.; Nabel, E. G.; Bishop, K.; Marquet, M.; Felgner, P. L.; Gordon, D.; and Chang, A. E. Direct gene transfer for treatment of human cancer. *Ann. N. Y. Acad. Sci* **1995**, *772*, 227-231.
98. Rosenberg, S. A.; Blaese, R. M.; Brenner, M. K.; Deisseroth, A. B.; Ledley, F. D.; Lotze, M. T.; Wilson, J. M.; Nabel, G. J.; Cornetta, K.; Economou, J. S.; Freeman, S.; Riddell, S. R.; Oldfield, E.; Gansbacher, B.; Dunbar, C.; Walker, R. E.; Schuening, F. G.; Roth, J. A.; Crystal, R. G.; Welsh, M. J.; Culver, K.; Heslop, H. E.; Simons, J.; Wilmott, R. W.; Tiberghien, P.; and et al Human gene marker/therapy clinical protocols. *Hum. Gene Ther.* **1996**, *7*, 2287-2313.
99. David, S. A.; Bechtel, B.; Annaiah, C.; Mathan, V. I.; and Balaram, P. Interaction of cationic amphiphilic drugs with lipid A: Implications for development of endotoxin antagonists. *Biochim. Biophys. Acta* **1994**, *1212*, 167-175.
100. David, S. A.; Mathan, V. I.; and Balaram, P. Interactions of linear dicationic molecules with lipid A: Structural requisites for optimal binding affinity. *J. Endotoxin. Res.* **1995**, *2*, 325-336.
101. Blagbrough, I. S.; Geall, A. J.; and David, S. A. Lipopolyamines incorporating the teraamine spermine bound to an alkyl chain, sequester bacterial lipopolysaccharide. *Bioorg. Med. Chem. Lett.* **2000**, *10*, 1959-1962.
102. David, S. A.; Perez, L.; and Infante, M. R. Sequestration of bacterial lipopolysaccharide by bis(arms) gemini compounds. *Bioorg. Med. Chem. Lett.* **2002**, *12*, 357-360.

103. Miller, K. A.; Suresh Kumar, E. V. K.; Wood, S. J.; Cromer, J. R.; Datta, A.; and David, S. A. Lipopolysaccharide Sequestrants: Structural Correlates of Activity and Toxicity in Novel Acylhomospermines. *J. Med. Chem.* **2005**, *48*, 2589-2599.
104. Burns, M. R.; Wood, S. J.; Miller, K. A.; Nguyen, T.; Cromer, J. R.; and David, S. A. Lysine-spermine conjugates: hydrophobic polyamine amides as potent lipopolysaccharide sequestrants. *Bioorg. Med. Chem.* **2005**, *13*, 2523-2536.
105. Burns, M. R.; Jenkins, S. A.; Wood, S. J.; Miller, K.; and David, S. A. Structure-activity relationships in lipopolysaccharide neutralizers: design, synthesis, and biological evaluation of a 540-membered amphipathic bisamide library. *J. Comb. Chem.* **2006**, *8*, 32-43.
106. David, S. A.; Silverstein, R.; Amura, C. R.; Kielian, T.; and Morrison, D. C. Lipopolyamines: novel antiendotoxin compounds that reduce mortality in experimental sepsis caused by gram-negative bacteria. *Antimicrob. Agents Chemother.* **1999**, *43*, 912-919.
107. Burns, M. R.; Jenkins, S. A.; Wood, S. J.; Miller, K.; and David, S. A. Structure-activity relationships in lipopolysaccharide neutralizers: design, synthesis, and biological evaluation of a 540-membered amphipathic bisamide library. *J. Comb. Chem.* **2006**, *8*, 32-43.

108. Wood, S. J.; Miller, K. A.; and David, S. A. Anti-endotoxin agents. 2. Pilot high-throughput screening for novel lipopolysaccharide-recognizing motifs in small molecules. *Comb. Chem. High. Throughput. Screen.* **2004**, *7*, 733-743.
109. Wood, S. J.; Miller, K. A.; Lushington, G. H.; Burns, M. R.; and David, S. A. Anti-endotoxin agents. 3. Rapid identification of high-affinity lipopolysaccharide-binding compounds in a substituted polyamine library. *Comb. Chem. High Throughput. Screen.* **2006**, *9*, 27-36.
110. Guo, J. X.; Wood, S. J.; David, S. A.; and Lushington, G. H. Molecular modeling analysis of the interaction of novel bis-cationic ligands with the lipid A moiety of lipopolysaccharide. *Bioorg. Med. Chem. Lett.* **2006**, *16*, 714-717.
111. Burns, M. R.; Jenkins, S. A.; Vermeulen, N. M.; Balakrishna, R.; Nguyen, T. B.; Kimbrell, M. R.; and David, S. A. Structural correlation between lipophilicity and lipopolysaccharide-sequestering activity in spermine-sulfonamide analogs. *Bioorg. Med. Chem. Lett.* **2006**, *16*, 6209-6212.
112. Burns, M. R.; Jenkins, S. A.; Wood, S. J.; Miller, K.; and David, S. A. Structure-activity relationships in lipopolysaccharide neutralizers: design, synthesis, and biological evaluation of a 540-membered amphipathic bisamide library. *J. Comb. Chem.* **2006**, *8*, 32-43.
113. Nguyen, T. B.; Adisechan, A.; Suresh Kumar, E. V. K.; Balakrishna, R.; Kimbrell, M. R.; Miller, K. A.; Datta, A.; and David, S. A. Protection from

- Endotoxic Shock by EVK-203, a Novel Alkylpolyamine Sequestrant of Lipopolysaccharide. *Bioorg. Med. Chem.* **2007**, *15*, 5694-5709.
114. Sil, D.; Shrestha, A.; Kimbrell, M. R.; Nguyen, T. B.; Adisechan, A. K.; Balakrishna, R.; Abbo, B. G.; Malladi, S.; Miller, K. A.; Short, S.; Cromer, J. R.; Arora, S.; Datta, A.; and David, S. A. Bound to Shock: Protection from Lethal Endotoxemic Shock by a Novel, Nontoxic, Alkylpolyamine Lipopolysaccharide Sequestrant. *Antimicrob. Agents Chemother.* **2007**, *51*, 2811-2819.
115. Wood, S. J.; Miller, K. A.; Lushington, G. H.; Burns, M. R.; and David, S. A. Anti-endotoxin agents. 3. Rapid identification of high-affinity lipopolysaccharide-binding compounds in a substituted polyamine library. *Comb. Chem. High Throughput. Screen.* **2006**, *9*, 27-36.
116. Khownum, K.; Wood, S. J.; Miller, K. A.; Balakrishna, R.; Nguyen, T. B.; Kimbrell, M. R.; Georg, G. I.; and David, S. A. Novel endotoxin-sequestering compounds with terephthalaldehyde-bis-guanylhydrazone scaffolds. *Bioorg. Med. Chem. Lett.* **2006**, *16*, 1305-1308.
117. Calnan, B. J.; Tidor, B.; Biancalana, S.; Hudson, D.; and Frankel, A. D. Arginine-mediated RNA recognition: the arginine fork. *Science* **1991**, *252*, 1167-1171.
118. Burns, M. R.; Jenkins, S. A.; Kimbrell, M. R.; Balakrishna, R.; Nguyen, T. B.; Abbo, B. G.; and David, S. A. Polycationic sulfonamides for the sequestration of endotoxin. *J. Med. Chem.* **2007**, *50*, 877-888.

119. David, S. A. Towards a rational development of anti-endotoxin agents: novel approaches to sequestration of bacterial endotoxins with small molecules. *J. Molec. Recognition* **2001**, *14*, 370-387.
120. Buchheit, K. H.; Gamse, R.; Giger, R.; Hoyer, D.; Klein, F.; Kloppner, E.; Pfannkuche, H. J.; and Mattes, H. The serotonin 5-HT₄ receptor. 2. Structure-activity studies of the indole carbazimidamide class of agonists. *J. Med. Chem.* **1995**, *38*, 2331-2338.
121. Nguyen, C.; Ruda, G. F.; Schipani, A.; Kasinathan, G.; Leal, I.; Musso-Buendia, A.; Kaiser, M.; Brun, R.; Ruiz-Perez, L. M.; Sahlberg, B. L.; Johansson, N. G.; Gonzalez-Pacanowska, D.; and Gilbert, I. H. Acyclic nucleoside analogues as inhibitors of *Plasmodium falciparum* dUTPase. *J. Med. Chem.* **2006**, *49*, 4183-4195.
122. Green, L. C.; Wagner, D. A.; Glogowski, J.; Skipper, P. L.; Wishnok, J. S.; and Tannenbaum, S. R. Analysis of nitrate, nitrite and [15-N] nitrate in biological fluids. *Anal. Biochem.* **1982**, *126*, 131.
123. Fennrich, S.; Fischer, M.; Hartung, T.; Lexa, P.; Montag-Lessing, T.; Sonntag, H.-G.; Weigandt, M.; and Wendel, A. Detection of endotoxins and other pyrogens using human whole blood. *Dev. Biol. Standards* **1999**, *101*, 131-139.
124. Remick, D.G.; Newcomb, D.E.; and Friedland, J.S. Whole-blood assays for cytokine production. In *Septic shock. Methods and protocols*. Evans, T. J. Ed.; Humana Press: New Jersey, 2000; pp 101-114.

125. Cook, E. B.; Stahl, J. L.; Lowe, L.; Chen, R.; Morgan, E.; Wilson, J.; Varro, R.; Chan, A.; Graziano, F. M.; and Barney, N. P. Simultaneous measurement of six cytokines in a single sample of human tears using microparticle-based flow cytometry: allergics vs. non-allergics. *J. Immunol. Methods* **2001**, *254*, 109-116.
126. Funato, Y.; Baumhover, H.; Grantham-Wright, D.; Wilson, J.; Ernst, D.; and Sepulveda, H. Simultaneous measurement of six human cytokines using the Cytometric Bead Array System, a multiparameter immunoassay system for flow cytometry. *Cytometry Res.* **2002**, *12*, 93-103.
127. Freudenberg, M. A. and Galanos, C. Tumor necrosis factor alpha mediates lethal activity of killed Gram-negative and Gram-positive bacteria in D-galactosamine- treated mice. *Infect. Immun.* **1991**, *59*, 2110-2115.
128. Tracey, K. J. and Cerami, A. Tumor necrosis factor, other cytokines and disease. . *Annu. Rev. Cell Biol.* **1993**, *9*, 317-343.
129. Kawai, T. and Akira, S. TLR signaling. *Semin. Immunol.* **2007**.
130. Kumagai, Y.; Takeuchi, O.; and Akira, S. Pathogen recognition by innate receptors. *J. Infect. Chemother.* **2008**, *14*, 86-92.
131. Kumagai, Y.; Takeuchi, O.; and Akira, S. Pathogen recognition by innate receptors. *J. Infect. Chemother.* **2008**, *14*, 86-92.
132. Takeda, K. and Akira, S. Toll-like receptors. *Curr. Protoc. Immunol.* **2007**, *Chapter 14*, Unit.

133. Akira, S. Toll-like receptors and innate immunity. *Adv. Immunol.* **1902**, 78, 1-56.
134. Akira, S.; Takeda, K.; and Kaisho, T. Toll-like receptors: critical proteins linking innate and acquired immunity. *Nature Immunol.* **2001**, 2, 675-680.
135. Cottalorda, A.; Vershelde, C.; Marcais, A.; Tomkowiak, M.; Musette, P.; Uematsu, S.; Akira, S.; Marvel, J.; and Bonnefoy-Berard, N. TLR2 engagement on CD8 T cells lowers the threshold for optimal antigen-induced T cell activation. *Eur. J. Immunol.* **2006**, 36, 1684-1693.
136. Kaisho, T. and Akira, S. Toll-like receptors as adjuvant receptors. *Biochim. Biophys. Acta* **2002**, 1589, 1-13.
137. Vollmer, W. and Holtje, J. V. The architecture of the murein (peptidoglycan) in gram-negative bacteria: vertical scaffold or horizontal layer(s)? *J. Bacteriol.* **2004**, 186, 5978-5987.
138. Baddiley, J. Bacterial cell walls and membranes. Discovery of the teichoic acids. *Bioessays* **1989**, 10, 207-210.
139. Fischer, W. Lipoteichoic acid and lipids in the membrane of *Staphylococcus aureus*. *Med. Microbiol. Immunol.* **1994**, 183, 61-76.
140. Henderson, B.; Poole, S.; and Wilson, M. Bacterial modulins: a novel class of virulence factors which cause host tissue pathology by inducing cytokine synthesis. *Microbiol. Rev.* **1996**, 60, 316-341.
141. Muhlradt, P. F.; Kiess, M.; Meyer, H.; Sussmuth, R.; and Jung, G. Isolation, structure elucidation, and synthesis of a macrophage stimulatory lipopeptide

- from *Mycoplasma fermentans* acting at picomolar concentration. *J. Exp. Med.* **1997**, *185*, 1951-1958.
142. Dziarski, R. and Gupta, D. The peptidoglycan recognition proteins (PGRPs). *Genome Biol.* **2006**, *7*, 232.
143. Schroder, N. W.; Morath, S.; Alexander, C.; Hamann, L.; Hartung, T.; Zahringer, U.; Gobel, U. B.; Weber, J. R.; and Schumann, R. R. Lipoteichoic acid (LTA) of *Streptococcus pneumoniae* and *Staphylococcus aureus* activates immune cells via Toll-like receptor (TLR)-2, lipopolysaccharide-binding protein (LBP), and CD14, whereas TLR-4 and MD-2 are not involved. *J. Biol. Chem.* **2003**, *278*, 15587-15594.
144. Buwitt-Beckmann, U.; Heine, H.; Wiesmuller, K. H.; Jung, G.; Brock, R.; and Ulmer, A. J. Lipopeptide structure determines TLR2 dependent cell activation level. *FEBS J.* **2005**, *272*, 6354-6364.
145. Nahori, M. A.; Fournie-Amazouz, E.; Que-Gewirth, N. S.; Balloy, V.; Chignard, M.; Raetz, C. R.; Saint, G., I; and Werts, C. Differential TLR recognition of leptospiral lipid A and lipopolysaccharide in murine and human cells. *J. Immunol.* **2005**, *175*, 6022-6031.
146. Melchers, F.; Braun, V.; and Galanos, C. The lipoprotein of the outer membrane of *Escherichia coli*: a B-lymphocyte mitogen. *J. Exp. Med.* **1975**, *142*, 473-482.
147. Muhlradt, P. F.; Quentmeier, H.; and Schmitt, E. Involvement of interleukin-1 (IL-1), IL-6, IL-2, and IL-4 in generation of cytolytic T cells from thymocytes

- stimulated by a *Mycoplasma fermentans*-derived product. *Infect. Immun.* **1991**, *59*, 3962-3968.
148. Quentmeier, H.; Schmitt, E.; Kirchhoff, H.; Grote, W.; and Muhlradt, P. F. *Mycoplasma fermentans*-derived high-molecular-weight material induces interleukin-6 release in cultures of murine macrophages and human monocytes. *Infect. Immun.* **1990**, *58*, 1273-1280.
149. Quentmeier, H.; Schumann-Kindel, G.; Muhlradt, P. F.; and Drexler, H. G. Induction of proto-oncogene and cytokine expression in human peripheral blood monocytes and the monocytic cell line THP-1 after stimulation with mycoplasma-derived material MDHM. *Leuk. Res.* **1994**, *18*, 319-325.
150. Deres, K.; Schild, H.; Wiesmuller, K. H.; Jung, G.; and Rammensee, H. G. In vivo priming of virus-specific cytotoxic T lymphocytes with synthetic lipopeptide vaccine. *Nature* **1989**, *342*, 561-564.
151. Muhlradt, P. F.; Meyer, H.; and Jansen, R. Identification of S-(2,3-dihydroxypropyl)cystein in a macrophage-activating lipopeptide from *Mycoplasma fermentans*. *Biochemistry* **1996**, *35*, 7781-7786.
152. Takeuchi, O.; Kaufmann, A.; Grote, K.; Kawai, T.; Hoshino, K.; Morr, M.; Muhlradt, P. F.; and Akira, S. Cutting edge: preferentially the R-stereoisomer of the mycoplasmal lipopeptide macrophage-activating lipopeptide-2 activates immune cells through a toll-like receptor 2- and MyD88-dependent signaling pathway. *J. Immunol.* **2000**, *164*, 554-557.

153. Morr, M.; Takeuchi, O.; Akira, S.; Simon, M. M.; and Muhlradt, P. F. Differential recognition of structural details of bacterial lipopeptides by toll-like receptors. *Eur. J. Immunol.* **2002**, *32*, 3337-3347.
154. Okusawa, T.; Fujita, M.; Nakamura, J.; Into, T.; Yasuda, M.; Yoshimura, A.; Hara, Y.; Hasebe, A.; Golenbock, D. T.; Morita, M.; Kuroki, Y.; Ogawa, T.; and Shibata, K. Relationship between structures and biological activities of mycoplasmal diacylated lipopeptides and their recognition by toll-like receptors 2 and 6. *Infect. Immun.* **2004**, *72*, 1657-1665.
155. Reutter, F.; Jung, G.; Baier, W.; Treyer, B.; Bessler, W. G.; and Wiesmuller, K. H. Immunostimulants and Toll-like receptor ligands obtained by screening combinatorial lipopeptide collections. *J. Pept. Res.* **2005**, *65*, 375-383.
156. Beutler, B. and Poltorak, A. The sole gateway to endotoxin response: how *LPS* was identified as *TLR4*, and its role in innate immunity. *Drug Metab. Dispos.* **2001**, *29*, 474-478.
157. Beutler, B. Tlr4: central component of the sole mammalian LPS sensor. *Curr. Opin. Immunol.* **2000**, *12*, 20-26.
158. Poltorak, A.; He, X.; Smirnova, I.; Liu, M. Y.; Huffel, C. V.; Du, X.; Birdwell, D.; Alejos, E.; Silva, M.; Galanos, C.; Freudenberg, M.; Ricciardi, C. P.; Layton, B.; and Beutler, B. Defective LPS signaling in C3H/HeJ and C57BL/10ScCr mice: mutations in Tlr4 gene. *Science* **1998**, *282*, 2085-2088.
159. Akira, S. and Takeda, K. Functions of toll-like receptors: lessons from KO mice. *C. R. Biol.* **2004**, *327*, 581-589.

160. Takeda, K. and Akira, S. TLR signaling pathways. *Semin. Immunol.* **2004**, *16*, 3-9.
161. Takeuchi, O.; Hoshino, K.; Kawai, T.; Sanjo, H.; Takada, H.; Ogawa, T.; Takeda, K.; and Akira, S. Differential roles of TLR2 and TLR4 in recognition of gram-negative and gram-positive bacterial cell wall components. *Immunity.* **1999**, *11*, 443-451.
162. Spohn, R.; Buwitt-Beckmann, U.; Brock, R.; Jung, G.; Ulmer, A. J.; and Wiesmuller, K. H. Synthetic lipopeptide adjuvants and Toll-like receptor 2--structure-activity relationships. *Vaccine* **2004**, *22*, 2494-2499.
163. Alexopoulou, L.; Thomas, V.; Schnare, M.; Lobet, Y.; Anguita, J.; Schoen, R. T.; Medzhitov, R.; Fikrig, E.; and Flavell, R. A. Hyporesponsiveness to vaccination with *Borrelia burgdorferi* OspA in humans and in. *Nat. Med.* **2002**, *8*, 878-884.
164. Takeuchi, O.; Sato, S.; Horiuchi, T.; Hoshino, K.; Takeda, K.; Dong, Z.; Modlin, R. L.; and Akira, S. Cutting edge: role of Toll-like receptor 1 in mediating immune response to microbial lipoproteins. *J. Immunol.* **2002**, *169*, 10-14.
165. Buwitt-Beckmann, U.; Heine, H.; Wiesmuller, K. H.; Jung, G.; Brock, R.; Akira, S.; and Ulmer, A. J. TLR1- and TLR6-independent recognition of bacterial lipopeptides. *J. Biol. Chem.* **2006**, *281*, 9049-9057.

166. Buwitt-Beckmann, U.; Heine, H.; Wiesmuller, K. H.; Jung, G.; Brock, R.; Akira, S.; and Ulmer, A. J. Toll-like receptor 6-independent signaling by diacylated lipopeptides. *Eur. J. Immunol.* **2005**, *35*, 282-289.
167. Jin, M. S.; Kim, S. E.; Heo, J. Y.; Lee, M. E.; Kim, H. M.; Paik, S. G.; Lee, H.; and Lee, J. O. Crystal structure of the TLR1-TLR2 heterodimer induced by binding of a tri-acylated lipopeptide. *Cell* **2007**, *130*, 1071-1082.
168. Kiura, K.; Kataoka, H.; Nakata, T.; Into, T.; Yasuda, M.; Akira, S.; Inoue, N.; and Shibata, K. The synthetic analogue of mycoplasmal lipoprotein FSL-1 induces dendritic cell maturation through Toll-like receptor 2. *FEMS Immunol. Med. Microbiol.* **2006**, *46*, 78-84.
169. Link, C.; Gavioli, R.; Ebensen, T.; Canella, A.; Reinhard, E.; and Guzman, C. A. The Toll-like receptor ligand MALP-2 stimulates dendritic cell maturation and modulates proteasome composition and activity. *Eur. J. Immunol.* **2004**, *34*, 899-907.
170. Espuelas, S.; Roth, A.; Thumann, C.; Frisch, B.; and Schuber, F. Effect of synthetic lipopeptides formulated in liposomes on the maturation of human dendritic cells. *Mol. Immunol.* **2005**, *42*, 721-729.
171. Borsutzky, S.; Kretschmer, K.; Becker, P. D.; Muhlrad, P. F.; Kirschning, C. J.; Weiss, S.; and Guzman, C. A. The mucosal adjuvant macrophage-activating lipopeptide-2 directly stimulates B lymphocytes via the TLR2 without the need of accessory cells. *J. Immunol.* **2005**, *174*, 6308-6313.

172. Mansson, A.; Adner, M.; Hockerfelt, U.; and Cardell, L. O. A distinct Toll-like receptor repertoire in human tonsillar B cells, directly activated by PamCSK, R-837 and CpG-2006 stimulation. *Immunology* **2006**, *118*, 539-548.
173. Ruprecht, C. R. and Lanzavecchia, A. Toll-like receptor stimulation as a third signal required for activation of human naive B cells. *Eur. J. Immunol.* **2006**, *36*, 810-816.
174. Reschner, A.; Moretta, A.; Landmann, R.; Heberer, M.; Spagnoli, G. C.; and Padovan, E. The ester-bonded palmitoyl side chains of Pam3CysSerLys4 lipopeptide account for its powerful adjuvanticity to HLA class I-restricted CD8+ T lymphocytes. *Eur. J. Immunol.* **2003**, *33*, 2044-2052.
175. Lau, Y. F.; Deliyannis, G.; Zeng, W.; Mansell, A.; Jackson, D. C.; and Brown, L. E. Lipid-containing mimetics of natural triggers of innate immunity as CTL-inducing influenza vaccines. *Int. Immunol.* **2006**, *18*, 1801-1813.
176. Borsutzky, S.; Fiorelli, V.; Ebensen, T.; Tripiciano, A.; Rharbaoui, F.; Scoglio, A.; Link, C.; Nappi, F.; Morr, M.; Butto, S.; Cafaro, A.; Muhlradt, P. F.; Ensoli, B.; and Guzman, C. A. Efficient mucosal delivery of the HIV-1 Tat protein using the synthetic lipopeptide MALP-2 as adjuvant. *Eur. J. Immunol.* **2003**, *33*, 1548-1556.
177. Borsutzky, S.; Ebensen, T.; Link, C.; Becker, P. D.; Fiorelli, V.; Cafaro, A.; Ensoli, B.; and Guzman, C. A. Efficient systemic and mucosal responses against the HIV-1 Tat protein by prime/boost vaccination using the lipopeptide MALP-2 as adjuvant. *Vaccine* **2006**, *24*, 2049-2056.

178. Mittenbuhler, K.; Loleit, M.; Baier, W.; Fischer, B.; Sedelmeier, E.; Jung, G.; Winkelmann, G.; Jacobi, C.; Weckesser, J.; Erhard, M. H.; Hofmann, A.; Bessler, W.; and Hoffmann, P. Drug specific antibodies: T-cell epitope-lipopeptide conjugates are potent adjuvants for small antigens in vivo and in vitro. *Int. J. Immunopharmacol.* **1997**, *19*, 277-287.
179. Ghielmetti, M.; Zwicker, M.; Ghielmetti, T.; Simon, M. M.; Villiger, P. M.; and Padovan, E. Synthetic bacterial lipopeptide analogs facilitate naive CD4+ T cell differentiation and enhance antigen-specific HLA-II-restricted responses. *Eur. J. Immunol.* **2005**, *35*, 2434-2442.
180. Bohnenkamp, H. R.; Papazisis, K. T.; Burchell, J. M.; and Taylor-Papadimitriou, J. Synergism of Toll-like receptor-induced interleukin-12p70 secretion by monocyte-derived dendritic cells is mediated through p38 MAPK and lowers the threshold of T-helper cell type 1 responses. *Cell Immunol.* **2007**, *247*, 72-84.
181. Haux, J. Infection and cancer. *Lancet* **2001**, *358*, 155-156.
182. Bauduer, F. [Medicine in ancient Egypt, a fascinating level of modernity]. *Presse Med.* **2001**, *30*, 1236-1239.
183. SPRUNT, W. H. Imhotep. *N. Engl. J. Med.* **1955**, *253*, 778-780.
184. Coley, W. B. A Preliminary Note on the Treatment of Inoperable Sarcoma by the Toxic Product of Erysipelas. *Post-graduate* **1893**, *8*, 278-286.
185. Medzhitov, R. and Janeway, C. A., Jr. Innate immunity: impact on the adaptive immune response. *Curr. Opin. Immunol.* **1997**, *9*, 4-9.

186. Medzhitov, R. and Janeway, C. A., Jr. An ancient system of host defense. *Curr. Opin. Immunol.* **1998**, *10*, 12-15.
187. Janeway, C. A., Jr. and Medzhitov, R. Introduction: the role of innate immunity in the adaptive immune response. *Semin. Immunol.* **1998**, *10*, 349-350.
188. Akira, S.; Uematsu, S.; and Takeuchi, O. Pathogen recognition and innate immunity. *Cell* **2006**, *124*, 783-801.
189. Kirschning, C. J. and Schumann, R. R. TLR2: cellular sensor for microbial and endogenous molecular patterns. *Curr. Top. Microbiol. Immunol.* **2002**, *270*, 121-144.
190. Kaisho, T. and Akira, S. Toll-like receptor function and signaling. *J. Allergy Clin. Immunol.* **2006**, *117*, 979-987.
191. Takeuchi, O. and Akira, S. Signaling pathways activated by microorganisms. *Curr. Opin. Cell Biol.* **2007**, *19*, 185-191.
192. Kanzler, H.; Barrat, F. J.; Hessel, E. M.; and Coffman, R. L. Therapeutic targeting of innate immunity with Toll-like receptor agonists and antagonists. *Nat. Med.* **2007**, *13*, 552-559.
193. Cheever, M. A. Twelve immunotherapy drugs that could cure cancers. *Immunol. Rev.* **2008**, *222*:357-68., 357-368.
194. Hunder, N. N.; Wallen, H.; Cao, J.; Hendricks, D. W.; Reilly, J. Z.; Rodmyre, R.; Jungbluth, A.; Gnjatic, S.; Thompson, J. A.; and Yee, C. Treatment of

- metastatic melanoma with autologous CD4+ T cells against NY-ESO-1. *N. Engl. J. Med.* **2008**, *358*, 2698-2703.
195. A controlled field trial of the effectiveness of cholera and cholera El Tor vaccines in the Philippines. Preliminary report; Philippines Cholera Committee. *Bull. World Health Organ* **1965**, *32*, 603-625.
196. Kimbrell, M. R.; Warshakoon, H.; Cromer, J. R.; Malladi, S.; Hood, J. D.; Balakrishna, R.; Scholdberg, T. A.; and David, S. A. Comparison of the immunostimulatory and proinflammatory activities of candidate Gram-positive endotoxins, lipoteichoic acid, peptidoglycan, and lipopeptides, in murine and human cells. *Immunol. Lett.* **2008**, *118*, 132-141.
197. Schmidt, J.; Welsch, T.; Jager, D.; Muhlradt, P. F.; Buchler, M. W.; and Marten, A. Intratumoural injection of the toll-like receptor-2/6 agonist 'macrophage-activating lipopeptide-2' in patients with pancreatic carcinoma: a phase I/II trial. *Br. J. Cancer* **2007**, *97*, 598-604.
198. Prass, W.; Ringsdorf, H.; Bessler, W.; Wiesmuller, K. H.; and Jung, G. Lipopeptides of the N-terminus of Escherichia coli lipoprotein: synthesis, mitogenicity and properties in monolayer experiments. *Biochim. Biophys. Acta.* **1987**, *900*, 116-128.
199. Bessler, W. G.; Cox, M.; Lex, A.; Suhr, B.; Wiesmuller, K. H.; and Jung, G. Synthetic lipopeptide analogs of bacterial lipoprotein are potent polyclonal activators for murine B lymphocytes. *J. Immunol.* **1985**, *135*, 1900-1905.

200. Metzger, J.; Wiesmuller, K. H.; Schauder, R.; Bessler, W. G.; and Jung, G. Synthesis of novel immunologically active tripalmitoyl-S-glycerylcysteinyl lipopeptides as useful intermediates for immunogen preparations. *Int. J. Pept. Protein Res.* **1991**, *37*, 46-57.
201. Metzger, J. and Jung, G. Mycoloylpeptides and other lipopeptide adjuvants from higher aldoketene dimers. *Angew. Chem. Int. Ed Engl.* **1987**, *26*, 336-338.
202. Metzger, J.; Olma, A.; Leplawy, M. T.; and Jung, G. Synthesis of a B-lymphocyte activating γ -methylserine containing lipopentapeptide. *Z. Naturforsch. B.* **1987**, *42*, 1197-1201.
203. Metzger, J.; Jung, G.; Bessler, W. G.; Hoffmann, P.; Strecker, M.; Lieberknecht, A.; and Schmidt, U. Lipopeptides containing 2-(palmitoylamino)-6,7-bis(palmitoyloxy) heptanoic acid: synthesis, stereospecific stimulation of B-lymphocytes and macrophages, and adjuvanticity in vivo and in vitro. *J. Med. Chem.* **1991**, *34*, 1969-1974.
204. Grabiec, A.; Meng, G.; Fichte, S.; Bessler, W.; Wagner, H.; and Kirschning, C. J. Human but not murine toll-like receptor 2 discriminates between tri-palmitoylated and tri-lauroylated peptides. *J. Biol. Chem.* **2004**, *279*, 48004-48012.
205. Nguyen, T. B.; Suresh Kumar, E. V.; Sil, D.; Wood, S. J.; Miller, K. A.; Warshakoon, H. J.; Datta, A.; and David, S. A. Controlling Plasma Protein Binding: Structural Correlates of Interactions of Hydrophobic Polyamine

- Endotoxin Sequestrants with Human Serum Albumin. *Mol. Pharm.* **2008**, *5*, 1131-1137.
206. Pierik, M.; Joossens, S.; Van Steen, K.; Van Schuerbeek, N.; Vlietinck, R.; Rutgeerts, P.; and Vermeire, S. Toll-like receptor-1, -2, and -6 polymorphisms influence disease extension in inflammatory bowel diseases. *Inflamm. Bowel Dis.* **2006**, *12*, 1-8.
207. Canto, E.; Ricart, E.; Monfort, D.; Gonzalez-Juan, D.; Balanzo, J.; Rodriguez-Sanchez, J. L.; and Vidal, S. TNF alpha production to TLR2 ligands in active IBD patients. *Clin. Immunol.* **2006**, *119*, 156-165.
208. Nara, K.; Kurokawa, M. S.; Chiba, S.; Yoshikawa, H.; Tsukikawa, S.; Matsuda, T.; and Suzuki, N. Involvement of innate immunity in the pathogenesis of intestinal Behcet's disease. *Clin. Exp. Immunol.* **2008**, *152*, 245-251.
209. Albert, E. J. and Marshall, J. S. Aging in the absence of TLR2 is associated with reduced IFN-gamma responses in the large intestine and increased severity of induced colitis. *J. Leukoc. Biol.* **2008**, *83*, 833-842.
210. Seyberth, T.; Voss, S.; Brock, R.; Wiesmuller, K. H.; and Jung, G. Lipolanthionine peptides act as inhibitors of TLR2-mediated IL-8 secretion. Synthesis and structure-activity relationships. *J. Med. Chem.* **2006**, *49*, 1754-1765.

211. Zarbin, P. H.; Arrigoni, E. B.; Reckziegel, A.; Moreira, J. A.; Baraldi, P. T.; and Vieira, P. C. Identification of male-specific chiral compound from the sugarcane weevil *Sphenophorus levis*. *J. Chem. Ecol.* **2003**, *29*, 377-386.
212. Zhou, D.; Lagoja, I. M.; Rozenski, J.; Busson, R.; Van Aerschot, A.; and Herdewijn, P. Synthesis and properties of aminopropyl nucleic acids. *Chembiochem.* **2005**, *6*, 2298-2304.
213. Enders, D.; Lenzen, A.; Backes, M.; Janeck, C.; Catlin, K.; Lannou, M. I.; Runsink, J.; and Raabe, G. Asymmetric total synthesis of the 1-epi-aglycon of the cripowellins A and B. *J. Org. Chem.* **2005**, *70*, 10538-10551.
214. Andre, C., Bolte, J., and Demuyneck, C. Syntheses of 4-deoxy-D-fructose and enzymic affinity study. *Tetrahedron Asymmetry.* **1998**, *9*, 3737-3739.
215. Prestat, G.; Baylon, C.; Heck, M. P.; Grasa, G. A.; Nolan, S. P.; and Mioskowski, C. New strategy for the construction of a monotetrahydrofuran ring in Annonaceous acetogenin based on a ruthenium ring-closing metathesis: application to the synthesis of Solamin. *J. Org. Chem.* **2004**, *69*, 5770-5773.
216. Fernandez, R., Ros, A., Magriz, A., Dietrich, H., and Lassaletta, J. M. Enantioselective synthesis of cis- α -substituted cycloalkanols and trans-cycloalkyl amines thereof. *Tetrahedron.* **2007**, *63*, 6755-6763.
217. Avenoza, A., Busto, J. H., Jimenez-Oses, G., and Peregrina, J. M. Stereoselective synthesis of orthogonally protected alpha-methylnorlanthionine. *Org.Lett.* **2009**, *8*, 2855-2858.

218. Rice, T. K.; Schork, N. J.; and Rao, D. C. Methods for handling multiple testing. *Adv. Genet.* **2008**, *60*:293-308., 293-308.
219. Sheldon, M. R.; Fillyaw, M. J.; and Thompson, W. D. The use and interpretation of the Friedman test in the analysis of ordinal-scale data in repeated measures designs. *Physiother. Res. Int.* **1996**, *1*, 221-228.